Title
Post-fire hydrologic behavior and recovery: Advancing spatial and temporal prediction with an emphasis on remote sensing

Author
Kinoshita, Alicia

Publication Date
2012

Peer reviewed|Thesis/dissertation

UNIVERSITY OF CALIFORNIA

Los Angeles

Post-fire hydrologic behavior and recovery: Advancing spatial and temporal prediction with an emphasis on remote sensing

A dissertation submitted in partial satisfaction of the requirements for the degree Doctor of Philosophy in Civil Engineering

by

Alicia Michiko Kinoshita

2012

ABSTRACT OF THE DISSERTATION

Post-fire hydrologic behavior and recovery:

Advancing spatial and temporal prediction with an

emphasis on remote sensing

by

Alicia Michiko Kinoshita

Doctor of Philosophy in Civil Engineering

University of California, Los Angeles, 2012

Professor Terri S. Hogue, Chair

This work has investigated the policy of wildfires, modeling techniques for post-fire assessment, and the influence of controlling variables on post-fire recovery. Post-fire mitigation and management require reliable predictions of immediate hydrologic consequences and long-term recovery to pre-fire conditions. This research shows that models used by agencies are not adaptable to all geographical and climatological conditions. Results show inconsistencies between model predictions for peak discharge events across the sites and less confidence associated with larger return periods (25- and 50-year peak flow events). Remote sensing techniques improve spatial and temporal resolution of data streams for model parameters and post-fire recovery predictions. This research shows that recovery is dependent on many variables, including burn severity, slope aspect, and vegetation biomass. The lack of vegetation recovery across watersheds results in significant changes in annual and seasonal discharge throughout the study period. Understanding these key controlling variables will improve post-fire hydrological predictions. Previously established remote sensing algorithms can be applied and adapted to burned areas to improve hydrologic and recovery predictions. This work encourages new tools that can be incorporated into policies that minimize development at the WUI, improve homeowner preparation in fire-prone areas, and improve post-fire recovery predictions. This work improves post-fire modeling and predictions primarily with remote sensing applications to guide accurate, efficient, and cost-effective management decisions.

The dissertation of Alicia Michiko Kinoshita is approved.

Steven A. Margulis

Rui Wang

William W-G. Yeh

Terri S. Hogue, Committee Chair

University of California, Los Angeles

2012

DEDICATION PAGE

This dissertation is dedicated to my parents, Michael and Margaret Kinoshita, who provided love and support throughout my decade at UCLA, without them this work would not have been possible. Without them I would not be leading an exciting life of a hydrologist and fire chaser! This is also dedicated to my friends and family, who have made graduate school doable. Don't be modest, you know who you are. Thank you for your patience, love, and encouragement! Because of you, my graduate school journey is filled with adventure and memorable moments.

TABLE OF CONTENTS

ACKNOWLEDGEMENTS

I would like to thank my advisor, Dr. Terri Hogue, for her inspiration and guidance necessary to accomplish this work. I would also like to acknowledge my committee members, Dr. Steve Margulis, Dr. Rui Wang, and Dr. William Yeh for their time and commitment to my success as a hydrologist at UCLA.

I would like to acknowledge all of my coauthors Terri S. Hogue (all chapters), Rui Wang (Chapter 1), Dr. Jongyoun Kim (Chapter 5), Brandon Hale (Chapter 3), Carolyn Napper (Chapter 3 and 6), Jess Clark (Chapter 6), Kevin Cooper (Chapter 6), and Mark Stamer (Chapter 6) for their contributions.

Finally, I would like to thank my fire team and research group from the Civil Engineering Department at UCLA for their amazing field help and support throughout my work, especially Dr. Helen Jung, Karen Chu, Brandon Hale, Tristan Acob, Dr. Megan Burke, Chris Wessel, David Moering, Steve Skinner, Shu-wen (Sharon) Liu, Laura McNerney, Nathan Griffin, Bryant Reyes, and Sonya Lopez. I would also like to thank the Forest Service for their knowledge, guidance, stories, jokes, trail mix, and cool field cars throughout my interactions with them in and out of the field. Many thanks to Carolyn Napper, Marc Stamer, Kevin Cooper, Jess Clark, Chris Stewart, and Pete Wohlgemuth for opening up the exciting world of post-fire to me.

VITA OF ALICIA MICHIKO KINOSHITA

Education

Master of Science, Civil Engineering *University of California, Los Angeles*	Jun 2009
Bachelor of Science, Civil Engineering **Minor**, Classical Civilization *University of California, Los Angeles*	Jun 2007

Experience

Graduate Student Researcher –Civil Engineering *University of California, Los Angeles*	Jun 2007 - present
Teaching Fellow–Civil Engineering *University of California, Los Angeles*	Sp 2012
Teaching Associate –Civil Engineering *University of California, Los Angeles*	W 2011, SP 2011
Teaching Assistant –Civil Engineering *University of California, Los Angeles*	Sp 2010,W 2009,Sp 2008

Undergraduate Student Research Mentor – Civil Engineering
University of California, Los Angeles

- Undergraduate research projects in remote sensing of post-fire environments: Karen Chu (F 2011 to SP 2012), Carolyn Chou (W 2011), and Audrey Lee (Sp 2011) and post-fire hydrological modeling: Nathan Griffin (F 2011 and W 2011)
- Research Aides in post-fire field work and modeling: Brandon Hale, Master's Thesis in Progress (Su 2010 - present), Tristan Acob (Su 2011 to present), Laura McNerney (Sp 2011 to Sp 2012)

Undergraduate Research Aide – Civil Engineering *University of California, Los Angeles*	Nov 2006 - Jun 2007

Select Publications &Presentations

- Kinoshita, A.M., Hogue, T.S., Hale, B., and Napper, C., Post-fire hydrologic model assessment for peak discharge estimates for western United States watersheds. *In review.*	Jun 2012
- Stein, E.D., Brown, J.S., Hogue, T.S., Burke, M.P., and Kinoshita, A., 2012: Regional patterns of storm water contaminant loading following southern California wildfires. Environmental Toxicology and Chemistry. *In review.*	Mar 2012
- **Kinoshita, A.M. and Hogue, T.S**., Wildfire and Hydrologic Consequences. National Science Foundation Hazards Research Expo and Hazards Day on the Hill, Capitol Hill, Washington D.C.	Sep 2011
- Kinoshita, A.M. and Hogue, T., Investigating Controls on Post-Fire Hydrologic Recovery in Southern California Watersheds. *Catena*.	Jun 2011
- Antos, Mike, T.S. Hogue, T. Longcore, S.J. Lee, A. Kinoshita, C. Milanes, K. Morris, S. Pincetl, F. Shilling, N.L.C Steele, R. Vos, B. Washburn. Assessing Ecosystem Values of Watersheds in Southern California. Los Angeles and San Gabriel Rivers Watershed Council, Los Angeles, CA.	Feb 2011
- **Kinoshita, A.M.** and Hogue, T., 2010, Evaluating controls on hydrologic recovery in burned watersheds in the San Bernardino Mountains. Southern California Academy of Sciences (SCAS) Annual Meeting, California State University, Los Angeles, CA. *(Oral Presentation Award in Physical Sciences)*	May 2010

Extracurricular

American Geophysical Union Member	2009 - present
American Society of Civil Engineers – UCLA Chapter	2006 - present
Student Advisor – Transportation Design Project	2007 - 2008
Member - Seismic Design Project Team	2006 - 2007
Director – Transportation Design Project	2006 - 2007
Institute of Transportation Engineers	2006 - 2009
Founding President – UCLA Chapter	2006 - 2007

Chapter 1. Introduction

Changing climate and increasing size and frequency of wildfires threaten western United States watersheds (Westerling et al., 2006). According to CalFrap (2009a) more than half of the twenty largest fires in southern California occurred within the last decade. In the past, remote fires in the wildlands were not cause for concern, but development into fire-prone regions (i.e. rural areas, foothills, mountainsides) has altered natural fire regimes and increased damage and post-fire consequences to urban areas and downstream communities (Dombeck et al., 2004; Pausas et al., 2008). This contributes to increased suppression and mitigation expenditures (Busby and Albers, 2010). As fire incidents increase, preparation and management is imperative for maintaining healthy ecosystems and sustainable urban-fringe development (Dombeck et al., 2004). Burned land surfaces encourage flooding and debris flows (Debano, 2000; Ice et al., 2004), often resulting in altered water quality and damage to nearby development (Burke et al., 2011; Wohlgemuth et al., 2008).

There is a need for wildfire policies that can bridge gaps between fire science, management, and local communities. The effects of wildfire and post-fire hydrological consequences are well known to the scientific community; however, insurance programs and zoning policies do not seem to reflect these issues. Similarly, understanding the effects of post-fire hydrologic behavior and recovery time is critical for local and regional short- and long-term water resources management in regions which experience periodic and extensive burns. Agencies such as the U.S. Forest Service (USFS) are interested in reliable post-fire prediction in order to efficiently and cost-effectively minimize post-fire impacts (debris flows and flooding) on values at risk (Foltz et al., 2009).

Remote sensing has greatly improved techniques for acquiring and studying variables in ungaged and large spatial areas and has potential for post-fire application. Remote sensing provides convenient data acquisition at high spatial and temporal resolutions and makes estimating key hydrologic parameters that govern post-fire recovery possible. The development of predictive models to large regional areas affected by wildfire will ultimately improve planning for downstream communities and resource monitoring in semi-arid regions where water resources are limited and highly impacted by upstream burns.

1.1 Wildfires

Wildfires are increasing in intensity and size across the western U.S. (Westerling et al., 2006). Climate change, altered land use patterns, and fire suppression policies have contributed to the threat of catastrophic wildfires (Keeley et al., 2004; Pincetl, et al., 2008; Service, 2004). In southern California more than half of the twenty largest fires in California have occurred within the last decade (CalFrap, 2009a). Within the last decade, there have been several large wildfires in southern California near large cities (Figure 1-1). Table 1-1 includes characteristics of these fires. Many of these large and destructive fires are occurring at the wildland-urban fringe and raise concerns for fire management issues.

Table 1-1: Six southern California wildfire events, including name, date, county, acres burned, structures burned, deaths, cause, and rank within the last decade (CalFrap, 2009a)

Fire Name	Date	County	Acres Burned	Structures Burned	Death	Cause	Rank
Cedar	Oct 2003	San Diego	273,246	2,820	15	Human	1
Zaca	Jul 2007	Santa Barbara	240,207	1	0	Human	2
Witch	Oct 2003	San Diego	197,990	1,650	2	Power lines	4
Day	Sep 2006	Ventura	162,702	11	0	Human	9
Station	Aug 2009	Los Angeles	160,557	209	2	Human	10
Simi	Oct 2003	Ventura	106,668	13	0	Unknown	16

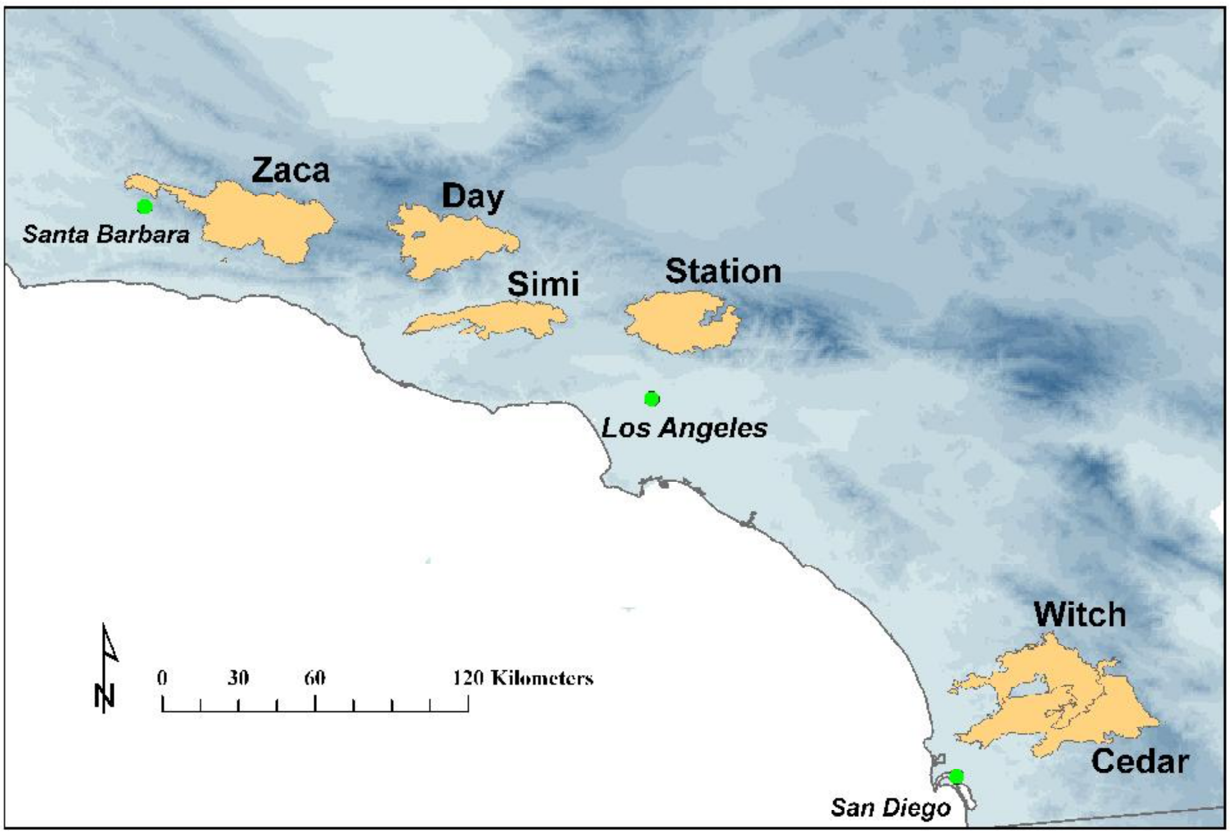

Figure 1-1: Six southern California wildfire perimeters within the last decade since 1932 (CalFrap 2009a and b)

Increasing variability in wildfire regimes is a concern as fire dramatically alters ecosystem characteristics and in situ processes. Vegetation loss and acute changes in soil properties significantly change land-atmosphere interactions and overall water balance within a burned system (Debano, 2000; Ice et al., 2004; Meixner and Wohlgemuth, 2003). Immediately post-fire, land surface alterations contribute to increased overland flow and related hazards for downstream communities. Loss of vegetation and soil transformation alters normal flow patterns, disrupts ecologic and hydrologic behavior, and water quality (surface and ground water) and sediment transport to urban fringe communities not only the first post-fire year (i.e. debris flows and flooding), but also years after fire (Burke et al., 2010, 2011; Debano, 2000; Cydzik and Hogue, 2009; Ice et al.. 2004; Jung et al., 2009; Kinoshita and Hogue, 2011; Martin and Moody, 2001; Pierson et al., 2008; Rulli and Rosso, 2007; Wohlgemuth et al., 2008). Post-fire consequences also include altered water quality (i.e. increased chemical and sediment loads) (Burke et al., 2011; Debano, 2000; Ice et al., 2004). Accurate prediction of post-fire hydrological behavior and assessing impacts on water supply and quality is critical for post-fire storm preparation and response, especially at the wildland-urban interface.

1.2 Wildfire management

1.2.1 Wildfire suppression

Wildfire suppression became a popular technique to limit the adverse impacts of wildfires to development at the urban-fringe. However, this policy has not been successful as the number of fires per year increased. Suppression has adverse impacts on forest fire patterns (North et al., 2009) and is not effective in chaparral environments (Keeley et al., 2004). In forests, suppression often leads to fuel build-up and competition between trees for resources, leading to type conversion. In chaparral environments climate and fuel type often result in unstoppable fires.

The shift from healthy forest structure to unhealthy structure results in catastrophic and stand-replacing wildfires (Miller and Woolfenden, 1999; USDA Forest Service, 2004) (Figure1-

2) Sierran old-growth or healthy forest structures consist of spacious stands, where natural fire disturbances are slow burning and of low intensity, clearing small to medium vegetation and allowing the dominant and tolerant trees to age (USDA Forest Service, 2004). Unhealthy forest structures consist of dense and unevenly aged vegetation, creating a "fuel ladder" (small and medium vegetation) that provides fuel for wildfires to burn at high intensity and allow easy spreading from the ground (understory) to treetops, resulting in large "crown fires" (Figure 1-2)(USDA Forest Service, 2004). Fire suppression and recent climate variability, primarily increasing temperatures; have contributed to unhealthy forest structures. Additionally, logging and beetle infestations have led to large accumulations of dead timber (standing and downed). Unhealthy stand structures not only threaten forests with catastrophic wildfires, but also wildlife and local communities. Restoring a natural fire-regime and old-growth forest structure should minimize catastrophic wildfire events (Abella et al., 2007; North et al., 2009).

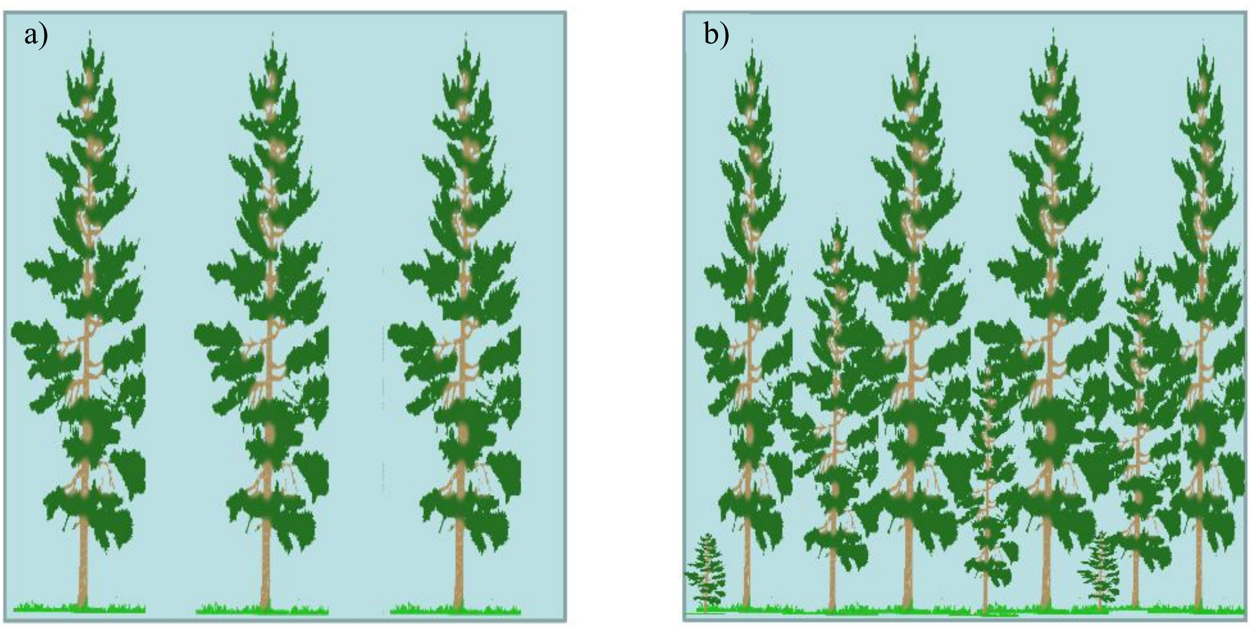

Figure 1-2: Healthy forest (a) and unhealthy forest structures (b) in the Sierra

In southern California's chaparral systems, fire suppression is less predictable and promotes an unhealthy and unnatural over-accumulation of vegetation, changing the natural fire regime (Syphard et al., 2007). This accumulation of vegetation biomass or high fuel loads contributes to catastrophic and costly fires, especially within recent years (Baker, 1993; Beeson et al., 2001; Dwire and Kauffman, 2003; Fairbrother and Turnley, 2005; Kumagai et al., 2003). Keeley et al. (2004) note that wildfires combined with southern Californian fire weather are only minimally controlled by vegetation age (stand age) or spatial patterns of fuels, evidenced by the 2003 and 2007 fire storms. Under moderate winds, fuel breaks are an effective tool against wildfire, but fail when winds are capable of pushing the fire through barriers or spreading embers (1-2 km from a source). Despite efforts to prevent and fight wildfires, the average frequency of wildfires consistently appears to be 30-40 years (Keeley et al., 2004).

1.2.2 Hydrologic post-fire management

Increased post-fire runoff and sediment response threaten lives, natural resources, and property and the ability to quickly and accurately predict hydrologic behavior is critical for deciding values most at risk and guiding management decisions and treatments. The primary responsibility for mitigation focuses on human lives, values at risk, and ecosystems (not private property). Uncertainties in storm intensity, duration, and location affect ecosystem and hydrologic response; however the first storm season post-fire poses the largest threat to downstream communities. In southern California the storm season (November through February) quickly follows the fire season (July through October). Rapid mobilization of resources to prepare for post-fire response is necessary. However, the public often misinterprets a passing storm with no damage as an indication that post-fire threats are gone or minimal. It was observed in the 2009 Station Fire (largest wildfire in Los Angeles County history), that with each successive storm the public participation in preparation and evacuations decreased (Cannon, 2010). This behavior demonstrates the lack of communication between the scientific and the local communities. Public perceptions of post-fire events should be made transparent before a fire occurrence. Warning the public of post-fire hydrologic consequences during and immediately after a fire does not benefit the community and steps to improve community preparedness are necessary. For managers, all safety and management decisions such as opening evacuations, closed recreation areas, roads, or removing k-rails depend on accurate post-fire predictions and understanding of increased threats. The length of time that communities remain at risk has important economic and resource implications.

Understanding the impact of wildfire on long-term water budgets, water resources, and water quality is critical, especially for downstream communities (Meixner and Wohlgemuth, 2003; Barnett et al., 2004). The recovery of areas affected by wildfire varies based on many parameters and has the potential to remain susceptible to adverse post-fire consequences for prolonged periods of time. Accurate prediction of post-fire hazards can better guide cost effective (allocation of agency funds and resources) and efficient management policies and solutions. Integrating remote sensing data into relevant modeling systems can facilitate improved post-fire hydrologic predictions. Changes from pre- to post-fire conditions in characteristics are readily observable using remote sensing products, including albedo, vegetation biomass, and land surface temperature. These and other parameters can be applied within various algorithms to better understand and predict system recovery. Collaborative work with the U.S. Forest Service reveals a need to initially validate vegetation biomass indicators, reducing uncertainty in predictions centered on use of these data.

1.3 Research goals and research questions

The overarching goal of this research is to understand post-fire management needs and concerns of society, agencies, and ecosystems and to improve post-fire modeling and predictions primarily with remote sensing applications to guide accurate, efficient, and cost-effective management decisions. This research evaluates current wildfire management issues and investigates improvements for policies. This research also evaluates current hydrological models used in USFS post-fire assessments in order to provide guidance on model use across diverse hydro-climatic regimes. Finally, this research strives to understand post-fire hydrologic recovery and prediction utilizing remote sensing and in situ geophysical data. This work is guided by the following questions:

- *What are current hydrological post-fire management protocols in the western U.S. and how are communities affected by both pre- and post-fire management and policy decisions?*
- *What are commonly used models in post-fire assessments and how do these models perform across diverse hydroclimatic regimes? What models are optimal for post-fire hydrologic predictions?*
- *Does the integration of remote sensing products improve post-fire modeling and management, especially in semi-arid regions? Can current remote sensing algorithms be adapted for post-fire systems? What key variables can be used to assess post-fire hydrologic behavior?*
- *How do we utilize answers to the above questions to inform future modeling, prediction, and post-fire response efforts, especially for responsible agencies such as the USFS or the National Weather Service (NWS)?*

1.4 Research approach and organization of dissertation

To understand the consequences that wildfire poses to communities and ecosystems the following framework is proposed to address the aforementioned goals:

- Management of post-fire consequences at the WUI. Many agencies as well as the public are unaware of the risk that post-fire consequences pose. Raising awareness to these issues is critical at the WUI for safety and remedial decisions.
- Current pre- and post-fire modeling practices using various regional wildfires in collaboration with the USFS to assess the performance of selected hydrological models. Preliminary results show inconsistencies in model parameter selections and results (Kinoshita et al., 2012).
- Kinoshita and Hogue (2011) investigated short- and long-term post-fire hydrologic response utilizing Moderate Resolution Imaging Spectroradiometer (MODIS) enhanced vegetation index (EVI) and ground-based hydrologic variables. Results offer insight on factors that influence hydrologic recovery in post-fire chaparral systems such as precipitation patterns, level of burn severity, watershed slope aspects, and vegetation recovery.
- Expansion of methods to include more characteristics and indicators of ecosystem resilience, such as evapotranspiration and soil moisture, through the optimization of remote sensing algorithms for post-fire systems.

The organization of this dissertation includes background on wildfires, policy and management practices, and the importance of hydrological modeling and prediction; discussion of preliminary work on assessment of hydrological models used by the USFS and investigation of controls on recovery in post-fire watersheds; development of a post-fire ET algorithm based only on remote sensing variables, discussion of contributions and continuation of work on the investigation of ecosystem resilience and post-fire recovery.

1.5 References

Abella, S.R., Convington, W.W., Fule, P.Z., Lentile, L.B., and Sanchez Meador, A.J., 2007. Past, present, and future old growth in frequent-fire Conifer Forests of the Western United States. Faculty Publications (Sepa), paper 56.

Baker, W.L., 1993. Spatially heterogeneous multi-scale response of landscapes to fire suppression. Oikos 66:66-71.

Barnett, T., Malone, R., Pennell, W., Stammer, D., Semtner, B., and Washington, W., 2004. The effects of climate change on water resources in the west: Introduction and overview. Climatic Change 62: 1-11.

Beeson, P.C., Martens, S.N., Breshears, D.D., 2001. Simulating overland flow following wildfire: mapping vulnerability to landscape disturbance. Hydrological Processes, 15:2917-2930.

Burke, M.P., Hogue, T.S., Ferreira, M., Mendez, C.B., Navarro, B., Lopez, S., and Jay, J.A., 2010. The Effect of Wildfire on Soil Mercury Concentrations in Southern California Watersheds. Water, Soil and Air Pollution 212:369-385.

Burke, M.P., Hogue, T.S., Barco, J., Wessel, C., Kinoshita, A.M., and Stein, E., 2011.Dynamics of Pre- and Post-fire Pollutant Loads in an Urban Fringe Watershed. Chemosphere (In review).

Busby, G. and Albers, H.J., 2010. Wildfire Risk Management on a Landscape with Public and Private Ownership: Who Pays for Protection? Environmental Management 45: 296-310.

California Department of Forestry and Fire Protection (CalFrap), 2009a. 20 Largest California Wildland Fires (By Acreage Burned). http://www.fire.ca.gov/about/downloads/20LACRES.pdf.

CalFrap, 2009b. Fire Perimeters (fire09_1).http://frap.cdf.ca.gov/data/frapgisdata/select.asp.

Cannon, S., 2010. Lessons learned from an emergency release of a post-fire debris-flow hazard assessment for the 2009 Station fire, San Gabriel Mountains, Southern California. American Geophysical Union Conference, San Francisco, December 13-17, 2010.

Cydzik, K. and Hogue, T.S., 2009. Modeling Post-Fire Response and Recovery Using the Hydrologic Engineering Center Hydrologic Modeling System (HEC-HMS). Journal of the American Water Resources Association 45(3):702-714.

Debano, L.F., 2000. The role of fire and soil heating on water repellency in wildland environments: a review. Journal of Hydrology 231-232: 195-206.

Dombeck, M.P., Williams, J.E., and Wood, C.A., 2004. Wildfire Policy and Public Lands: Integrating Scientific Understanding with Social Concerns across Landscapes. Conservation Biology 18(4): 883-889.

Dwire, K.A. and Kauffman, 2003.Fire and riparian ecosystems in landscapes of the western USA. Forest Ecology and Management 178:61-74.

Fairbrother, A. and Turnley, J.G., 2005. Predicting risks of uncharacteristic wildfires: Application of the risk assessment process. Forest Ecology and Management 211:28-35.

Foltz, R.B., Robichaud, P.R., and Rhee, H., 2009. A Synthesis of Post-Fire Road Treatments for BAER Teams: Methods, Treatment Effectiveness, and Decision making Tools for Rehabilitation. Gen. Tech. Rep. RMRS-GTR-228 Fort Collins, CO: U.S. Department of Agriculture, Forest Service, Rocky Mountain Research Station. 152 p.

Ice, G.G., Neary, D.G., and Adams, P.W., 2004. Effects of Wildfire on Soils and Watershed Processes. Journal of Forestry 16-20.

Jung, H., Hogue, T.S., Rademacher, L., and Meixner, T., 2009. Impact of Wildfire on Source Water Contributions in Devil Creek, CA: Evidence from End-member Mixing Analysis. Hydrological Processes 23: 183 – 200.

Keeley, J.E., Fotheringham, C.J., and Moritz, M.A., 2004. Lessons from the October 2003 Wildfires in southern California. Journal of Forestry 102(7):26-31.

Kinoshita, A.M. and Hogue, T.S., 2011. Investigating Controls on Post-Fire Hydrologic Recovery in southern California Watersheds. Catena 87(2): 240-252.

Kinoshita, A.M., Hogue, T.S., Hale, B., and Napper, C., 2012. Post-fire hydrologic model assessment for peak discharge estimates for western United States watersheds. In Review.

Kumagai, Y., Carroll, M.S., and Cohen, P., 2004. Coping with Interface Wildfire as a Human Event: Lessons from the Disaster/Hazards Literature. Journal of Forestry 102(6): 28-32.

Martin, D.A. and Moody, J.A., 2001. Comparison of soil infiltration rates in burned and unburned mountainous watersheds. Hydrological Processes 15:2893-2903.

Meixner T., Wohlgemuth, P. 2003. Climate variability, fire, vegetation recovery, and watershed hydrology. In Proceedings of First Inter-Agency Conference on Research in the Watersheds, Benson, Arizona 651-656.

Miller, C.I. and Woolfenden, W.B., 1999. Sierra Nevada Forests: Where Did They Come From? Where Are They Going? What Does It Mean? Trans. 64th No. Am. Wildl. And Nature. Resour. Conf.

Moody, J.A., Martin, D.A., Haire, S.L., and Kinner, D.A., 2007. Linking runoff response to burn severity after a wildfire. Hydrological Processes, 22, pp. 2063–2074.

North, M., Stine, P., O'Hara, K., Zielinski, W., and Stephens, S., 2009.An ecosystem management strategy for Sierran mixed-conifer forests. Gen Tech. Rep. PSW-GTR-220.

Albany, CA: U.S. Department of Agriculture, Forest Service, Pacific Southwest Research Station.

Pausas, J.G., Llovet, J., Rodrigo, A., and Vallejo, R., 2008. Are wildfires a disaster in the Mediterranean basin? – A Review. International journal of Wildland Fire 17: 713-723.

Pierson, F.B., Robichaud, P.R., Moffet, C.A., Spaeth, K.E., Hardegree, S.P., Clark, P.E., Williams, C.J., 2008. Fire effects on rangeland hydrology and erosion in a steep sagebrush-dominated landscape. Hydrological Processes 22: 2916-2929.

Pincetl, S., Rundel, P.W., Blasio, J.C, Silver, D., Scott, T., Keeley, J.E., and Halsey, R., 2008. It's the Land Use, Not the Fuels: Fires and Land Development in southern California. Real Estate Review 37: 25-42.

Rulli, M.C. and Rosso, R., 2007. Hydrologic response of upland catchments to wildfires. Advances in Water Resources 30:2072-2086.

Service, R., 2004. As the West Goes Dry. Science 20(303), no. 5661, pp1124-1127.

Syphard, A.D., Radeloff, V.C, Keeley, J.E., Hawbaker, T.J., Clayton, M.K., Steward, S.I., and Hammer, R.B., 2007. Human influence on California fire regime. Ecological Applications 17(5):1388-1402.

USDA Forest Service, 2004. Forests with a Future.

Westerling, A.L., Hidalgo, H.G., Cayan, D.R., and Swetnam, T.W., 2006. Warming and Earlier Spring Increase Western U.S. Forest Wildfire Activity. Science 313: 940-943.

Wohlgemuth, P.M., Hubbert, K.R., Beyers, J.L., and Narog, M.G., 2008.Post-Fire Watershed Response at the Wildland-Urban Interface, Southern California. The Third Interagency Conference on Research in the Watersheds, 8-11 September, 2008, Estes Park, CO.

Chapter 2. Management Policies at the Wildland-Urban Interface

2.1 Wildland-urban interface

In the western states, the population is growing faster than the national average (Randeloff et al., 2005). As the population grows, development pushes the urban boundary further into wildlands, increasing the interaction at the wildland-urban interface (WUI). The WUI is characterized as the transitional area between undeveloped and human developed land. Persistent development in wildfire prone regions such as rural areas, foothills, and mountainsides contribute to more severe threats at the WUI (Dombeck et al., 2004; Pausas et al., 2008). According to Randeloff et al., 2005, 9% of the United States is covered by WUI and California has the largest number of homes at the WUI. In California, over five million homes are included in the WUI and this number continues to rise as people seek more natural resources (Randeloff et al., 2005; Stephens et al., 2009). As the number of wildfire incidents increased, an increase in contribution to fire suppression and mitigation expenditures increased (Busby and Albers, 2010). Since 2001, agencies have dramatically increased fire management allocations and expenses to protect properties at the WUI (Dombeck et al., 2004). Land use patterns such as single-family homes or large communities that are allowed to expand into naturally fire-prone areas are supported by inadequate fiscal and fire management policies (Pincetl et al., 2008).

Since the late 1800s, wildfires at the WUI in the western United States gave rise to federal fire suppression policies. To protect development, fire suppression aims to extinguish a wildfire immediately, this responsive technique does not solve the problem. Suppression promotes an unhealthy and unnatural over accumulation of vegetation, changing the natural fire regime (Syphard et al., 2007). This accumulation of vegetation biomass or high fuel loads contributes to the outbreak of catastrophic and costly fires within the recent years (Baker, 1993;

Beeson et al., 2001; Dwire and Kauffman, 2003; Fairbrother and Turnley, 2005; Kumagai et al., 2004). After World War II, policies aimed to completely suppress fires seemed attainable with firefighting resources and technology dramatically increasing (firefighters, construction equipment, aerial tankers, etc.) (Dombeck et al., 2004).

Despite the enormous fire suppression efforts, wildfires still prevailed evidencing the unpredictability of wildfire regimes and the ineffectiveness of reliable suppression practices (Dombeck et al., 2004). Even with advancing fire-fighting technology, the total amount of landscape burned has increased – with more than 6 million acres burned in the mid- to late 1900s and early 2000 (Dombeck et al., 2004). Under moderate winds, fuel breaks are an effective tool against wildfire, but fail when winds are capable of pushing the fire through barriers or spreading embers (1-2 km from a source) (Keeley et al., 2004). Despite efforts to prevent and fight wildfires, the average frequency of natural wildfires appears to be 30-40 years (Keeley et al., 2004). Figure 1-1 shows the major fire events in southern California relative to major cities within the last decade and Table 1-1 provides information for these fires (CalFrap, 2009b). Table 1-1 demonstrates that these large fires are human induced as a result of increased wildland-urban conflict. Consequently, increased damage and costs accompany increased wildfire at the WUI.

2.2 Motivation

Many Americans desire to live in undeveloped and remote areas and since 1982; over 8.6 million new homes in the Western United States are built within 30 miles of a national forest (McKinley and Johnson, 2007). Destructive wildfires such as the 2009 Station Fire and more recent fire storms in Texas and Arizona have made wildfire and post-fire management and policies a primary concern, especially at the WUI (Randeloff et al., 2005). For example, the 2009

Station Fire in the Angeles National Forest (Los Angeles County, California) is the largest wildfire in Los Angeles County history and the tenth largest fire in California since the early 1930s (CalFrap, 2009b). The Station Fire burned 161,189 acres, damaged over 80 homes, and cost over $95 million to suppress, impacting four major watersheds – the Los Angeles River, San Gabriel River, Mojave River, and Santa Clara River (USDA Forest Service, 2009). The watersheds experienced damage to vegetation, soil, wildlife, and water resources (USDA Forest Service, 2009 and communities were threatened by winter storms that would inevitably cause adverse hydrologic impacts.

Many factors played a role in the tremendous size of this fire, such as prior drought conditions, immense fuel loads (area not recently burned), and steep and remote terrain. Although the Santa Ana winds were not present, the Station Fire was not quickly contained as steep and inaccessible terrain made immediate fire suppression impossible, allowing the fire to easily spread. After the containment of the wildfire, the threat to downstream communities was not over as winter storms threatened development with debris flows and flooding. Many homes in the foothills were damaged by erosion and hundreds of people were evacuated during the following storms. After the fire, most of the burned area was closed to the public to allow the ecosystem to recover and protect the public from post-fire hazards such as debris flows, flash flooding, or falling trees (USDA Forest Service, 2009).

The Arizona Wallow Fire in 2011 was the largest in the state's history. It burned over 538,048 acres with estimated damage of $109 million. The fire was human ignition, but is still under investigation. The Bastrop Fire in the summer of 2011 was the largest in Texas' state history. The cause of the fire was electrical. This fire is expected to cause over $325 million in insured losses. Both the Arizona and Texas fire are only one out of the many that burned throughout each state. Both states have been added to National Oceanic and Atmospheric Administration's (NOAA) $1 billion weather disaster list. The recent large fires mentioned above are examples of costly wildfires that do not yet include post-fire damages, which may be brought on by monsoon and winter storms.

The relationship between wildfire and flooding is well studied in the scientific community, but is not incorporated at the policy level. This study aims to provide analytical tools to understand post-fire flooding and improve local and regional policies. This study is part of a larger study that will suggest dynamic insurance policy adjustments based on analytical tools to alter community behavior and reduce exposure to post-fire flooding threats at the wildland-urban interface. The post-fire flooding rate will be a function of pre- and post-fire flood rate that is dependent on the wildfire properties. Specifically, we will investigate the geography of fire and post-fire flooding in the southwest, California and Arizona, and policy and market tools to reduce risks to communities.

2.3 Policies and management

The primary responsibility for implemented mitigation by local management agencies focuses on human lives, values at risk, and ecosystems (not private property). These mitigation measurements may include k-rails, sandbags, and public closures of roads and spaces. The cost, resources invested, and duration of these measures are dependent on post-fire predictions of value-at-risk and recovery time. Insurance plays an important role in safeguarding private development at the WUI. Insurance is a method to share the risk of loss, making coping with disasters manageable. However, current policies are ineffective at protecting property and discouraging further development at the WUI. Large insurance companies in the Nevada County in California are becoming more selective and more costly for those that choose to live in high-risk areas (Brown, 2011), which is progression towards encouraging homeowners to take more responsibility for their location. In both California and Arizona, the fire season is immediately followed by rain events – winter storm season and monsoons. The recent 2011 Arizona wildfires brought a rush to insure homes against post-fire floods. Basic home insurance does not cover floods and homeowners that do not possess flood insurance are encouraged to purchase flood insurance. Homeowners in danger of post-fire flooding should be aware that property does not need to be located in a floodplain for damage to occur (post-fire flooding).

The Federal Emergency Management Agency (FEMA) has offered the National Flood Insurance Program (NFIP) since 1968 and provides homeowners in disaster areas with the option to purchase federally sponsored flood insurance. Less than half of the floods in the U.S. result in federal disaster declaration, but the NFIP are available even if a disaster is not declared. The NFIP offers flood insurance to any property owners and renters in communities (approximately 21,000 communities nationwide) that participate in the program. NFIP policies are sold through private insurance agents throughout the country (www.floodsmart.gov). The NFIP program has a 30-day waiting period, which generally gives Californians adequate time to become policyholders before the winter storms. However, Arizona homeowners often have less time to purchase their policies within the 30-day window before the summer monsoons (2011 fires). Homeowners unaware of post-fire risks are often caught unprepared. This study presents parameters such as fire frequency, severity, and vulnerability, which can be implemented in policy development and adapted to decrease adverse post-fire consequences at the WUI.

2.4 Arroyo Seco case study and analytical tools

The entire Arroyo Seco watershed stretches from the San Gabriel Mountains to the Los Angeles River in downtown Los Angeles (Figure 2-1). The land surfaces have been aggregated into main land surface categories for simplicity and the transportation layer gives an estimate of the amount of development present. The Upper Arroyo Seco is a smaller urban-fringe watershed that contributes water to cities such as Pasadena, Sierra Madre, Arcadia, Altadena, and La Canada-Flintridge (Figure 2-2).The Upper Arroyo Seco (here on referred to as Arroyo Seco) will be used as a case study to investigate analytical tools that can be used to identify areas vulnerable to wildfire and post-fire flooding. It is 42 km^2 and the dominant vegetation includes chaparral, sage, shrubs, and mixed conifer at the higher elevations (Figure 2-2).

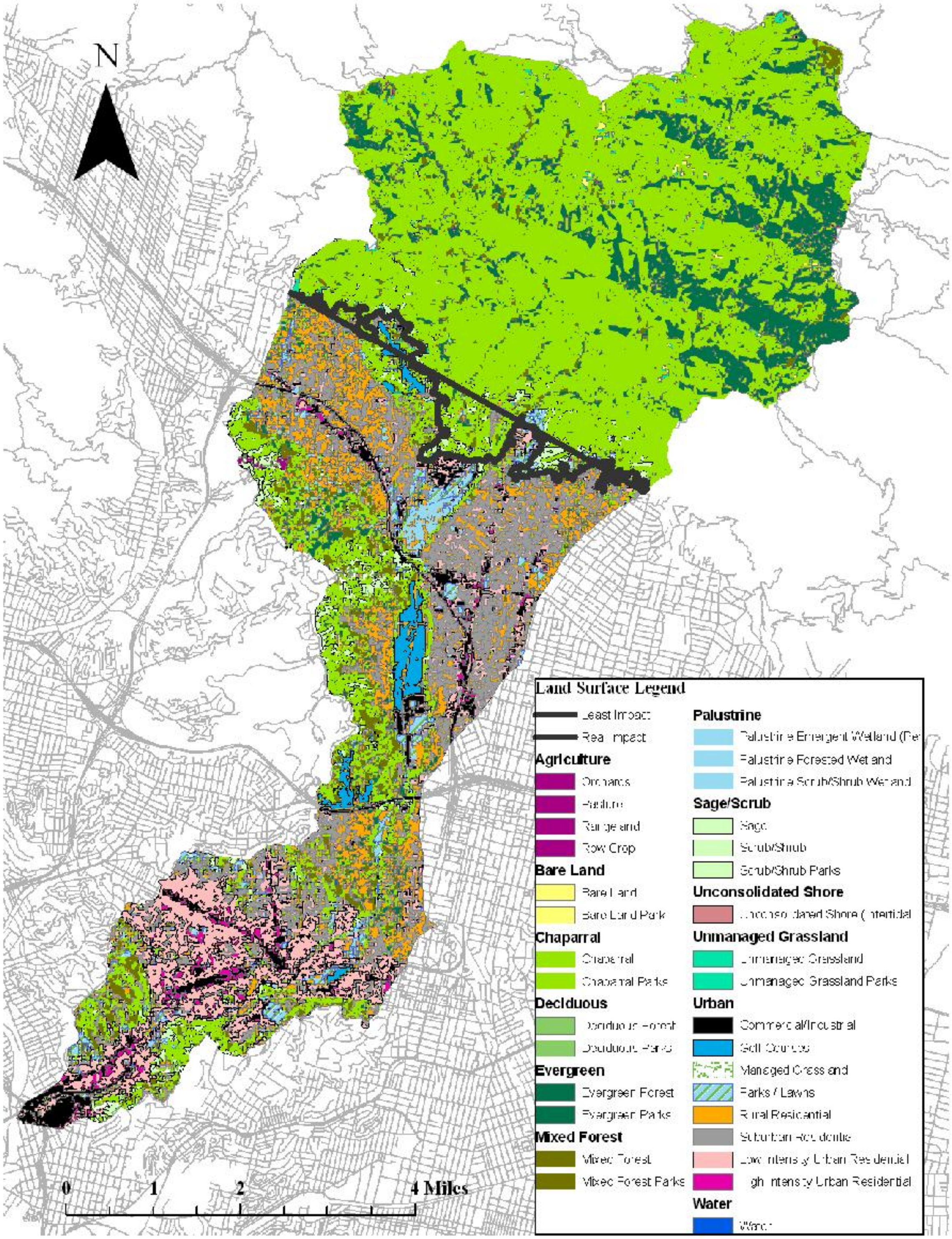

Figure 2-1: Land surface for the Arroyo Seco watershed, retrieved from the Landsat Thematic Mapper layer (30m; NOAA C-CAP, 2000) with a Los Angeles County transportation layer in the background. The Upper Arroyo Seco is predominantly chaparral, while the mid- to lower Arroyo Seco becomes increasingly urbanized to its end at the Los Angeles River. The fire vulnerability lines (least impact and real impact) at the wildland/urban interface are shown.

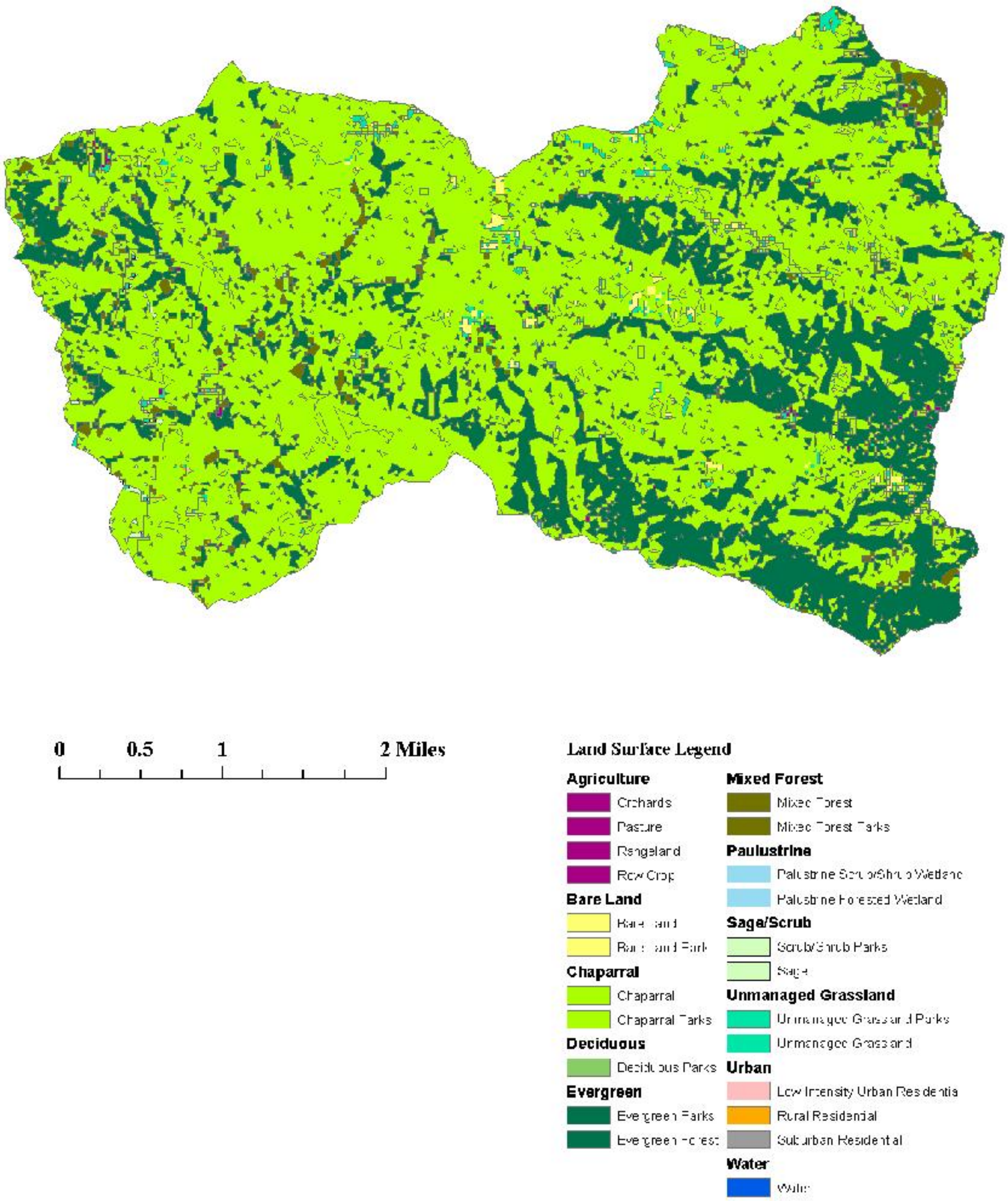

Figure 2-2: NOAA C-CAP 2001 landcover over the Arroyo Seco, California

Fire frequency

Fire frequency can be used to estimate the historical occurrence in fire regimes within affected watersheds. Fire frequency is an estimation of the size of the area burned within the watershed and its corresponding date (year of the occurrence) of the wildfire event. Estimation of fire frequency provides insight into the health of an ecosystem (relative to natural wildfire regime) and provides guidance for wildfire and post-fire consequence preparedness.

Fire data such as acreage burned, derived from the fire perimeter data (boundaries) obtained from the historical fire data set provided by the California Department of Forestry and Fire Protection (CalFrap, 2009a) and Rocky Mountain Geographic Science Center (RMGSC, 2010) are used to estimate fire frequency in the Los Angeles County and Arroyo Seco (Figure 2-3). Prior to the Station Fire in 2009 (in which Arroyo Seco was 100% burned), large fires in the Arroyo Seco included 57% burned in 1896 and the earliest burn recorded in 1959 (83%). The red line represents the total area of the Arroyo Seco, and each point represents a major fire event for the history of the Upper Arroyo Seco. Keeley et al. (2004) note that fires are a regular occurrence in southern California chaparral systems and generally have a natural frequency rate of 30-40 years, despite suppression policies. In the Upper Arroyo Seco, smaller fires appear to occur every 5-10 years, while the three observed large fires are about 50-60 years apart (Figure 2-3), slightly longer than the 30-40 year cycle noted by Keeley et al. (2004) and possibly a result of fire suppression. Information such as fire frequency can provide planners with a better understanding of the natural fire cycle and can be incorporated in future management plans.

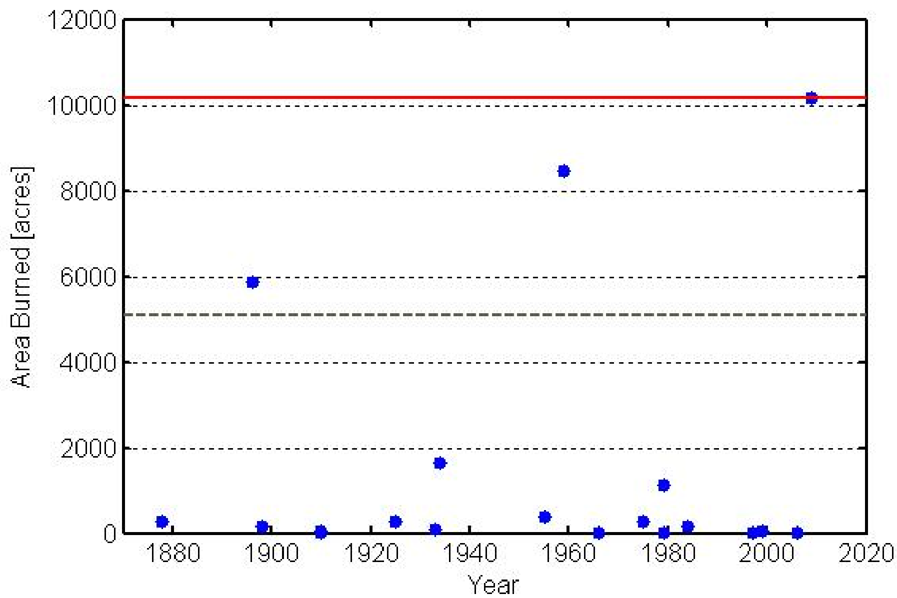

Figure 2-3: Fire frequency for a small watershed (Upper Arroyo Seco) in the Los Angeles County, near Pasadena. This figure shows the acres of the Upper Arroyo that burned in each fire. The red horizontal line (about 10,200 acres) represents the area of Upper Arroyo Seco.

Fire vulnerability

Fire vulnerability is the measure and assessment of the risk wildfire poses to human populations at the WUI. Fire vulnerability can be used as an indicator of the interaction between the urban and wildland interface. Ideally, minimal deviation from a straight linear distance across the WUI would indicate the lowest risk to human life and property. Minimal interaction simulates natural disturbance processes and benefits both humans and ecosystems. The fire vulnerability indicator is the ratio of the actual length of the urban-wildland interface to the linear length across the urban-wildland interface (theoretical best-case scenario). The relative difference or ratio between the two distances serves as an indicator that quantifies the risk to human life and property on the fringe of the urban development.

Fire vulnerability also establishes the threat of fire ignition (potential for human interaction).Keeley et al. (2004) show that 95% of all urban-fringe fires are started by people.

Extensive urban development has resulted in an urban fringe with increased risk to wildfire compared to borders that have minimal urban-wildland interaction. The Arroyo Seco watershed and fire vulnerability indicator (Figure 2-1) at the interface is a linear edge (direct line across the WUI) of 4.6 miles and the developed or real edge for Arroyo Seco is approximately 15.50 miles. The fire vulnerability ratio at the WUI is 3.34, which represents three times the vulnerability risk associated with urban development. More interaction at the urban interface results in increased potential for fire ignition and post-fire risks such as floods, debris flows, or water quality issues.

Burn Severity

Fire severity or burn severity is used to characterize the degree to which an ecosystem is altered (quantifies the amount of organic matter lost above ground) by fire and is used to evaluate potential risks to downstream populations and guide management and treatment decisions. Fire severity is strongly influenced by pre-fire vegetation, landscape, climate regime, and historical fire practices (suppression, defensible space, building into fire perimeters, etc.) (Baker, 1993; Keeley et al., 2005; Pausas et al., 2008). Higher burn severity results in more vegetation damage, directly influencing soil structure and integrity, and increasing flood and debris flow potential (Martin and Moody, 2001; Rulli and Rosso, 2007; Pausas et al., 2008; Cydzik and Hogue, 2009; and Jung et al., 2009). The burn severity acquired from the US Forest Service Remote Sensing Center for the Station Fire and Arroyo Sec show the spatial distribution of the burn severity, which can aid planners by identifying which areas are more vulnerable to post-fire debris and flooding (Figure 2-4).

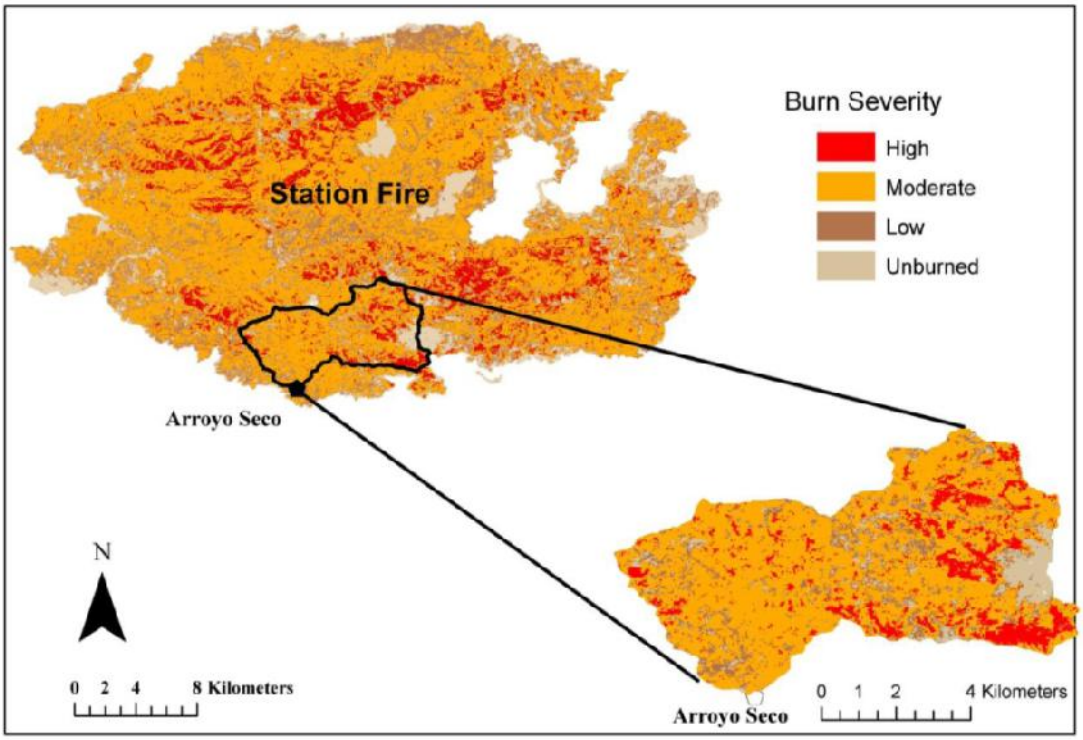

Figure 2-4: The burn severity for the Station Fire and the Arroyo Seco (US Forest Service Remote Sensing Center, 2011)

2.5 Summary of research needs

This preliminary study investigates the relationship between variables indicative of wildfire behaviors and post-fire consequences. Fire studies show that post-fire flooding is influenced by many parameters (i.e. climate, topography, available fuel, etc.) and we advocate that these should be incorporated into current policies. This study requires further understanding of NFIP rates and qualifications necessary for communities to be included in areas deemed floodplain and disaster zones. Specifically, we will continue our research to understand how the NFIP bases its rates and if rate adjustments based on fire hazards and parameters (presented in this study) exist. We will continue to examine home fire insurances, local government, and land use policy cases in California and Arizona and the incorporation of new tools to stimulate policies that minimize development at the WUI, improve homeowner preparation in fire-prone areas, and improve post-fire recovery predictions.

2.6 References

Baker, W.L., 1993. Spatially heterogeneous multi-scale response of landscapes to fire suppression. Oikos 66:66-71.

Brown, L., 2011. Insuring homes in wooded areas increasingly difficult. Special to the Union.http://www.theunion.com/apps/pbcs.dll/article?AID=/20110001/BREAKINGNEWS/111009998/1053&parentprofile=1053&template=printart. Accessed: October 2011.

Busby, G. and Albers, H.J., 2010. Wildfire Risk Management on a Landscape with Public and Private Ownership: Who Pays for Protection? Environmental Management 45: 296-310.

CalFrap (California Department of Forestry and Fire Protection), 2009a.Fire Perimeters (fire09_1). CalFrap: http://frap.cdf.ca.gov/data/frapgisdata/select.asp.

CalFrap, 2009b. "20 Largest California Wildland Fires (By Acreage Burned)." http://www.fire.ca.gov/communications/downloads/fact_sheets/20LACRES.pdf.

Cydzik, K. and Hogue, T.S., 2009. Modeling Post-Fire Response and Recovery using the Hydrologic Engineering Center Hydrologic Modeling System (HEC-HMS). Journal of the American Water Resources Association 45(3):702-714.

Dombeck, M.P., Williams, J.E., and Wood, C.A., 2004. Wildfire Policy and Public Lands: Integrating Scientific Understanding with Social Concerns across Landscapes. *Conservation Biology* 18(4): 883-889.

Dwire, K.A. and Kauffman, 2003.Fire and riparian ecosystems in landscapes of the western USA. Forest Ecology and Management 178:61-74.

Fairbrother, A. and Turnley, J.G., 2005. Predicting risks of uncharacteristic wildfires: Application of the risk assessment process. Forest Ecology and Management 211:28-35.

Keeley, J.E., Fotheringham, C.J., and Moritz, M.A., 2004. Lessons from the October 2003

Wildfires in southern California. Journal of Forestry 102(7):26-31.

Jung, H., Hogue, T.S., Rademacher, L., and Meixner, T., 2009. Impact of Wildfire on Source Water Contributions in Devil Creek, CA: Evidence from End-member Mixing Analysis. Hydrological Processes 23: 183 – 200.

Keeley, J.E., Fotheringham, C.J., and Baer-Keeley M., 2005. Determinants of Postfire Recovery and Succession in Mediterranean-Climate Shrublands of California. Ecological Applications 15(5): 1515-1534.

Kumagai, Y., Carroll, M.S., and Cohen, P., 2004. Coping with Interface Wildfire as a Human Event: Lessons from the Disaster/Hazards Literature. Journal of Forestry 102(6): 28-32.

Martin, D.A. and Moody, J.A., 2001. Comparison of soil infiltration rates in burned and unburned mountainous watersheds. Hydrological Processes 15:2893-2903.

Pausas, J.G., Llovet, J., Rodrigo, A., and Vallejo, R., 2008. Are wildfires a disaster in the Mediterranean basin? – A Review. International journal of Wildland Fire 17: 713-723.

Pincetl, S., Rundel, P.W., Blasio, J.C, Silver, D., Scott, T., Keeley, J.E., and Halsey, R., 2008. It's the Land Use, Not the Fuels: Fires and Land Development in southern California. *Real* Estate Review 37: 25-42.

Randeloff, V.C., Hammer, R.B., Stewart, S.I., Fried, J.S., Hocomb, S.S., and McKeefry, J.F., 2005. The wildland-urban interface in the United States. Ecological Applications 15(3): 799-805.

Rulli, M.C. and Rosso, R., 2007. Hydrologic response of upland catchments to wildfires. Advances in Water Resources 30:2072-2086.

Stephens, S.L., Adams, M.A., Handmer, J., Kearns, F.R., Leicester, B., Leonard, J., and Moritz, M.A., 2009. Urban-wildland fires: how California and other regions of the U.S. can learn from Australia. Environmental Research Letters 4: 1-5.

Syphard, A.D., Radeloff, V.C, Keeley, J.E., Hawbaker, T.J., Clayton, M.K., Steward, S.I., ad Hammer, R.B., 2007.Human influence on California fire regime. Ecological Applications 17(5):1388-1402.

USDA Forest Service, 2009. US Forest Service Fact Sheet: Station Fire Restoration.

Chapter 3. Post-Fire Hydrologic Model Assessment

3.1 Motivation

Wildfires alter land surfaces, land-atmosphere interactions, and hydrologic response (i.e. post-fire runoff and sediment response) (Debano, 2000; Moody and Martin, 2001; Ice et al., 2004; Cydzik and Hogue, 2009; Pierson et al., 2008; Jung et al., 2009; Burke et al., 2010). Wildfires are also occurring more frequently at the wildland-urban interface and impose threats on development (Randeloff et al., 2005; Cannon and DeGraff, 2009). Climate change and increasing wildfire frequency add to post-fire hydrologic variability (Westerling et al., 2006; Trouet et al., 2008; Cannon and DeGraff, 2009). The ability to accurately model and predict post-fire consequences is vital for human safety, ecosystem impacts, as well as effective and efficient management of state and regional resources.

The U.S. Department of Agriculture (USDA) Forest Service Burn Area Emergency Response (BAER) teams are deployed immediately after a wildfire is contained and determine values at risk. With respect to hydrology, BAER teams focus on estimating potential increases in post-fire runoff and sediment that place downstream values at risk or threaten human life and natural resources. The hydrologic models incorporated into BAER assessments vary by region, fire, modeler, accessibility, and ease of use (Foltz et al., 2009), and lack conformity. Furthermore, many of these models' performances have not been well documented within the post-fire context.

Numerous models and techniques exist for post-fire peak discharge prediction, varying in complexity (as a function of number of parameters), are used by BAER teams. The BAER teams typically use empirical, event-based models. A U.S. Forest Service (USFS) survey on BAER models (Napper, 2010), found that out of 44 responses, 25 modelers use the U.S. Geological

Survey (USGS) Linear Regression Model, 10 use the USDA Windows Technical Release 55 (Win TR-55), 22 use Curve Number (CN) methods, 19 use the Water Erosion Prediction Project (WEPP), 2 use the Fire Enhanced Runoff and Gully Initiation (FERGI), 8 use the Rowe Countryman and Storey (RCS), and 2 use the United States Army Corps of Engineers (USACE)Hydrologic Modeling System (HEC-HMS) model. The BAER survey brings attention to the wide-range of models being utilized by the wildfire community and the need for more systematic approaches (i.e. gathering parameters and adjusting models for post-fire conditions). The models have not been evaluated over an extensive range of conditions and there is limited literature on post-fire model performance evaluation and validation (Cydzik and Hogue, 2009). Models not well tested or validated contribute to prediction uncertainty and should be used with caution in post-fire conditions.

Models chosen for review in the current study include the Rowe Countryman and Story (RCS), USGS Linear Regression Equations, WinTR-55, Wildcat5, and HEC-HMS. The RCS method consists of look-up-tables (LUTs) for discharge and erosion rates for southern Californian watersheds based on in-situ observations (Rowe et al., 1949). Notable fires such as the 2003 Old and Grand Prix Fires, and the 2009 Station Fire in California, utilized the RCS method for BAER post-fire hydrological predictions and management assessments (Biddinger et al., 2003; Moore et al., 2009).

The USGS Linear Regression Equations have been used to estimate discharge across the southwestern United States, primarily under pre-fire conditions. This method uses relationships between discharge and climatic and physical characteristics of the contributing area. The 2010 BAER hydrological assessment of the Bull Fire (Stewart and Kaplan-Henry, 2010) used a variation of the USGS Linear Regression Model, calibrated towards local conditions (Kaplan-Henry, 2007).

The Win TR-55, Wildcat5, and HEC-HMS utilize curve number (CN) methodology, but the three systems vary by model parameters, constraints and developed interface. Several of the models have been previously applied to the Hayman Fire (Wildcat4) and Valley-Complex (Soil Conservation Service (SCS) runoff curve number method, customized in Excel; Burned Area Emergency Rehabilitation Team, Valley Fire Complex, 2000) and the Old Fire (HEC-HMS; Cydzik and Hogue, 2009). The CN method has been noted for having more uncertainty in predictions when estimating at the extremes, especially during low flow and low rainfall conditions (Hawkins, 1975). The HEC-HMS model was analyzed by Cydzik and Hogue (2009) under pre- and post-fire conditions. Results showed significant changes from pre- to post-fire parameters values as well as trends in several variables (initial abstractions, curve number, and lag time) over a three-year recovery period. The CN returned to pre-fire values by the end of the second post-fire year, initial abstractions reached pre-fire conditions after the third rainy season, and the lag time remained lower than pre-fire values throughout the three-year study period (Cydzik and Hogue, 2009).

The current study undertakes one of the first model intercomparisons for a range of event-based hydrologic models utilized under pre- and post-fire watershed conditions. We also outline the various modeling platforms, parameter acquisition (inputs and outputs), and necessary parameter alterations for pre- and post-fire simulations. All study models are used extensively by the USFS BAER teams as well as other operational and research communities. Specifically the objectives of our work are to: 1) review a range of event-based hydrologic models utilized in post-fire modeling of peak flow events, 2) evaluate the models' performance across a range of diverse fire sites in California, Colorado, and Montana, 3) demonstrate potential improvements in calibrated models where data are available, and 4) provide guidance on model constraints and application in diverse post-fire regimes. Ultimately, we hope to facilitate a uniform framework and calibration approach for improved post-fire hydrologic practices and modeling assessments across multi-jurisdictional fires in the western U.S.

3.2 Methods

3.2.1 Models

Study models and related descriptions of requirements as well as system outputs have been organized by level of complexity (Table 3-1). Most models include geomorphic parameters that describe the physical watershed such as size, slope, or lengths. Forcing data typically includes precipitation, storm intensity, or storm duration. In the current study, smaller basins are modeled as lumped (basin inputs and parameter are uniform) and larger watersheds are distributed (basin inputs and parameters vary by sub-basin). In both cases, modeled basin outputs include peak discharge or a complete discharge hydrograph at the outlet. After pre-fire models are established, models are altered using published literature or documentation to create post-fire models. It is important to note that the tested hydrologic models do not include algorithms for sediment or debris bulking factors. Bulking factors increase the clear water discharge to represent the high concentrations of sediment typical of post-fire conditions (Gusman et al., 2009).

Table 3-1: Summary of models utilized in the current study, including model creator, platform for application, constraints on watershed size, and model outputs.

Model	Creator	Platform	Most suitable watershed size	Outputs
RCS	Rowe Countryman Storey	LUTs	N/A	Qpk, sediment
USGS Linear Regression	USGS	Regional USGS regression eqns	>5 mi2	Qpk
Curve Number (CN) Methods				
TR-55	USDA NRCS	WinTR-55	<25 mi2	Qpk and time, hydrograph
Wildcat 5	USFS, Stream Team, Fort Collins, CO	Microsoft Excel macros (2003 or later)	<5 mi2	Qpk and time, hydrograph
USACE HEC-HMS	U.S. Army Corps	Windows	Flexible	Storm hydrograph, Qpk and time

RCS

The Rowe Countryman and Storey (RCS) is a method for estimating flood peaks and erosion for basins within the national forests of southern California (Rowe et al., 1949). The RCS method establishes reasonable estimates through detailed look-up-tables of the average frequency and size of peak flow events and erosion rates associated with normal (unburned) conditions, the effect of burned vegetation, and the recovery of vegetation and hydrology with respect to time. Rowe et al. (1949) undertook extensive observations across southern California watersheds (along the coast from the Mexican border to San Luis Obispo) and developed relationships for peak discharge frequencies for over 250 watersheds within five zones. Relationships were then established between storm precipitation and post-fire peak discharge for watersheds in each specific storm zone and determined the changes in these flows for subsequent post-fire years. The method is still used for runoff estimates in many southern Californian watersheds.

USGS Linear Regression Equations

The USGS Linear Regression Equations (USGS) is developed for estimating 2-, 5-, 10-, 25-, 50-, and occasionally 100-yr peak discharge for ungaged sites across the southwestern United States. The least squares regression equations are produced for broad regions using long-term discharge observations. In the current study we implement regression equations previously developed for the Sierra (California), South Coast (California), Mountain (Colorado), Upper Yellowstone (Montana), and West (Montana) regions. The general regional equations and variables used in this study are outlined below (relevant coefficients are provided in Table 3-2):

Sierra, California (Waananen and Crippen, 1977): $Q_t = kA^aP^bH^c$

South Coast, California (Waananen and Crippen, 1977): $Q_t = kA^aP^b$

Mountain, Colorado (Vaill, 2000): $Q_t = kA^a(S+1)^b$

Upper Yellowstone-Central Mountain, Montana (Omang, 1992): $Q_t = kA^a(E/1000)^b(HE+10)^c$

West, Montana (Omang, 1992): $Q_t = kA^aP^b$

where:

t = recurrence interval

A = watershed area [mi^2]

P = mean annual precipitation [in]

H = altitude index (average of elevations at points 10% and 85% along the channel in thousands of feet)

E = mean basin elevation [ft]

S = slope

HE = basin high elevation index (percentage of the total basin area above 6,000 ft)

Table 3-2: USGS Linear Regression Models and coefficients for each recurrence interval used in the current study, where t = recurrence interval, A = watershed area [mi2], P = mean annual precipitation [in], H = altitude index (average of elevations at points 10% and 85% along the channel in thousands of feet), E = mean basin elevation [ft], S = slope, and HE = high elevation index (percentage of the total basin area above 6,000 ft).

Regional Equation	Sierra	South Coast	Mountain	Upper Yellowstone-Central Mountain	West
State	California	California	Colorado	Montana	Montana
Sites	Bull	Arroyo Seco Devil Canyon	Hayman	Fridley	Valley-Complex
Equation	$\mathbf{Q_t=kA^aP^bH^c}$	$\mathbf{Q_t=kA^aP^b}$	$\mathbf{Q_t=kA^a(S+1)^b}$	$\mathbf{Q_t=kA^a(E/1000)^b(HE+10)^c}$	$\mathbf{Q_t=kA^aP^b}$
t =2-yr	k=0.24, a=0.88, b=1.58, c=-0.80	k=0.14, a=0.72, b=1.62	k=11.0, a=0.663, b=3.465	k=0.177, a=0.85, b=3.57, c=-0.57	k=0.042, a=0.94, b=1.49
t =5-yr	k=1.20, a=0.82, b=1.37, c=-0.64	k=0.40, a=0.77, b=1.69	k=17.9, a=0.677, b=2.739	k=0.960, a=0.79, b=3.44, c=-0.82	k=0.140, a=0.90, b=1.31
t =10-yr	k=2.63, a=0.80, b=1.25, c=-0.58	k=0.63, a=0.79, b=1.75	k=23.0, a=0.685, b=2.364	k=2.71, a=0.77, b=3.36, c=-0.94	k=0.253, a=0.89, b=1.25
t =25-yr	k=6.55, a=0.79, b=1.12, c=-0.52	k=1.10, a=0.81, b=1.81	k=29.4, a=0.695, b=2.004	k=8.54, a=0.74, b=3.16, c=-1.03	k=0.379, a=0.87, b=1.19
t =50-yr	k=10.4, a=0.78, b=1.06, c=-0.48	k=1.50, a=0.82, b=1.85	k=34.5, a=0.700, b=1.768	k=19.0, a=0.72, b=2.95, c=-1.05	k=0.496, a=0.86, b=1.17

Curve Number Methodology

The Curve Number (CN) method is an empirical method commonly used for runoff estimation and was developed by the USDA Natural Resources Conservation Service (NRCS) to estimate runoff depth (USDA SCS, 1991). The USDA Win TR-55, Wildcat5, and USACE HEC-HMS models all utilize the CN method with varying user interfaces and parameter requirements.

The SCS CN method considers rainfall, hydrologic soils, land cover type, treatment and conservation practices, hydrologic conditions, and topography. The selected CN value is a function of land cover type, soil properties, and antecedent moisture conditions, which can be estimated from look-up-tables or geospatial data sets. The SCS method considers four hydrologic soil groups (A, B, C, and D), categorized by similar physical structure (i.e. texture), infiltration and runoff characteristics (i.e. degree of swelling when saturated, transmission rate of water) (USDA NRCS, 2007). Soil group runoff potential increases from low (A) to high (D) and decreases from free water transmission (A) to restricted water transmission (D). The models accommodate three pre-defined rainfall distributions types – Type I, IA, and III, which are based on climate zones across the United States (USDA NRCS, 2009). Type I and IA represent the Pacific maritime climate (wet winters and dry summers). Type IA is the most gradual rainfall distribution type and Types II and III represent similar distributions of intense, short duration rainfall.

The volume of runoff (P_e) is estimated using the CN and cumulative precipitation for a specified duration. The empirical formulation of the uniform loss applied throughout a storm includes:

$$S = \frac{1000}{CN} - 10$$

Equation 3-1

where:

S = Storage

CN = estimated CN value

$$I_a = (0.1)S$$

Equation 3-2

where:

I_a=initial abstractions [in]

$$P_e = \frac{(P - I_a)^2}{P - I_a + S}$$

Equation 3-3

where:

P_e= precipitation excess (runoff depth) [in]

P=total storm precipitation [in]

For consistency, the SCS Dimensionless Unit Hydrograph (UH), an empirical method used to route flow to a designated output location or design point, is selected for use in the Wildcat5, Win TR-55, and the HEC-HMS models. The SCSUH method uses time of concentration, T_c, which is defined as the time for a particle of water to travel from the furthest point of the watershed to the design point (SCS, 1991):

$$T_c = \frac{L^{0.8}(S+1)^{0.7}}{1140Y^{0.5}}$$

Equation 3-4

where:

T_c = time of concentration [hours]

L = watershed length [ft]

Y = watershed slope [%]

S = storage

The UH provides a simple method for quantifying the effect of a unit of rainfall on a corresponding unit of runoff and estimates peak discharge by constructing a hydrograph based on the variables lag time, time to peak, and base time.

Lag time is subsequently defined as:

$$T_L = 0.6T_c$$

Equation 3-5

where:

T_L = lag-time [hours]; which is the time from the center of mass of rainfall to the time of peak discharge

Time to peak (T_p) is defined as:

$$T_p = 0.67T_c$$

Equation 3-6

where:

T_p = time to peak [hours]; which is the time from the beginning of rainfall to the time of peak discharge

Base time (T_b) is defined as:

$$T_b = 2.67T_p$$

Equation 3-7

where:

T_b = base time [hours]; which is the duration of the storm response

Finally, peak discharge (*Qp)* is defined as:

$$Q_p = 484\frac{A}{T_p}$$

Equation 3-8

where:

Q_p = peak discharge [cfs]

A = area [mi^2]

Wildcat5

The Wildcat5 is used extensively in US Forest Service applications to wildlands (Hawkins and Munoz, 2011). The model is spreadsheet based (Microsoft Office Excel (2003 or later)) whose inputs include storm characteristics, watershed soil and cover (to calculate runoff depths), timing parameters (related to time of concentration), and unit hydrograph selection. The outputs include a calculated hydrograph and peak runoff (Hawkins and Munoz, 2011).

Win TR-55

Win TR-55 (TR-55) is a CN-based model for small watersheds (less than 25 mi^2) that is capable of accommodating up to ten homogenous sub-basins. The model calculates storm runoff volume, peakflow rate, hydrograph, and storage volume for storm water management (USDA NRCS, 2009). Storm data required by TR-55 includes: rainfall return period (year), 24-hour rainfall amount (inch), and rainfall distribution type (function of rainfall intensity). The TR-55 uses the Muskingum-Cunge for routing with time of concentration manually inputted or calculated using the following parameters: length (ft), slope (ft/s), surface (Manning's n), and velocity (ft/s), for sheet, shallow concentrated, and channel flow types. Using the NOAA Atlas of precipitation to determine 24-hour storm depths for each recurrence interval, the TR-55 outputs corresponding peak streamflow values.

HEC-HMS

The HEC-HMS is a modular framework developed by the United States Army Corps of Engineers (USCAE) where the CN methodology is used to simulate precipitation-runoff processes based on physiographic data within watershed systems. The model can be used to simulate observed events over a system (user-defined meteorological forcing) or to simulate pre-defined design storms. The HEC-HMS has a more complex GUI interface, however the modeling framework includes options for numerous physical configurations of a watershed (sub-basin, reach, junction, etc.), including a variety of sub-basin loss methods (SCS CN selected for this study), runoff transformation methods (SCS unit hydrograph selected), and open channel routing methods (Muskingum-Cunge selected) (USACE, 2010). In addition to parameters necessary for the SCS method, the HEC-HMS model has options to include storm baseflow in runoff prediction.

3.2.2 Post-fire models

To simulate post-fire conditions, model parameters are adjusted to reflect changes in watershed properties. The look-up-tables for the RCS method incorporate post-fire peak flow and erosion rates for time intervals up to 30 years after fire. The USGS regression equations and CN models are altered using the following methodology (Foltz et al., 2009).

USGS Linear Regression Equations

The USGS uses estimated modifiers to scale pre-fire runoff values to post-fire runoff values. The modifier is a function of the burn severity and a parameter that accounts for increased runoff. The pre-fire Q_n is then multiplied by the modifier to produce an estimate of post-fire runoff for each return interval. There are no standard guidelines to determine post-fire modifiers; BAER team members utilize their own methods, varying by region, model, or modeler (Foltz et al., 2009). For this study the modifier is calculated using Foltz et al. (2009):

$$Modifier = 1 + \left[\left(\%RO_{increase}\right) * \frac{\left(A_H + A_M\right)}{A_T} \right]$$

Equation 3-9

where:

A_H = Area of high burn severity [mi^2]

A_M = Area of moderate burn severity [mi^2]

A_T = total watershed area [mi^2]

$\%RO_{increase}$ = percent of runoff increase, post-fire [%]

Methods for estimating the %RO increase for the post-fire year are not well defined. In the current study, the %RO increase is estimated using long-term streamflow records from burned watersheds or previously published studies. Regional watersheds, City Creek (USGS gage 11055800), Devil Canyon (USGS gage 11063680), and Arroyo Seco (USGS gage11098000) that have pre- and post-fire streamflow records are used to estimate a %RO parameter for the southern California watersheds. The Colorado and Montana %RO parameter values are based on Robichaud et al. (2008), while the Bull Fire %/RO increase parameter is based on Moore et al. (2009). There is significant uncertainty in the modifier method as the increase in runoff is basically estimated a priori through the %RO parameter. Reducing the uncertainty in the modifier value for the USGS regression equation approach is outside the scope of this study, but is a subject for future investigation.

Curve Number Models

To adjust the CN parameter for post-fire land cover conditions, the following guidelines developed by Higginson and Jarnecke (2007) are utilized (note that the maximum CN value is 100):

Low burn severity CN = pre-fire CN + 5

Moderate burn severity CN = pre-fire CN + 10

High burn severity CN = pre-fire CN + 15

3.2.3 Data resources and parameters

A range of parameters must be acquired for pre- and post-fire model development. These parameters are often estimated using various methods (including maps, local knowledge, etc.) and implemented into models to predict peak flow events. Electronic databases provide objective and readily accessible tools for the acquisition of relevant model parameters (Table 3-3). A Digital Elevation Map (DEM) can be utilized to determine contributing watershed area, basin geophysical characteristics (slope, slope aspect, or lengths), and stream features, and are acquired from the US Geological Survey (USGS) (http://seamless.usgs.gov/). Land cover classification is used to estimate pre-fire land cover and is provided by the USGS (http://www.mrlc.gov/finddata.php). National Land Cover datasets (2001 and 2006) are 16-class land cover products across the United States with 30 meter spatial resolution. The classification is developed from the unsupervised Landsat Enhanced Thematic Mapper+ (ETM+) satellite data. The USDA Natural Resources Conservation Services (NRCS) provides a Web Soil Survey for the contiguous United States (http://websoilsurvey.nrcs.usda.gov/app/HomePage.htm). Soil type is used to establish model infiltration parameters and the partitioning between incoming precipitation and surface runoff.

Burn severity, required for post-fire CN adjustment, is a representation of the boundary and degree of burn within a wildfire (Key and Benson, 2004). Digital burn severity maps are typically generated from remote sensing products such as Landsat and are validated in situ by BAER teams. The validated maps are known as Burned Area Reflectance Classification (BARC) maps and can be acquired from a remote sensing database developed by the USDA Forest Service Remote Sensing Applications Center (RSAC) (http://www.fs.fed.us/eng/rsac/baer/).

All study models require representation of precipitation amount, frequency, intensity or duration. Alternatively, a design storm or a representation of the variation of precipitation depth over time can be used. The National Oceanic and Atmospheric Administration (NOAA) National Weather Service (NWS) provides the NOAA Precipitation Frequency Estimates at various durations (i.e. 5-min, 10-min, 24-hour, weekly, etc.) and recurrence intervals (i.e. 1-, 2-, 5-, 10-year, etc.) for the United States with 90% confidence intervals (http://hdsc.nws.noaa.gov/hdsc/pfds/index.html).

Table 3-3: Websites with relevant databases used to obtain pre- and post-fire model parameters and input data.

Electronic Resources	Source	Parameters
Digital Elevation Map	USGS Digital Elevation Map (http://seamless.usgs.gov/)	Geophysical parameters; routing
Land cover	National Land Cover Database (2001 and 2006) (http://www.mrlc.gov/finddata.php)	Curve number
Soil classification	USDA Natural Resources Conservation Service (http://websoilsurvey.nrcs.usda.gov/app/HomePage.htm)	Curve number
Climate	National Oceanic and Atmospheric Administration (http://hdsc.nws.noaa.gov/hdsc/pfds/index.html)	Design storms
Burned Area Reflectance Classifications	Remote Sensing Applications Center (http://www.fs.fed.us/eng/rsac/baer/)	Burn severity

3.2.4 Study areas

Model evaluation was undertaken for six basins in the Western U.S. for both pre- and post-fire conditions (Tables 3-4 and 3-5).The study sites are located within California, Colorado and Montana and provide a range of hydroclimatic conditions and burn severity levels (Table 3-5). Where observations are available, the models are calibrated for pre- and post-fire conditions (Table 3-4). Southern California sites include the 2003 Old Fire in the San Bernardino Mountains (Devil Canyon) and the 2009 Station Fire in the San Gabriel Mountains (Arroyo Seco). The 2010 Bull Fire in the southern Sequoia, California (Bull #3), is also utilized within the current study. Other study sites include the Hayman Fire in Colorado (2002), and the Valley-Complex (2000) and Fridley Fires in Montana (2001) (Robichaud et al., 2008; 2010).

Table 3-4: Available pre- and post-fire models for each basin, where * indicates observational data is available for pre-fire model calibrations and indicates post-fire models adjusted from the calibrated pre-fire models.

Model	Valley-Complex, MT	Fridley, MT	Hayman, CO	Devil Canyon, CA	Arroyo Seco, CA	Bull #3, CA
RCS	---	---	---	Pre, Post	Pre, Post	---
USGS Linear Regression	Pre, Post	Pre, Post	Pre, Post	Pre, Post	Pre, Post	Pre, Post
TR-55	Pre, Post	Pre, Post	Pre, Post	Pre*, Post*	Pre*, Post*	Pre, Post
Wildcat 5	Pre, Post	Pre, Post	Pre, Post	---	---	Pre, Post
HEC-HMS	Pre, Post	Pre, Post	Pre, Post	Pre*, Post*	Pre*, Post*	Pre, Post

Table 3-5: General basin characteristics, including, nearest city/state, fire name and year, latitude and longitude of basin outlet, area, outlet elevation, basin slope, and dominant pre-fire vegetation.

Basin	Location; nearest city	Fire, year	°N lat., °W long.	Area [km^2]	Outlet elev. [m]	Slope [%]	Pre-fire dominant vegetation
Valley-Complex	Western MT; Sula	Valley-Complex, 2000	45.91, -114.03	0.036	1720	46	forest[•,†]
Fridley	Southern MT; Emigrant	Fridley, 2001	45.51, -110.78	0.13	1930	43	shrubland/ herbaceous[•,†]
Hayman	Central CO; Lake George	Hayman, 2002	39.18, -105.36	0.03	2440	33	forest[•]
Devil Canyon	Southern CA; San Bernardino	Old, 2003	34.208, -117.331	14	634	15	shrubland/ forest[•]
Arroyo Seco	Southern CA; La Canada	Station, 2009	34.221, -118.178	40	426	6	shrubland/ forest[†]
Bull #3	Southern Sequoia, CA; Kernville	Bull, 2010	35.835, -118.46	4.12	893	26	shrubland/ forest[†]

[•]Homer et al., 2004 (National Land Cover Database, 2001)
[†]Fry et al., 2011 (National Land Cover Database, 2006)

3.2.5 Model evaluation

Pre-fire

Pre- and post-fire parameters and model forcing for the CN models were established using the digital data bases and sources (Tables 3-3 and 3-6).We first undertake an assessment of the pre-fire model performance to determine the relative accuracy of models where in situ data (gage observations) are available. The Weibull method is commonly used to analyze streamflow and estimate expected frequency of flows. It is based on the assumption that the peak discharge over a long period of time is evenly distributed and can be used to estimate a return period for specific discharge peaks. Events that occur more frequently (2-yr, 5-yr, etc.) have smaller flow volumes and consequently have higher probabilities of being exceeded. For each basin where a long-term streamgage exists, a Weibull frequency distribution is generated using the observed peak flow values (established USGS time series). The Weibull-generated discharge value for each recurrence event is considered a reasonable approximation of the associated storm frequency and allows comparison of modeled design storm simulations to an “observed” storm frequency.

Table 3-6: Summary of pre- and post-fire CN model parameters used in the Wildcat5, TR-55, and HEC-HMS models.

Watershed	Rainfall Distribution°	Hydrologic Soil Type	Pre-fire			Post-fire	
			Curve Number	T_c [hr]	Dominant Burn Severity	Curve Number	T_c [hr]
Arroyo Seco	Type I	C	72	5.14	66% Moderate	81	3.94
AS* - Little Bear	Type I	D	71	1.99	46% Low; 22% High	78	1.63
AS* - Lower	Type I	C	73	4.33	49% Low; 31% High	81	3.41
AS* - Colby	Type I	C	73	2.69	24% Low; 45% Moderate	80	2.19
Bull Fire #3	Type IA	D	82	0.49	68% Moderate	90	0.37
Devil Canyon	Type I	C	73	2.09	63% High	86	1.39
Fridley	Type II	B	74	0.17	100% High	89	0.11
Hayman	Type II	D	79	0.14	100% High	94	0.08
Valley-Complex	Type II	A	44	0.22	100% High	59	0.15

°24-hour rainfall distribution from NRCS
AS*indicates one of three sub-basins of the Arroyo Seco used in the distributed models

Post-fire

Evaluation of simulated discharge where no observed flow is available requires an alternative approach. This occurs at our ungaged pre-fire sites and all post-fire sites. In these cases, each model's simulated discharge is compared to the mean of the modeled values for that frequency. Given the lack of observations, we make the assumption that the multi-model is a reasonable proxy of the observed flow (Georgakakos et al., 2004; Ajami et al., 2006; Duan et al., 2007).

3.2.6 Statistical evaluation

To evaluate performance, we utilize two metrics commonly used in model assessment (Hogue et al., 2000, 2006; Cydzik and Hogue, 2009), root mean square error (RMSE) and percent bias:

$$Root\ Mean\ Square\ Error = \frac{\sqrt{\left(Q_{model} - Q_{obs}\right)^2}}{n}$$

Equation 10

where:

n=1

$$Percent\ Bias = \frac{Q_{model} - Q_{obs}}{Q_{obs}} * 100\%$$

Equation 11

where:

Q_{model} = modeled discharge at a specific recurrence interval

Q_{obs} = observed discharge (either Weibull or multi-model average)

3.2.7 Model calibration

Pre-fire models are calibrated to improve peak flow estimations, where observational data are available (Arroyo Seco and Devil Canyon). Similarly, only models whose parameters allow for adjustment are calibrated (TR-55 and HEC-HMS). Curve numbers and parameters dependent on the curve number are adjusted to better match pre-fire observations using statistics and visual inspection of hydrographs. Calibration efforts focus primarily on matching peak discharge, with a secondary focus on discharge volume. The TR-55 is calibrated by adjusting the CN until the peak discharge matches for each recurrence interval, while the HEC-HMS model is calibrated by adjusting the CN, Ia, and lag time (Table 3-7). The calibrated pre-fire models are then adjusted for post-fire conditions using established modifier methods.

Table 3-7: Uncalibrated (Uncal) and calibrated (Cal) parameters for Arroyo Seco lumped and distributed models (the distributed model consist of three sub-basins denoted with AS). S5 and S7 identify the storms shown in this study.

TR-55	Type	CN	TL[hr]	Tc [hr]	Ia [cm]
Lumped	Uncal	72	---	5.14	---
	Cal	51	---	6.80	---
HEC-HMS	Type	CN	TL[hr]	Tc [hr]	Ia [cm]
Lumped	Uncal	72	6.17	10.28	0.99
	Cal S5	45.5	3.17	5.28	10.39
	Cal S7	35.25	5.25	8.75	10.80
AS - Colby	Uncal	73	1.61	2.69	1.88
	Cal S5	21	2.08	3.47	8.13
	Cal S7	21	2.33	3.89	7.87
AS - Little-Bear	Uncal	71	1.19	1.99	2.08
	Cal S5	21	2.67	4.44	7.62
	Cal S7	21	1.67	2.78	7.87
AS - Lower	Uncal	73	2.59	4.32	1.88
	Cal S5	21	6.67	11.11	8.13
	Cal S7	21	3.75	6.25	7.87

3.3 Results and discussion

3.3.1 Pre- and post-fire peak discharge

The TR-55, HEC-HMS, and USGS Regression method are adaptable to all of our study sites (all basins are modeled; Table 3-5). The RCS method is only applicable to the two study sites in southern California (Arroyo Seco and Devil Canyon). The Wildcat5 is applied to all sites except the Arroyo Seco and Devil Canyon. Only the TR-55 and HEC-HMS are utilized for calibration – and only for the Arroyo Seco and Devil Canyon watersheds where pre-fire data is available. We normalize each modeled outflow by basin area to evaluate performance across the study sites.

Model performance across the sites is highly variable under both pre- and post-fire conditions (Figure 3-1).Modeled discharge increases from small to large events for each watershed and at each event there is variability as a function of site. Where applicable, the RCS performs relatively well compared to observational data (Figures 3-1a and 3-1b). The USGS performs well at the lower peak discharge events and generally shows increasing error for larger events (Figures 3-1c and 3-1d). The Wildcat5 is the most limited in application of the CN models, but seems to perform the best overall without calibration (Figures 3-1e and 3-1f). For one of the smallest study sites (Valley-Complex; 0.036 km^2) the model did not generate runoff (Fig 3-1e and 3-1f). The uncalibrated TR-55 (Figures 3-1g and 3-1h) and HEC-HMS (Figures 3-1i and 3-1j) models significantly over-predict discharge for all basins. The calibrated models (Arroyo Seco and City Creek) significantly reduce discharge predictions, by decreasing the CN and increasing initial abstractions. Both models at both sites produce improved estimates of observed peak discharge. Uncalibrated model predictions for the Bull, Hayman, Valley, and Fridley (smaller watersheds) are significantly larger than the calibrated Arroyo Seco and City Creek values, indicating that these models would benefit from calibration.

The peak discharge per unit area is highly influenced by watershed elevation and slope (Table 3-5). In the CN models, slope influences the time of concentration; steeper slopes equate to smaller residence time within the basin. The shorter time of concentration values produce more immediate discharge, especially under post-fire conditions. Higher elevation watersheds generally receive more precipitation, also contributing to larger runoff. Similarly the location of each site determines the rainfall distribution type used as input to the USGS and CN models, which has a significant influence in the predicted discharge. Type II rainfall distributions (Colorado and Montana) have larger runoff in response to more intense precipitation events. This is extremely pronounced in the Q25, Q50, and all post-fire events. Type I rainfall distributions (Devil Canyon and Arroyo Seco) show similar discharge per unit area for the TR-55 and HEC-HMS. Type IA (Bull Fire) is the least intense distribution type and generally predicts less discharge per unit area than the other sites.

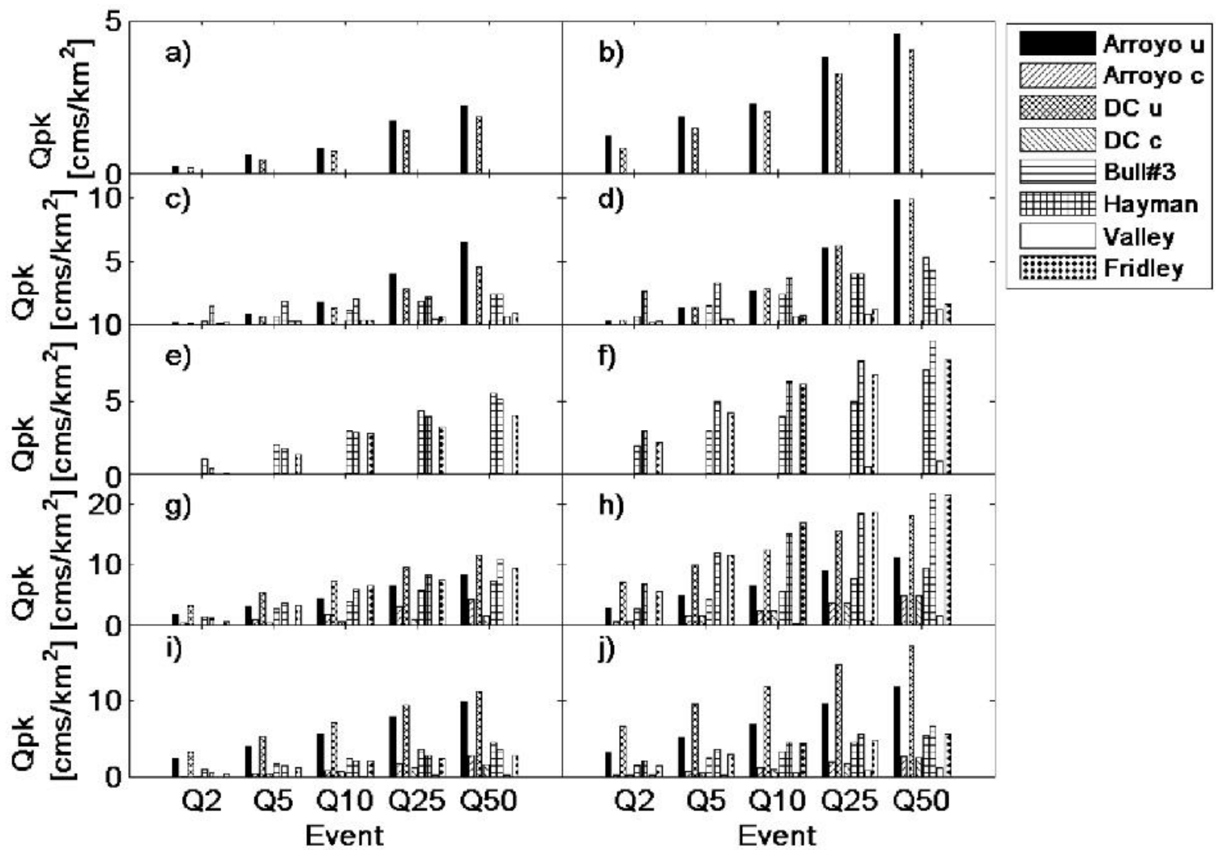

Figure 3-1: Modeled discharge for each basin according to each pre- and post-fire model: RCS (a and b), USGS (c and d), Wildcat5 (e and f), TR-55 (g and h), and HEC-HMS (i and j). For the Arroyo Seco and Devil Canyon watersheds, uncalibrated and calibrated models are the average of the lumped and distributed uncalibrated and calibrated results.

Further analysis shows that peak discharge for each recurrence interval is highly variable between the study models for three focus watersheds – the Arroyo Seco (Figures 3-2a and 3-2b), Bull Fire #3 (Figures 3-2c and 3-2d), and Hayman (Figures 3-2e and 3-2f) fires. Bull Fire #3 pre- and post-fire models (Figures 3-2c and 3-2d) do not include the RCS (outside of southern California), calibrated TR-55 (no observational data), or calibrated HEC-HMS models (no observational data). The Hayman pre- and post-fire models do not include the RCS (outside of southern California), calibrated TR-55 (no observational data), or calibrated HEC-HMS models (no observational data). The USGS model is available for all study sites. In general, the models show more discrepancy at the larger events (Q25 and Q50) where there is more intra-model variability and larger uncertainty. The uncalibrated TR-55 and HEC-HMS pre-fire models for the Arroyo Seco watershed, where there is observational data, significantly over-predict peak discharge, while the other models under-predict for Q2-Q10 events (Figure 3-2a). At the Q25 and Q50, the USGS, uncalibrated TR-55, calibrated TR-55, and uncalibrated HEC-HMS models over-predict peak discharge. The Wildcat5 appears to perform the best with the model average for the pre-fire Bull Fire #3 and Hayman, while the TR-55 uncalibrated model estimates the most discharge for each event (Figures 3-2c and 3-2d).When the Wildcat5 is applied to the Arroyo Seco despite recommended watershed size (not shown), the model significantly over-estimates peak discharge. The Wildcat5 seems the most well adapted for peak discharge modeling, but application is limited by watershed size. The Bull #3 and Hayman (Figures 3-2c-3-2f) show similar intra-model variability for each event. Generally, in the Bull Fire #3 and Hayman, the uncalibrated TR-55 predicts significantly more discharge than the other models; contributing to increased post-fire runoff response, while the HEC-HMS modeled discharge tends to be similar to the model average.

A sensitivity analysis (not shown) showed discharge estimated using the CN models is highly sensitive to rainfall input and curve number (refer to Table 3-5 for CN model parameters). Some of the California watersheds are on the boundary between NRCS Type I and IA rainfall distribution types. Type IA is less intense rainfall than Type I; both types were modeled for these basins and results showed significant influence of rainfall type on runoff production. Type I was ultimately chosen given this distribution provided simulations that better matched observational discharge. Similarly, the CN significantly influences the volume of predicted runoff. Lowering the CN decreases the volume of discharge and raising the CN increases the volume. Both parameters are subjective and contribute to model uncertainty due to the inconsistencies in CN acquisition and rainfall distribution type.

The CN parameter is also significantly influenced by soil group (Table 3-6). The California sites and Hayman site are generally characterized by soil types C (Arroyo Seco, City Creek, Devil Canyon) and D (Bull Fire and Hayman), which generate moderate (type C) and high (type D) runoff potential when thoroughly wet. In both soil groups, C and D, water transmission is restricted. The Fridley site is characterized by soil type B, which is defined as moderately low runoff potential and unimpeded water transmission. The Valley-Complex site is characterized by soil type A, which is defined as low runoff potential and free water transmission through the soil. This is seen in the Valley-Complex site, which is comparable in size to the Hayman site, but generates significantly less discharge (Figure 3-1). Immediately post-fire the soils are highly hydrophobic and increase runoff. Recovery to pre-fire conditions, the breakdown of the hydrophobic layer is dependent on amount and intensity of rainfall. The post-fire CN parameters are simply modified (Higginson and Jarnecke, 2007) to reflect an increase in surface runoff and a decrease in infiltration.

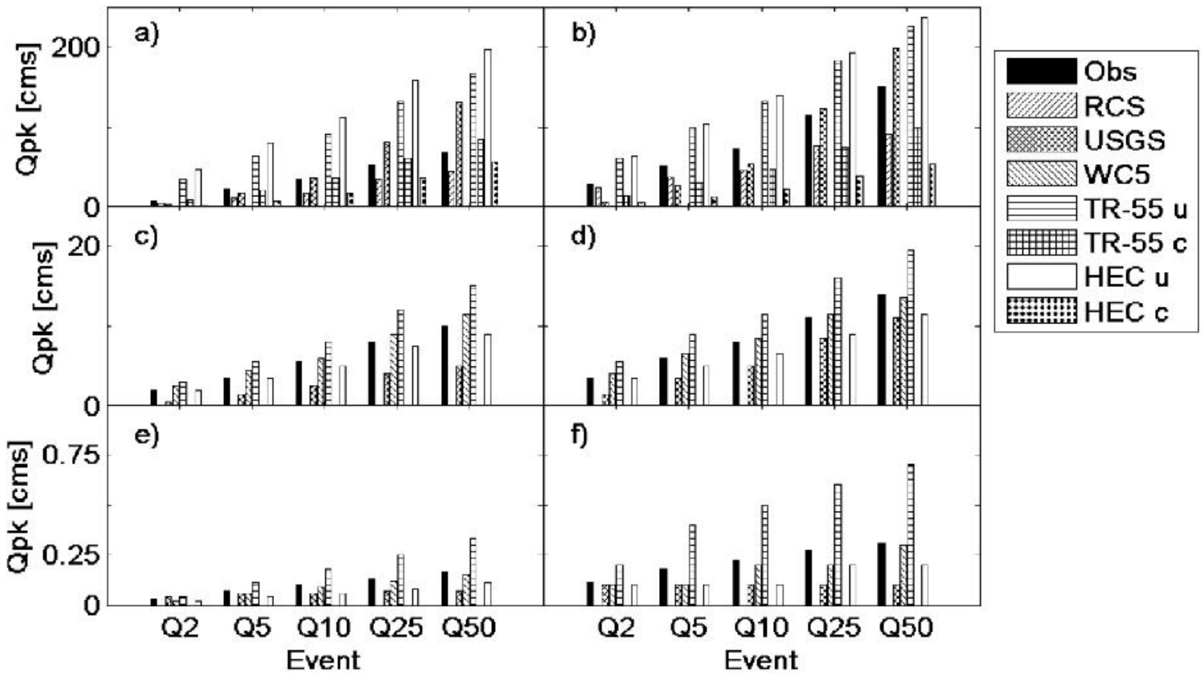

Figure 3-2: Arroyo Seco (a and b), Bull Fire #3 (c and d), and Hayman (e and f) pre- and post-fire peak discharge estimates for applicable models. The observational flow (Obs) for each watershed is the USGS gage data (a) or the model average (b-f).

3.3.2 Calibration

The lumped and distributed Arroyo Seco design for the HEC-HMS model result in distinct differences for both uncalibrated and calibrated parameters (Table 3-7).The CN significantly decreases and the initial abstractions significantly increase in both the calibrated lumped and distributed models, as a result of having to lower the water volume. The alteration in CN and initial abstraction reflect sensitivity to soil type and land cover, which govern the transmission of runoff into the soil. By decreasing the CN and increasing the initial abstraction we are essentially altering the soil characteristics of our models to accommodate more infiltration.

The lag time for the lumped Arroyo Seco and Lower Arroyo Seco sub-basin are lowered to move water more quickly from the upper parts of the basin to the outlet, which more appropriately accounts for the steepness of the watershed. The lumped and distributed simulations for two observed storms in the Arroyo Seco (24-28 December 2003 and 19-26 October 2004) show significant improvement after calibration (Figures 3-3b and 3-3d (uncalibrated) vs. Figures 3-3a and 3-3c (calibrated)). The observed discharge is greatly over-estimated by the uncalibrated lumped and uncalibrated distributed hydrographs for each storm (Figures 3-3a and 3-3c). The calibrated distributed model is able to capture the peak and volume of the observed storm better than the lumped model. Amore challenging storm from October 2000 resulted in simulations that did not adequately match the observed discharge (Figure 3-3d). This may be due to the second pulse of precipitation, where both models over-predict discharge response. Overall, the distributed calibrated model performs better than the lumped calibrated model (Figure 3-3d).

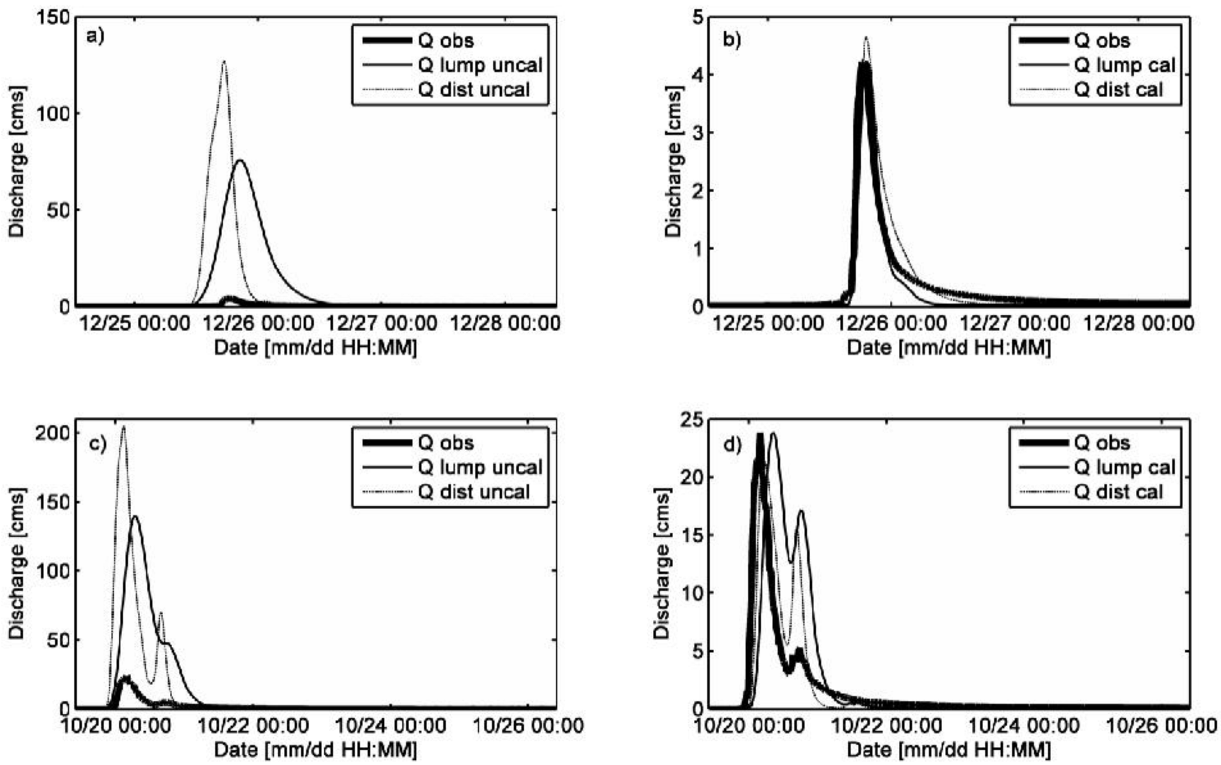

Figure 3-3: Uncalibrated (a and c) and calibrated (b and d) lumped and distributed hydrographs for two observed storms in the Arroyo Seco.

The final calibrated parameters are next evaluated on two independent storm events (Figure 3-4). The final parameter values generally results in adequate performance for the lumped and distributed models for the27 February – 3 March 2006 storm (Figure 3-4a). A less successful validation is highlighted for a storm occurring 5-11 February 2009 (Figure 3-4b). Both validation storms show that both models are sensitive to precipitation volumes and intensity, which is influenced by the initial abstraction parameter in the model. Overall the distributed model performs better than the lumped model, demonstrating the influence of including parameter variability throughout the basin.

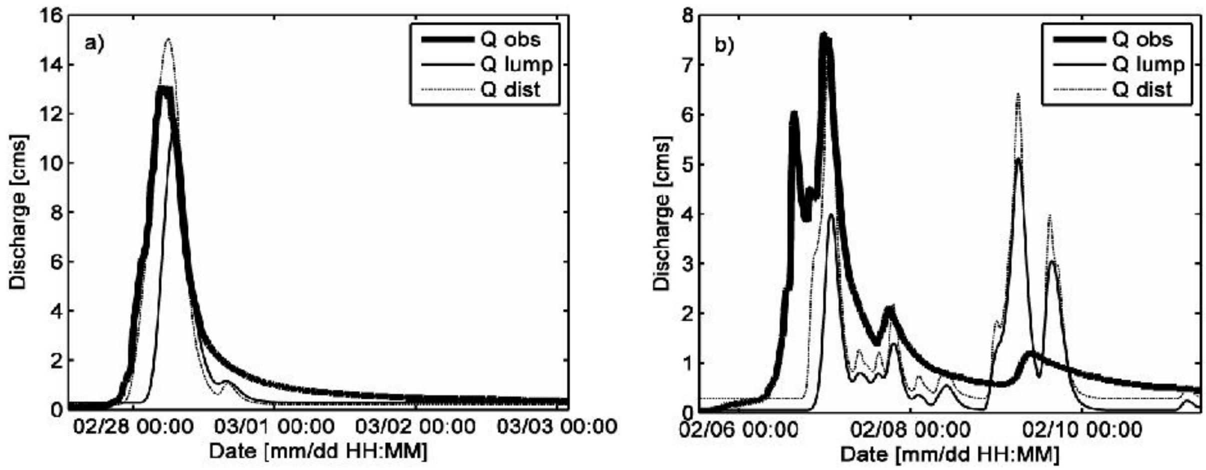

Figure 3-4: Selected validation storms for the Arroyo Seco lumped and distributed models.

3.3.3 Model uncertainty and errors

In general, model errors are highly variable across the basins and fire systems studied. We show that model selection considerably affects errors in peak discharge for the pre- and post-fire Arroyo Seco (Figures 3-5a, 3-5b, 3-6a, 3-6b), Bull #3 (Figures 3-5c, 3-5d, 3-6c, 3-6d), and Hayman (Figures 3-5e, 3-5f, 3-6e, 3-6f) simulations. Generally, the RMSE for each model and watershed increases with event size (Q2-Q50) and increased volume of runoff. The RCS predicts pre-fire discharge well but also tends to show larger errors with larger events. The USGS predictions are more variable between events and watersheds and have the largest error for all the models for the pre- and post-fire Arroyo Seco (Figures 3-5a and 3-5b) and pre-fire Bull Fire #3 (Figure 3-5c). The Arroyo Seco HEC-HMS uncalibrated distributed model has the largest RMSE deviation relative to the other models for all events (Figures 3-5a and 3-5b). Pre-fire, the HEC-HMS uncalibrated distributed, uncalibrated lumped, and uncalibrated TR-55 have the largest RMSE. The USGS shows larger RMSE at the Q25 and Q50 events. For the Bull #3, the USGS and TR-55 (Figures 3-5c and 3-5d) show the largest RMSE for all events. Overall, the Wildcat5 shows more consistent RMSE for all events pre- and post-fire (Figures 3-5c and 3-5d).

The Hayman fire models show increasing RMSE with larger events and the TR-55 has the largest RMSE followed by the USGS model (Figures 3-5e and 3-5f). Generally the TR-55 (uncalibrated) over-predicts discharge for all watersheds and has the highest error for the post-fire Bull Fire #3 (Figure 3-5d) and pre- and post-fire Hayman (Figures 3-5e and 3-5f). The Wildcat5 does well relative to the other models and generally has the lowest error for the pre- and post-fire Bull Fire #3 and Hayman sites (Figures 3-5c-3-5f). Calibration of the TR-55 and HEC-HMS results in decreased peak discharge for each event and improves RMSE for both pre- and post-fire models.

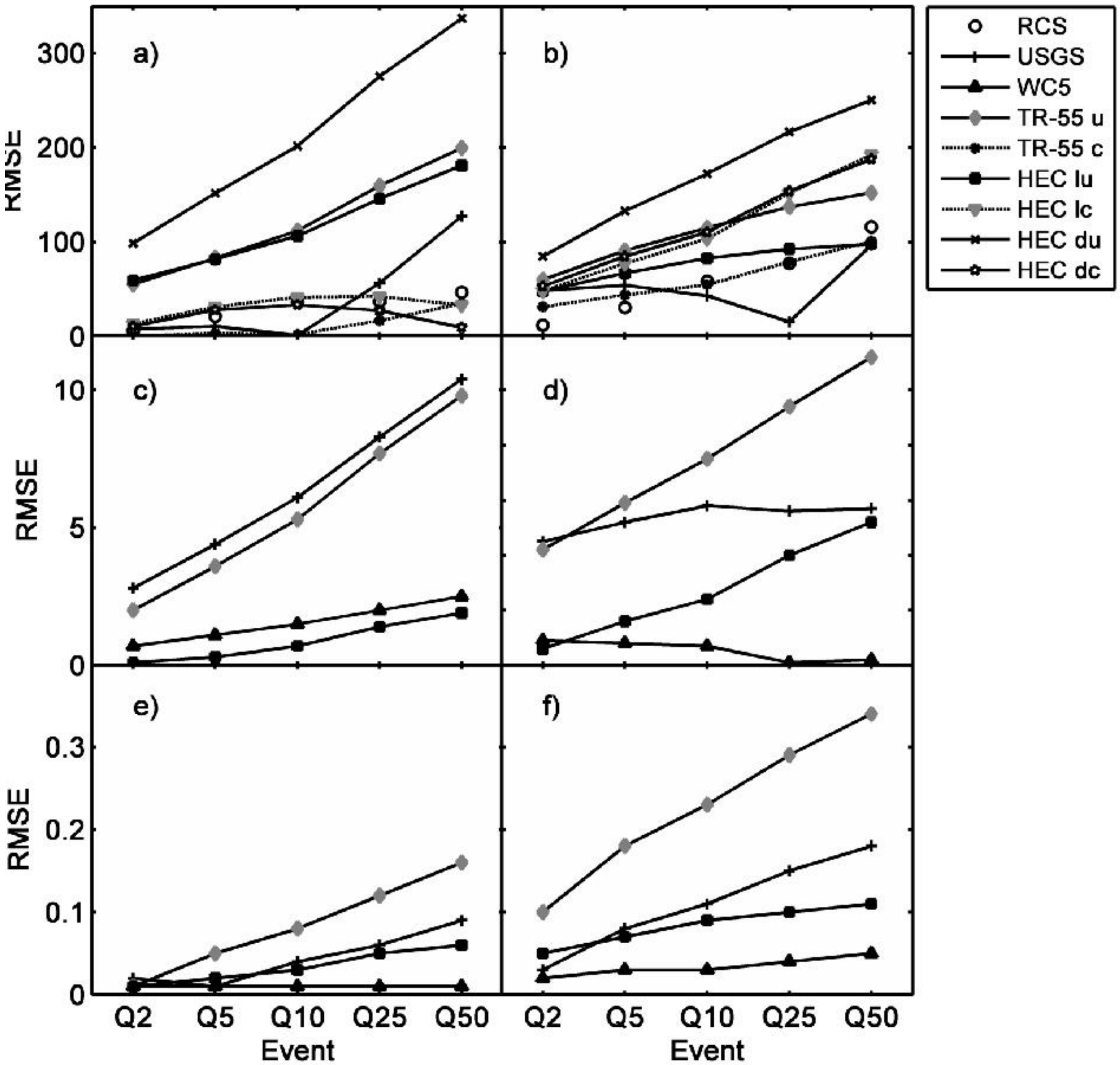

Figure 3-5: RMSE for each model for pre- and post-fire Arroyo Seco (a, b), Bull #3 (c, d), and Hayman (e, f) models.

The percent bias (Figure 3-6) highlights the tendency of models to under- or over-predict peak discharge. The Arroyo Seco pre-fire HEC-HMS uncalibrated lumped and distributed models and the TR-55 uncalibrated models all significantly over-estimate peak discharge (Figure 3-5a). The post-fire Arroyo Seco models also tend to under- and over-predict (Figure 3-5b). The Bull #3 percent bias is less than the Arroyo Seco, which is likely due to sensitivity to the size of the watersheds. The uncalibrated TR-55 and USGS have the largest absolute percent bias

(Figures 3-6c and 3-6d). The uncalibrated TR-55 over-estimates the peak discharge for the Hayman basin (Figures 3-6e and 3-6f).

The importance of model selection for a basin of interest is shown by the spread and variance of modeled peak discharge values for each recurrence interval (Figure 3-7). Larger basins with more flow show more inter-model variability for each prediction. The largest basin, Arroyo Seco shows the largest spread between modeled discharge (Figures 3-7a and 3-7b) and the smallest basin, Hayman shows the smallest spread between the models for each event (Figures 3-7e and 3-7f). The models appear most sensitive to storm data (precipitation) and the CN parameter. Undefined methods of estimating CNs (current methods consist of maps, field, GIS, look-up-tables, or "user experience") result in highly variable and uncertain peak flow estimates. Results show that lack of calibration for pre- and post-fire models contribute to inaccurate peak flow estimates and that models are not well adapted for variability in watershed size.

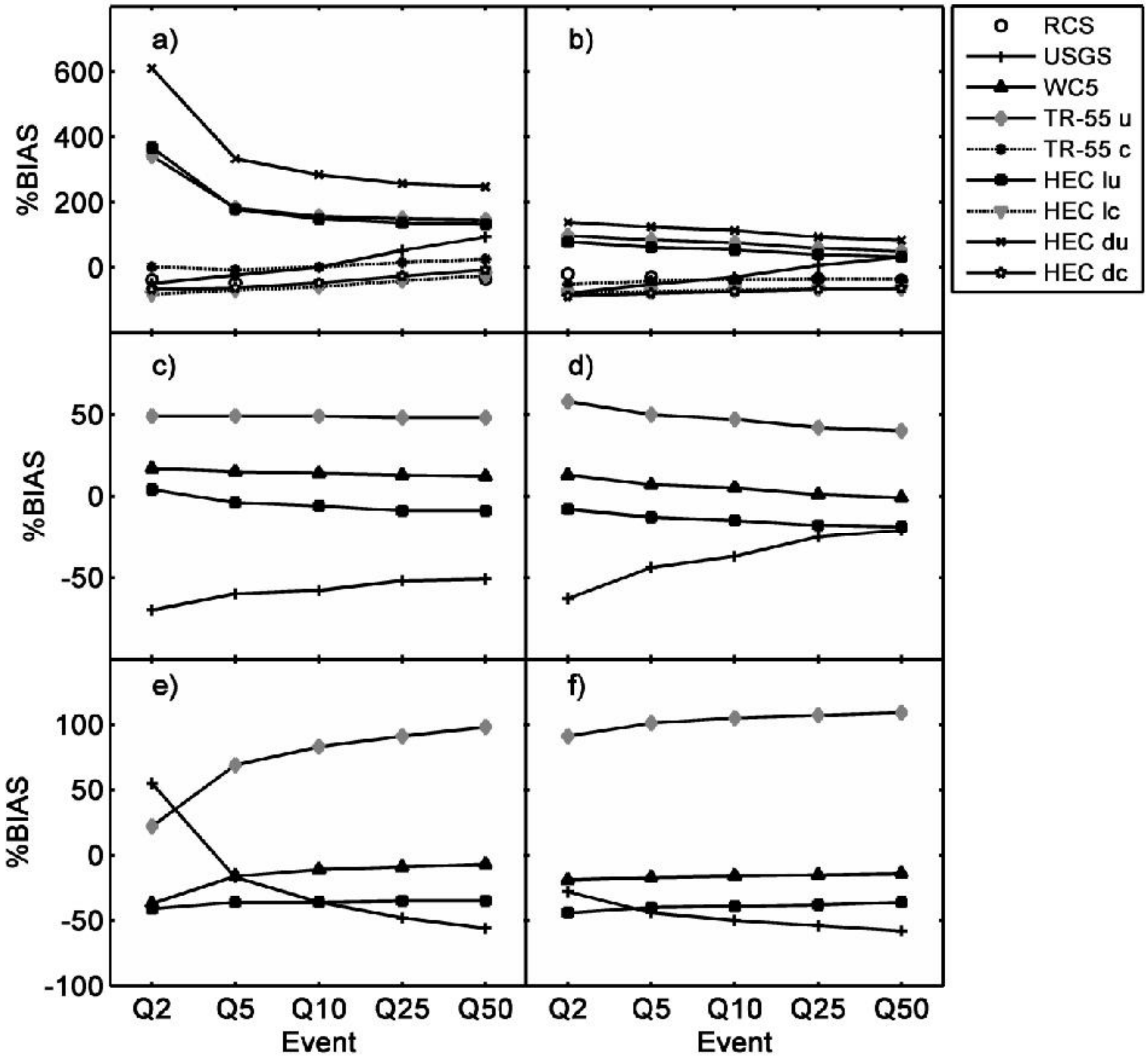

Figure 3-6: Percent bias for each model for pre- and post-fire Arroyo Seco (a, b), Bull #3 (c, d), and Hayman (e, f) models.

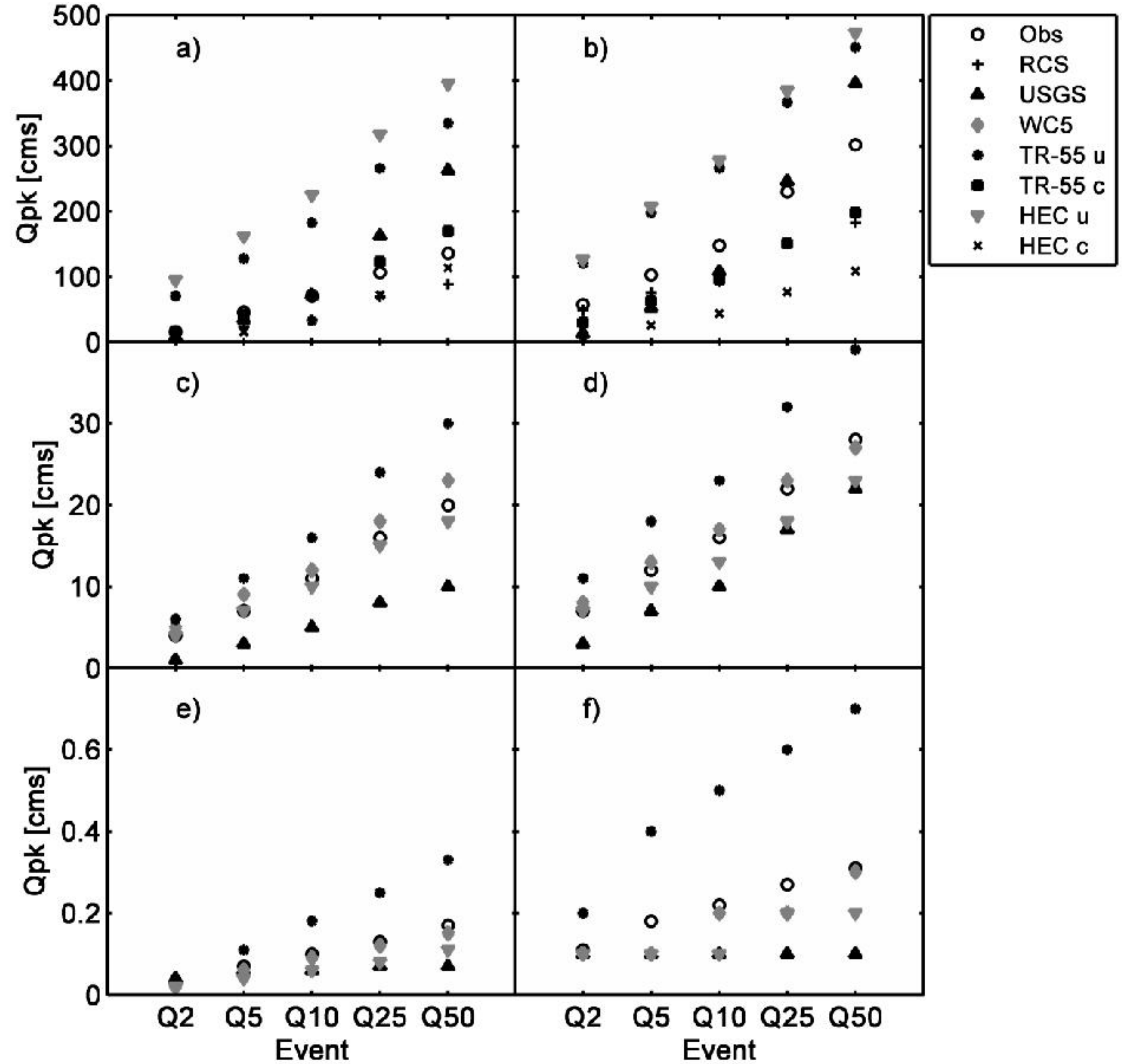

Figure 3-7: Spread of modeled peak discharge for the pre- and post-fire Arroyo Seco (a and b), Bull #3 (c and d), and Hayman (e and f) models.

3.4 Conclusions

Wildfires drastically alter land surfaces and have significant post-fire consequences for downstream communities and ecosystems. Climate change and increasing wildfire frequency add to post-fire hydrologic variability (Cannon and DeGraff, 2009; Trouet et al., 2008; Westerling et al., 2006), requiring a balance between efficient and accurate hydrologic modeling for post-fire predictions. Post-fire consequences at the WUI are especially of concern and require rapid and accurate assessments to mitigate immediate and long-term threats. The USDA Forest Service BAER teams and other scientists utilize hydrologic models to predict post-fire discharge that help guide assessment and treatment decisions. Hydrologic models used during post-fire assessments vary based on modeler preference, geographic region, parameter availability, and ease of use and do not include algorithms for sediment or debris bulking factors. Lack of standardized parameter acquisition, model usage, and assessment of model uncertainty reduce confidence in model performance and ultimately affects management decisions and mitigation costs.

In the current study, we review six models commonly used in post-fire hydrologic assessments: RCS, USGS Linear Regression Equations, USDA Win TR-55, Wildcat5, and USACE HEC-HMS. The models are tested on a range of diverse geographical and hydro-climatic conditions. We also provide a compilation of resources used to collect parameters for each study basin. Model performance is summarized as follows:

- Estimated peak discharge is highly variable depending on the model and parameter selection within the system.
- The RCS method performs well compared to watersheds where there are observations, but RCS has limited regional applicability (only applicable to southern California). The RCS is also a static model that is not adaptable to changing geomorphology and climate conditions.
- The USGS linear regression model includes a subjective modifier used to adjust towards post-fire peak runoff (requires percent of runoff increase a priori), adding significant

uncertainty in discharge estimates. The regional regression equations are broad and not fine-tuned for specific watersheds, resulting in more variable performance.

- The Wildcat5 seems to perform the best overall without calibration, but application is limited by basin size.
- The uncalibrated TR-55 tends to over-estimate peak discharge events for all watersheds, and has more uncertainty during low flow events.
- The HEC-HMS model has a moderate learning curve due to its complex GUI and high number of required parameters, but provides relatively good results, especially after calibration. In addition, the HEC-HMS provides more flexibility for watershed set up (i.e. loss methods, runoff transformations, routing) with user-defined model selections and parameter input.
- The utilized CN models are sensitive to the rainfall distribution and the CN parameter. Currently a standardized method to acquire and calibrate the CN models does not exist, increasing uncertainty in model results.

Our results show that discharge estimates are highly variable for each watershed and event and that no one model appears suitable for all watersheds. We recommend the HEC-HMS if there is sufficient time and data to, at the minimum, calibrate a pre-fire model for the area of interest. This model provides the most customizable model, which if used properly, can best reflect watershed behaviors and properties. However, if calibration data or adequate time is not available, the Wildcat5 is a good choice for watersheds meeting size requirements. Hydrologic modelers may also keep in mind that a combination of models may best represent peak discharge. Where one model is not applicable or representative, another model may perform better. Models in agreeance can provide more confidence in post-fire model predictions. CN model variability is partly attributed to parameter input. Our study shows that hydrologic soil group and rainfall distribution significantly alter model predictions. Generally, CN models tend to over-estimate discharge and stems from CN over-estimation. Attention to model limitations (i.e. geography, climate, watershed size) must be considered when selecting an appropriate framework for simulation of pre- and post-fire peak discharge. The ability to accurately model and predict post-fire hydrological consequences with improved confidence is critical for reducing management costs and improving regional resource allocation.

3.5 References

Ajami, N.K., Duan, Q., Gao, X., and Sorooshian, S., 2006. Multimodel Combination Techniques for Analysis of Hydrological Simulations: Application to Distributed Model Intercomparison Project Results. American Meteorological Society 7: 755-768.

Biddinger, T., Gallegos, A.J., Janicki, A., TenPas, J., and Weaver, R., 2003. BAER Watershed Assessment Report, 2003 Grand Prix and Old Fire. San Bernardino National Forest.

Burke, M.P., Hogue, T.S., Ferreira, M., Mendez, C.B., Navarro, B., Lopez, S., and Jay, J.A., 2010.The Effect of Wildfire on Soil Mercury Concentrations in Southern California Watersheds. Water, Soil and Air Pollution 212:369-385.

Burned Area Emergency Rehabilitation Team, Valley Fire Complex, 2000.Storm Flow Resource Assessment.

Cannon, S.H. and DeGraff, J., 2009. The Increasing Wildfire and Post-Fire Debris-Flow Threat in Western USA, and Implications for Consequences of Climate Change. Landslides – Disaster Risk reduction. Springer-Verlag Berlin Heidelberg; K. Sassa, P. Canuti (eds) Chapter 9 177-190

Cydzik, K. and T.S. Hogue, 2009.Modeling Post-fire Response and Recovery using the Hydrologic Engineering Center Hydrologic Modeling System (HEC-HMS), Journal of the American Water Resources Association, 45(3):702-714.

Debano, L.F., 2000. The role of fire and soil heating on water repellency in wildland environments: a review. Journal of Hydrology 231-232: 195-206.

Duan, Q., Ajami, N.K., Gao, X., and Sorooshian, S., 2007. Multi-model ensemble hydrologic prediction using Bayesian model averaging. Advances in Water Resources 30(5): 1371-1386.

Earles, T.A., Wright, K.R., Brown, C., and Langan, T.E., 2004.Los Alamos Forest Fire Impact Modeling. Journal of the American Water Resources Association, 40(2): 371-384.

Foltz, R.B., Robichaud, P.R., and Rhee, H., 2009. A Synthesis of Post-Fire Road Treatments for BAER Teams: Methods, Treatment Effectiveness, and Decision making Tools for Rehabilitation. Gen. Tech. Rep. RMRS-GTR-228 Fort Collins, CO: U.S. Department of Agriculture, Forest Service, Rocky Mountain Research Station. 152 p.

Fry, J., Xian, G., Jin, S., Dewitz, J., Homer, C., Yang, L., Barnes, C., Herold, N., and Wickham, J., 2011. Completion of the 2006 National Land Cover Database for the Conterminous united States, PE&RS, Vol. 77(9): 858-864.

Georgakakos, K.P., Seo, D., Gupta, H., Schaake, J., and Butts, M.B., 2004.Towards the characterization of streamflow simulation uncertainty through multimodel ensembles. Journal of Hydrology 298:222-241.

Hawkins, R.H. and Munoz, A.B., 2011. Wildcat5 for Windows (W5W): Documentation and Manual. School of Natural Resources and Environment, University of Arizona, Tucson.

Higginson, B., Jarnecke, J., 2007. Salt Creek BAER-2007 Burned Area Emergency Response. Prvo, UT: Unita National Forest; Hydrology Specialist Report. 11 p.

Hogue, T.S., S. Sorooshian, H. Gupta, A. Holz, and D. Braatz, 2000: A Multi-step Automatic Calibration Scheme for River Forecasting Models, Journal of Hydrometeorology, 1, 524-542.

Hogue, T.S., H.V. Gupta, and S. Sorooshian, 2006a: A “User-Friendly” Approach to Parameter Estimation in Hydrologic Models, Journal of Hydrology, 320, 202–217.

Homer, C. C. Huang, L. Yang, B. Wylie and M. Coan. 2004. Development of a 2001 National Land Cover Database for the United States. Photogrammetric Engineering and Remote Sensing, Vol. 70, no 7, July 2004, pp. 829-840.

Ice, G.G., Neary, D.G., and Adams, P.W., 2004.Effects of Wildfire on Soils and Watershed Processes. Journal of Forestry 16-20.

Jung, H., Hogue, T.S., Rademacher, L., and Meixner, T., 2009. Impact of Wildfire on Source Water Contributions in Devil Creek, CA: Evidence from End-member Mixing Analysis. Hydrological Processes 23: 183 – 200.

Kaplan-Henry, T.A., 2007.McNally Post-Fire Discharge and the Relationship of Sierra Nevada-wide Flood Frequency Curves and Local Kern River Discharge Curves. Advancing the Fundamental Sciences: Proceedings of the Forest Service National Earth Sciences Conference, San Diego, CA, 18-22 October 2004, PNWGTR-689, Portland, OR: U.S. Department of Agriculture, Forest Service, Pacific Northwest Research Station.

Key C.H., Benson C.N., 2004. Landscape Assessment (LA) Sampling and Analysis Methods. FIREMON Landscape Assessment.

Moody, J.A. and Martin, D.A., 2001. Post-fire, rainfall intensity-peak discharge relations for three mountainous watersheds in the western USA. Hydrological Processes, 15: 2981-2993.

Moore, M., Biddinger, T., Thornton, J., Wright, K., and Stewart, C., 2009. Hydrology Specialist Report, Station Fire BAER Assessment – Los Angeles River Ranger District. Angeles National Forest.

Napper, C., 2010 BAER Hydrology Model Questionnaire Results.

Omang, R.J., 1992. Analysis of the magnitude and frequency of floods and the peak-flow gaging network in Montana. US Geological Survey Water-Resources Investigations Report 92-4048.

Pierson, F.B., Robichaud, P.R., Moffet, C.A., Spaeth, K.E., Hardegree, S.P., Clark, P.E., Williams, C.J., 2008.Fire effects on rangeland hydrology and erosion in a steep sagebrush-dominated landscape. Hydrological Processes 22: 2916-2929.

Radeloff, C.C., Hammer, R.B., Stewart, S.I., Fried, J.S., Holcomb, S.S., McKeefry, J.F., 2005. The Wildland Urban Interface in the United States. Ecological Applications, 15: 799-805.

Robichaud, P.R., Wagenbrenner, J.W., Brown, R.E., Wohlgemuth, P.M., and Beyers, J.L., 2008.Evaluating the effectiveness of contour-felled log erosion barriers as a post-fire runoff and erosion mitigation treatment in the western United States. International Journal of Wildland Fire 17(2): 255-273.

Robichaud, P.R., Ashmun, L.E., and Sims, B.D., 2010. Post-Fire Treatment Effectiveness for Hillslope Stabilization. Gen. Tech. Rep. RMRS-GTR-240. Fort Collins, CO: U.S. Department of Agriculture, Forest Service, Rocky Mountain Research Station. 62 p.

Rowe, P.B., Countryman, C.M., and Storey, H.C., 1949. Probably peak discharge and erosion rates from southern California watersheds as influenced by fire. Pacific Southwest Forest and Range Experiment Station, US Department of Agriculture, Forest Service.

Rulli, M.C. and R. Rosso, 2007. Hydrologic Response of Upland Catchments to Wildfires. Advances in Water Resources 30:2072-2086.

Stewart, C. and Kaplan-Henry, T., 2010. Hydrology Specialist Report, Bull Fire BAER Assessment - Sequoia National Forest.

Trouet, V., Taylor, A.H., Carleton, A.M., Skinner, C.N., 2008.Interannual variations in fire weather, fire extent, and synoptic-scale circulation patterns in northern California and Oregon. Theoretical and Applied Climatology, 95:349-360.

US Army Corps of Engineers (USACE), 2010. Hydrologic Modeling System HEC-HMS: User's Manual version 3.5. Institute for Water Resources, Hydrologic Engineering Center.

U.S. Department of Agriculture, Natural Resources Conservation Service (USDA NRCS), 2007. Engineering field handbook: chapter 7 – Hydrologic Soil Groups. In: National engineering handbook. Washington, DC: U.S. Department of Agriculture, Soil Conservation Service: part 650.

U.S. Department of Agriculture, Soil Conservation Service (USDA SCS), 1991. Engineering field handbook: chapter 2 – estimating runoff. In: National engineering handbook. Washington, DC: U.S. Department of Agriculture, Soil Conservation Service: part 650.

U.S. Department of Agriculture, Natural Resources Conservation Service, 2009. Small Watershed Hydrology: WinTR-55 U.S.er Guide. Conservation Engineering Division.

Vafeidis, A.T., Drake, N.A., Wainwright, J., 2007. A proposed method for modeling the hydrologic response of catchments to burning with the use of remote sensing and GIS. Catena, 70: 396-409.

Vaill, J.E., 2000. Analysis of the magnitude and frequency of floods in Colorado. US Geological Survey Water-Resources Investigations Report 99-4190.

Waananen, A.O. and Crippen, J.R., 1977. Magnitude and frequency of floods in California. US Geological Survey Water-Resources Investigations Report 77-21.

Westerling, A.L., Hildago, H.G., Cayan, D.R., Swetnam, T.W., 2006. Warming and earlier spring increase western U.S. forest wildfire activity. Science, 313(5789): 940-943.

Wilson, C.J., J.W. Carey, P.C. Beeson, M.O. Gard, and I.J. Lane, 2001. A GIS-Based Hillslope Erosion and Sediment Delivery Model and Its Application to the Cerro Grande Burn Area. Hydrological Processes 15:2011-3023.

Chapter 4. Controls on Recovery in Post-Fire Watersheds

4.1 Motivation

Fire dramatically alters watershed processes. Loss of vegetation and soil transformation alter normal flow patterns and disrupt expected hydrologic behavior for years after fire (Debano, 2000; Ice et al., 2004; McMichael et al., 2004; Pierson et al., 2008; Cydzik and Hogue, 2009; Jung et al., 2009). Mediterranean systems are generally resilient to fire and have been noted to exhibit fairly quick recovery (Horton and Kraebel, 1955; Wittenberg et al., 2007). However, non-native plants can invade post-fire landscapes and alter hydrology and energy balances in semi-arid regions (Prater and DeLucia, 2006). Succession of vegetation or type conversion due to fire may also result in decreased evaporation and may be partly responsible for increased summer streamflow in post-fire semi-arid systems (Meixner and Wohlgemuth, 2003). Although ecosystem behavior and hydrologic recovery are linked, few studies have explicitly coupled investigation of both processes in post-fire systems. Typical studies of post-fire dynamics in chaparral dominated systems include field observations of vegetation recovery and resilience (Horton and Kraebel, 1955; Keeley and Sterling, 1981; Keeley et al., 2008). Plant recovery studies in post-fire chaparral shrublands demonstrate that parameters such as slope aspect and stand age (last fire event) are important determinants of burn severity; older vegetation implies more biomass, ground litter and fallen debris available to burn (Keeley et al., 2008). However, fire history, pre-fire land attributes (i.e. plant species and land-use history), and event-dependent characteristics such as fire severity and post-fire precipitation complicate predictions of post-fire vegetation recovery (Duguy and Vallejo, 2008; Keeley et al., 2005; Pausas, 2003; Roder et al., 2008).

Various studies have utilized remotely-sensed data to link burn or fire severity to hydrologic or soil behavior (Moody et al., 2007; Gonzalez-Pelayo et al., 2006). Vegetation regeneration after fire has also been evaluated in Mediterranean systems using a range of vegetation indices (Diaz-Delgado et al., 2002; McMichael et al., 2004; Roder et al., 2008; Wittenberg et al., 2007; Wittenberg and Inbar, 2009). Many remotely-sensed vegetation indices are available, with most studies utilizing Leaf Area Index (LAI) or Normalized Difference Vegetation Index (NDVI) (i.e. Landsat-TM or spectral mixture analysis (SMA) from Airborne Visible/Infrared Imaging Spectrometer (AVIRIS)) as a proxy of green biomass or vegetation activity present in post-fire systems (Diaz-Delgado et al., 1998, 2002; McMichael et al., 2004, 2006; Riano et al., 2002; Roder et al., 2008).

LAI is the leaf area per unit ground area and estimates the structural property of vegetation canopy (Myneni et al., 1995). LAI is estimated through the inversion of a canopy radiative transfer model that simulates radiative absorption and vegetation scattering (Myneni et al., 1995). Uncertainties in the LAI product include background interference and atmospheric scattering at the top of the atmosphere and top of the canopy (Myneni et al., 1995). NDVI uses the normalized difference between red and near-infrared channels. The product is sensitive to vegetation fraction and the rate of absorption of photosynthetic solar radiation (Gitelson et al., 1996). NDVI is noted to be adequate for monitoring plant recovery processes, but has drawbacks due to atmospheric and soil reflectance interference (McMichael et al, 2004; Wittenberg et al., 2007). For example, darker soils result in higher NDVI values (Gao et al., 2000) and there are non-linear relationships between NDVI and other vegetation variables, particularly under increasing biomass conditions. NDVI reaches a saturation level before the maximum is reached and may be most useful during initial post-fire conditions (Diaz-Delgado et al., 2002).

Vegetation indices used in post-fire recovery studies typically have high spatial resolution (e.g. 30m), but the number of images utilized over study sites has been limited (McMichael et al., 2006; Roder et al., 2008).

Investigators have also worked toward improving vegetation indices and validating new observations (Chen et al., 2005; Huete et al., 2002; Gao et al., 2000). The difference between the reflectance of the blue and red bands can be used to correct the atmospheric influences afflicting the NDVI parameter (Chen et al., 2005). The result is an Enhanced Vegetation Index (EVI) that is less sensitive to atmospheric influences and contains a blue band correction factor (Gao et al., 2000; Chen et al., 2005). EVI effectively monitors plant resilience, while reducing the effect of soil and atmospheric background interference. Unlike NDVI, EVI remains sensitive to vegetation at high biomass levels due to its sensitivity to canopy structure (Matsushita et al., 2007; Chen et al., 2005; Huete et al., 2002; Gao et al., 2000). EVI has been shown to detect variations in LAI, canopy type and architecture, plant structure, seasonal vegetation patterns, land cover, and biophysical variations (Gao et al., 2000; Wittenberg et al., 2007).

Despite the extensive literature on the application of remote-sensing products to study vegetation behavior, there is a lack of studies evaluating coupled ecosystem and hydrologic response in burned watersheds – especially integrating data from advanced satellite platforms. Several recent studies utilize field observations and five LANDSAT-based EVI images to evaluate the resilience of vegetation in semi-arid (Mediterranean) systems and the long-term effects of repeat fires on plant recovery (Wittenberg et al., 2007; Wittenberg and Inbar, 2009). The authors conclude that north facing slopes tend to return to pre-fire conditions faster than south facing slopes (in the northern hemisphere) and that remotely-sensed EVI helps detect pre- and post-fire vegetation cover but does not provide information on specific vegetation species. A recent study by Casady et al. (2009) also utilizes MODIS EVI time series (every 16 days for 5 years) as a proxy for green biomass recovery with respect to slope aspect and burn severity and develops a decision tree model to predict post-fire vegetation behavior.

The segregation of hydrologic or ecosystem recovery in previous post-fire studies highlights the need for investigation of coupled ecohydrologic response in fire altered systems. We advocate that simultaneous evaluation of EVI, burn severity, slope aspect and post-fire climatology will improve our understanding of the dynamics of ecosystem regeneration in burned watersheds and the corresponding seasonal and annual hydrologic response. Similar to previous studies, our work focuses on the amount of post-fire green biomass detected as a proxy of vegetation recovery and does not specifically identify plant species recovery (Keeley et al., 2008; Wittenberg, et al., 2007; Casady et al., 2009).The objectives of the current study are to: 1) investigate the influence of aspect, burn severity and precipitation patterns on post-fire vegetation response (using EVI as a proxy), 2) determine the impact of selected determinants (vegetation, burn severity, aspect, and climate) on post-fire hydrologic variability, and 3) establish recovery patterns and trends of both vegetation and discharge in post-fire chaparral systems.

4.2 Methods

We investigate hydrologic and ecologic recovery in two watersheds located in the San Bernardino Mountains of Southern California that were burned during the Old Fire of 2003 (26 October 2003 - 06 November 2003). Both watersheds are predominantly covered by chaparral with mixed forests in the higher elevations of the watersheds. To evaluate pre- and post-fire vegetation activity, we utilize MODIS EVI (MOD13Q1), a 16-day product with 250m spatial resolution (Huete et al., 2002). Burn severity and slope aspect of each watershed are also extracted and aggregated to 250m resolution using MODIS and USGS Digital Elevation Models (DEMs). Estimates of EVI (16-day), burn severity, and slope aspect are then evaluated as to their influence and control on post-fire hydrologic response in each watershed system.

4.2.1 Study areas

Southern California has a semi-arid, Mediterranean climate, including a relatively short precipitation season (generally December to March) and an extended dry period over the summer and fall season (NOAA, 2009a). Vegetation is primarily chaparral, sage, and scrub, with mixed conifer in the upper elevations. Chaparral typically have deep rooted systems necessary for obtaining water and surviving in hot dry climates (Schenk and Jackson, 2002), while shallow-rooted vegetation (grasses) cannot access deeper water stores and are senescent when moisture at the surface is depleted (Prater and DeLucia, 2006). The hydrology and vegetation of Southern California are heavily influenced by periodic El Nino events (NOAA, 2009b), which typically result in cooler, wetter conditions, and enhance vegetation growth. During the dry (fall) season, the Santa Ana Winds are a natural occurrence, where hot, dry air is moved west from the desert towards the ocean, drying out vegetation and encouraging ignited fires to spread (Keeley et al., 2004).

The Devil Canyon watershed (Figure 4-1) is approximately 14 km^2 and receives an average of 840 mm of precipitation each year (San Bernardino County Flood Control District (SBCFCD), 2008; data period from 1985-2010). Pre-fire vegetation for Devil Canyon watershed was retrieved from Landsat Thematic Mapper and consists primarily of chaparral (55%) and mixed forest at higher elevations (29%); the remaining 16% consists of a mixture of coastal sagescrub, developed areas, riparian zones, unvegetated areas, water, and woodlands (Minnich, 1988; NOAA, 2003). Devil Canyon exhibits vegetation, soil, relief, and atmospheric conditions typical to Southern Californian urban-fringe watersheds. Devil Canyon was 97% burned during the Old Fire. A historical fire perimeter data set provided by the California Department of Forestry and Fire Protection (from ~1900 to 2010) reveals notable fire events in Devil Canyon during 1918 (24% burned), 1924 (27% burned), and 1980 (28% burned). The last major fire event was about twenty years ago in 1954 (92% burned). Keeley et al. (2004) note that Southern California chaparral systems generally have a natural frequency rate of 30-40 years, indicating that Devil Canyon is generally close to a natural fire regime. The elevation range in Devil Canyon is 500 to 1700 meters and the overall watershed slope is 15% (USGS 7.5 min, Quadrangle Map; Silverwood Lake and San Bernardino North). The soil in Devil Canyon is associated with gravelly loamy sand, loamy sand, coarse loamy sand, sandy loam, and clay loam (Hromadka, 1986; Mays, 2001).

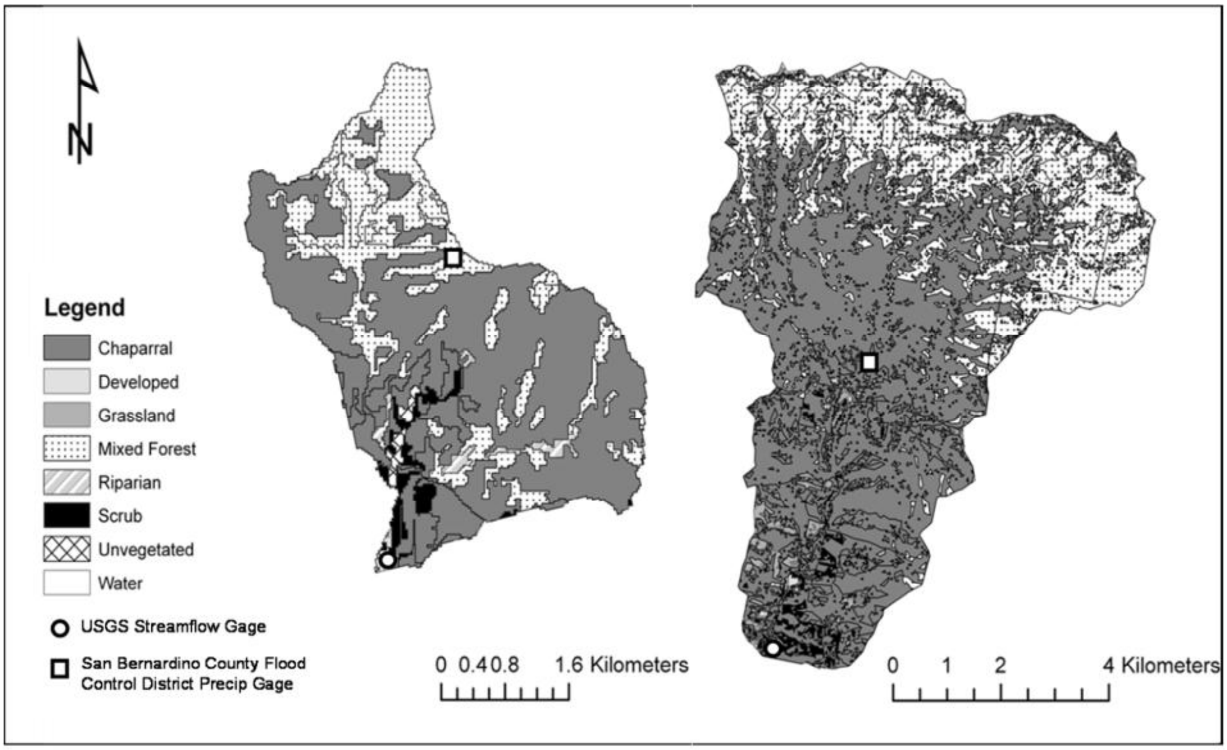

Figure 4-1: Pre-fire vegetation for Devil Canyon (left) and City Creek (right) retrieved from the Landsat Thematic Mapper layer (30m; NOAA C-CAP, 2000). USGS Gage locations are also plotted

The City Creek watershed (Figure 4-1) is approximately 51 km^2 and is located just southeast of the Devil Canyon catchment. The basin receives an average of 600 mm of precipitation a year (San Bernardino County Flood Control District (SBCFCD), 2010; data period from 1985-2010). City Creek consists primarily of chaparral (72%) and mixed evergreen and mixed conifer forests (20%) at higher elevations; the remaining 8% consists of a mixture of coastal sagescrub, developed areas, riparian zones, unvegetated areas, water, and woodlands (Minnich, 1988; NOAA, 2003). City Creek was estimated as 94% burned by the Old Fire. The California Department of Forestry and Fire Protection's historic fire perimeter set reveals notable fire events in City Creek in 1922 (53% burned), 1956 (61% burned), and 1970 (28% burned). In 2007, the Slide Fire burned less than five percent of the upper northeast of City Creek (predominantly mixed forest). The portion of City Creek re-burned during the 2007 fire was classified by the USDA Forest Service Remote Sensing Applications Center as mostly unchanged/very low and low burn severity (USDA Forest Service, 2007). City Creek's elevation range is 300 to 2100 meters and the overall watershed slope is estimated at 10% (USGS 7.5 min, Quadrangle Map Harrison). The soil in City Creek is associated with clay loams, shallow sandy loam, soils with low organic content, and soils higher in clay content (Hromadka, 1986; Mays, 2001). Refer to Table 4-1 for both watersheds' general characteristics.

Table 4-1: Devil Canyon and City Creek watershed characteristics with pre- and post-fire runoff ratios

		Devil Canyon (DC)	**City Creek (CC)**
Watershed Size		14.2 km^2	50.8 km^2
Watershed Slope		15%	10%
USGS Gage #		11063680	11055800
San Bernardino Precipitation Gage #		2840	2860 and 3377
% Burned		97%	94%
Pre-Fire Vegetation (%)	Chaparral	55%	72%
	Mixed Forest	29%	20%
Average Runoff Ratio	Pre-fire (WY85-03)	0.19	0.22
Yearly Post-fire runoff ratio	Post-fire (WY04-10)	0.37	0.36
	WY 2004	0.47	0.36
	WY 2005	0.48	0.62
	WY 2006	0.42	0.41
	WY 2007	0.45	0.3
	WY 2008	0.27	0.27
	WY 2009	0.25	0.23
	WY 2010	0.28	0.33

4.2.2 Hydrologic data

Precipitation data for the two watersheds are available from the San Bernardino County Flood Control District for water years (WY) 1985 to 2010 (01 October 1984 to 30 September 2010). The Devil Canyon rain gage (Gage 2840) is located at the top of the watershed, while the

City Creek rain gage (Gage 3377) is more centrally located in the middle elevation of the basin. There were about 160 days of missing data for the study period for the City Creek gage and additional gages (5140 and 5339) outside (5 and 5.5 miles respectively) of the watershed were used to estimate missing values (filled by the inverse-distance weighting method).Daily precipitation data for Devil Canyon is available for the period 02 October 1934 to present with only 373 days of missing data. Gage 3377 in City Creek is approximately 13 km directly south of the Devil Canyon gage, hence a linear regression was developed between the two gages to establish a relationship and estimate missing precipitation at the Devil Canyon gage. During the current study period, WY 2005 is noted as the second wettest year on record (NOAA, 2009a) and WY 2002 is noted as the driest year on record (NOAA, 2009c).

USGS discharge data are available at the outlet of both watersheds (gages 11055800 (City Creek) and 11063680 (Devil Canyon)). Hydrologic observations (discharge, runoff depth, and precipitation) were aggregated to various timescales, including monthly, seasonal and yearly totals for water years 1986 to 2010 to evaluate pre- and post-fire behavior of the watersheds. Additionally, discharge (Q) values were transformed to provide improved visualization of the full range of flows. In particular, the transformed flows are more ideal for observing baseflow, where the transformation expands the recessions (Hogue et al., 2000). Transformed flow, Q_t, is similar to a Box-Cox transformation (Box and Cox, 1964) and is calculated as follows:

$$Q_t = \frac{(Q+1)^{\lambda} - 1}{\lambda}$$

Equation 4-1

Where $\lambda = 0$ equates to a log transformation and $\lambda = 1$ implies no transformation. In the current study, we set $\lambda = 0.3$ (Hogue et al., 2000).Annual and seasonal discharge values are compared with corresponding EVI values for both pre- and post-fire periods. Each 250m EVI is further classified by aspect and level of burn severity.

4.2.3 Distributed watershed aspect

Aspect is defined as the compass direction of the slope face in the watershed and is classified using a Digital Elevation Model (DEM). Slope aspect influences the amount of radiative forcing that a respective land surface receives, facilitating or deterring growth rates. USGS DEMs were obtained for each watershed with a 10m resolution as Spatial Data Transfer Standard (SDTS) and aggregated to a 250m x 250m resolution to match the remote sensing data utilized in this study. Devil Canyon requires two DEM tiles (Silverwood Lake and San Bernardino North) and City Creek requires the Harrison Mountain tile. Similarly to Wittenberg et al. (2007), the current study categorizes the cell aspects into four primary directions; north (315° to 45°), east (45° to 135°), south (135° to 225°), and west (225° to 315°) facing slopes.

4.2.4 Differenced normalized burn ratio

MODIS is a multi-spectral sensor on board the Aqua and Terra satellite platforms containing 36 spectral bands with wavelengths between 0.4 to 14.4 µm. Spatial resolutions include 250m, 500m, and 1000m and temporal resolution include daily, 8-day, 16-day, monthly, quarterly, or yearly. Normalized Burn Ratio (NBR) is derived from remotely-sensed near infrared (NIR) and mid-infrared (MIR) MODIS bands and provides an estimate of the burn severity level (loss of vegetation) of a patch of land surface (Key and Benson, 2006). In the current study, NIR and MIR bands from the MOD13Q1 tile are used to derive NBR images for pre-fire (30 September 2003) and post-fire (17 November 2003) dates. The developed pre- and post-fire NBR images are differenced to create a differenced NBR (dNBR) image, which differentiates between burned and unburned areas (Key and Benson, 2006) and approximates the amount of vegetation density lost directly from wildfire. Based on Key and Benson's (2006) definition of severity levels, dNBR severity levels were classified into the following categories: unburned (<+100), low severity (+100 to +269), moderate severity (+270 to +659), and high severity (+660 to +1300). The relative amount of vegetation biomass lost during the wildfire (burn severity) provides insight on post-fire soil conditions (hydrophobicity, structure, etc.). 2.2.4

4.2.5 MODIS Vegetation Indices

MOD13Q1 is acquired from the EROS Data Center, whose database consists of various atmospheric, hydrologic, and energy variables that can be applied to global vegetation observations, hydrologic modeling, and other management applications. MOD13Q1 contains vegetation parameters such as NDVI, EVI, and relevant QA (quality analysis) data (Huete et al., 2002; Chen et al., 2005). The MOD13Q1 EVI data are utilized with a temporal resolution of 16 days and a spatial resolution of 250 meters. EVI data were collected from WY 2001 to 2010 (01 October 2000 – 30 September 2010). The equation used to derive MOD13Q1 (EVI) is noted as:

$$EVI = 2.5\left[\frac{\rho_{NIR} - \rho_{RED}}{\rho^*_{NIR} + C_1\rho^*_{NIR} - C_2\rho^*_{BLUE} + L}\right]$$

Equation 4-2

where ρ^*_{NIR} is the near infrared reflectance, ρ^*_{RED} is the red channel reflectance, ρ^*_{BLUE} is the blue channel reflectance, C_1andC_2 are the red and blue correction coefficients for atmospheric resistance, respectively, and L is the canopy background brightness correction factor (Huete et al., 2002; Cheng et al., 2005). Spatial and temporal EVI values were extracted and visualized, and various spatial aggregations are undertaken (per aspect type, per burn severity group, per basin area, etc.). The extracted EVI time series values are used to quantify the total annual EVI detected (summation of each 16-day EVI value per determinant over the entire water year) in order to represent the total vegetation biomass (dead or living) for each pre- and post-fire year. A single image or "snapshot" of EVI values will miss the variability present in vegetation, while the accumulation of EVI detected over the course of a year will capture the vegetation activity and variability. We also estimate a percent recovery for each post-fire year, relative to the three-year pre-fire average, with respect to each burn severity and aspect.

4.2.6 Savitzky-Golay analysis

Further assessment of vegetation recovery rates is undertaken using the Savitzky-Golay (S-G) least squares polynomial filter (Jonsson and Eklundh, 2004). An unfiltered EVI timeseries contains "noise" or small scale temporal variations and, similar to previous studies, steps are taken to filter this "noise" out to create a smoother signal for analysis. The EVI time series for each aspect for each burn severity level is smoothed using the S-G method where the degree of the polynomial regression is 1. After smoothing, the Casady et al. (2009) method is used to develop a relationship between post-fire years. The EVI time series is normalized by the pre-fire EVI mean (*f* EVI); making the post-fire EVI a fraction of the pre-fire EVI, also allowing for evaluation of the post-fire EVI vegetation relative to pre-fire EVI levels. For each succeeding post-fire year (WY 2004-2010), the *f* EVI is summed to derive the integrated annual EVI. The annual integral is subsequently fit with a regression line using the least squares method, using the following equation:

$$\int fEVI = \beta_0 + \beta_1(Year)$$

Equation 4-3

where $\int f$ EVI is the annual integration of the fraction of EVI for each successive post-fire year, $\beta 1$ is the slope that represents the recovery from year to year, and β_0 is the slope intercept. The derived regression provides an estimate of the annual progression (rate) of vegetation recovery throughout the study period for each slope aspect and burn severity level pair.

4.2.7 Analysis of variance

An Analysis of Variance (ANOVA) is employed to determine the significance of relationships between study parameters. Discharge and EVI are separated annually and seasonally (OND (Oct to Dec - fall), JFM (Jan to Mar - winter), AMJ (Apr to Jun - spring), and JAS (Jul to Sep - summer)) and evaluated for statistical differences from the pre-fire period. We test the null hypothesis that the mean of each discharge timeseries (WY 1986-2010; seasonal and annual periods) is similar to the mean from the pre-fire data period (WY 1986-2003) (α=0.05). For consistency, pre-fire discharge average is calculated by excluding El Nino years (given that no El Nino years were noted in the post-fire period). We also evaluate the null hypothesis that the mean of each yearly EVI timeseries (WY 2001-2010) is similar to the mean of the pre-fire EVI period (WY 2001-2003). We perform a multiple ANOVA comparison (pair-wise design) and evaluate successive pairs of post-fire means to the pre-fire average. This step-wise comparison allows us to evaluate when pre-fire conditions (behavior) are generally restored.

4.3 Results and discussion

4.3.1 General watershed behavior

Relevant characteristics, including precipitation, discharge, and average (basin-scale) EVI values are evaluated for each watershed for WY 2001-2010 (Figure 4-2). Both watersheds show a distinct (pulse) response to precipitation events during the winter season and minimal but consistent baseflow response in the summer period. Post-fire, discharge is significantly elevated for precipitation events that are of similar (or lower) amounts to pre-fire storms. In addition, baseflow values are heightened during the post-fire summer periods, especially after WY 2005 and WY 2006 winter seasons. Vegetation (EVI) in both basins shows a prolonged and increased response to precipitation events, with an extended sinusoidal seasonal pattern, peaking after the peak rainfall/discharge flux in each basin. Devil Canyon (Figure 4-2a) also shows a slightly higher basin-average EVI than City Creek (Figure 4-2b). We attribute this to the initial difference in vegetation distributions (Devil Canyon has a higher percentage of mixed forest and smaller percentage of chaparral than City Creek). Immediately post-fire (right of the vertical dashed line), the EVI of both watersheds shows a sharp decline, with EVI values decreasing by more than half. Significant winter rainfall during WY 2005 increases the EVI to near pre-fire levels in both Devil Canyon and City Creek; however the EVI response is dampened again during the next and subsequent seasons. This implies that the rainfall during WY 2005 resulted in a brief "green-up" of watershed vegetation; however the green-up was not sustained for either watershed. Discharge values remain elevated during the following summer period, and we hypothesize that mature (deeper) root systems, which can tap into deeper soil water stores, were not yet developed (Jung et al., 2009). Finally, the aggregate EVI signal of both watersheds does not appear to be back to pre-fire levels (maximum values are significantly lower) in the last year of the study period (WY 2010).

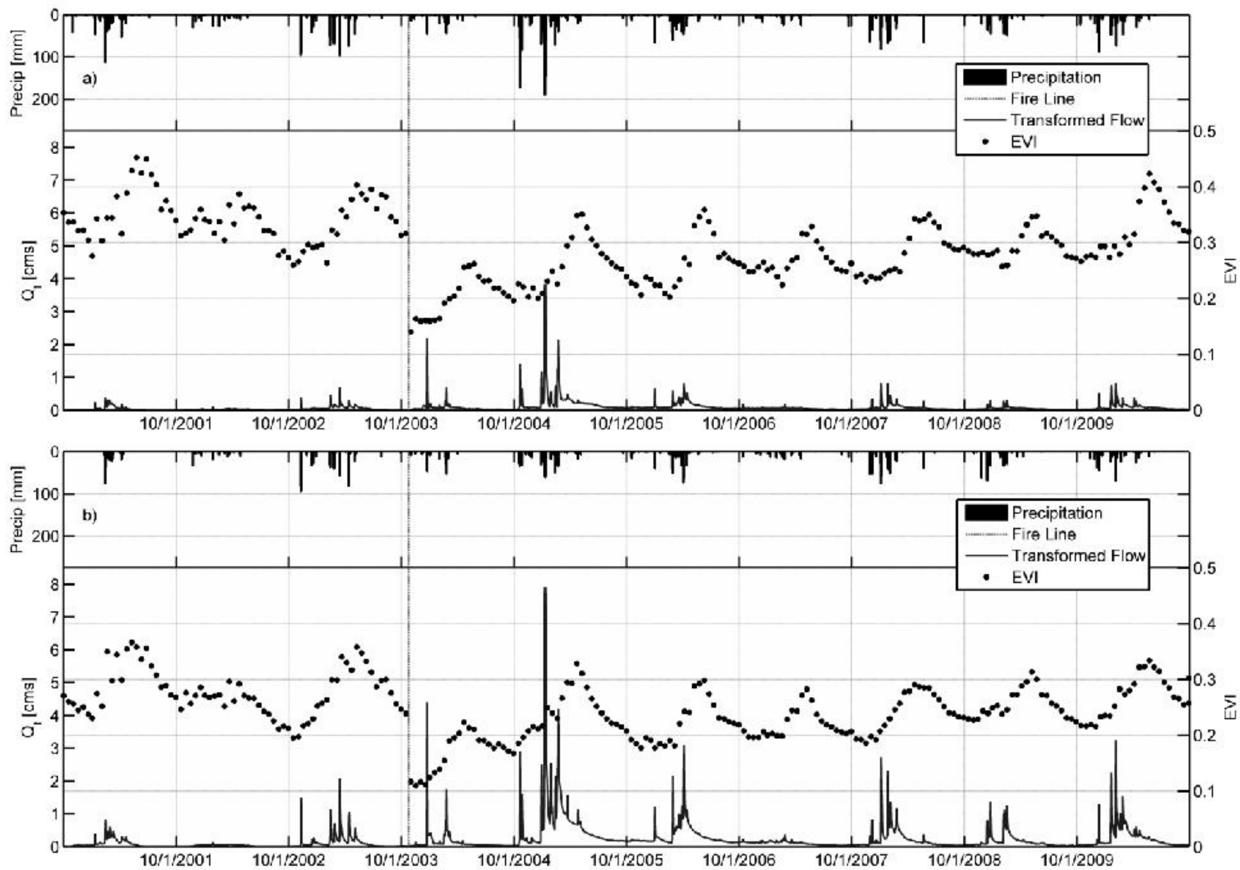

Figure 4-2: General hydrology of Devil Canyon (a) and City Creek (b) including precipitation, discharge (transformed) and16-day EVI. The dark grey line indicates the start date of the Old Fire (23 October 2003).

4.3.2 Seasonal runoff ratios

Annual and seasonal (wet and dry) runoff ratios (depth runoff:depth precipitation) are highlighted in Table 4-1 and Figure 4-3. In general, City Creek and Devil Canyon exhibit fairly similar runoff ratios over the pre-fire period, including 0.19 for Devil Canyon and 0.22 for City Creek. After fire, the average annual runoff ratios are significantly higher for both basins, with Devil Canyon having a runoff ratio of 0.37 and City Creek having a runoff ratio of 0.36 for the entire post-fire study period (Table 4-1). A cumulative distribution analysis also indicates that post-fire precipitation patterns are generally similar to the pre-fire cumulative precipitation patterns. However, the post-fire runoff depth is significantly altered (larger) in both watersheds relative to the pre-fire period (Table 4-1).

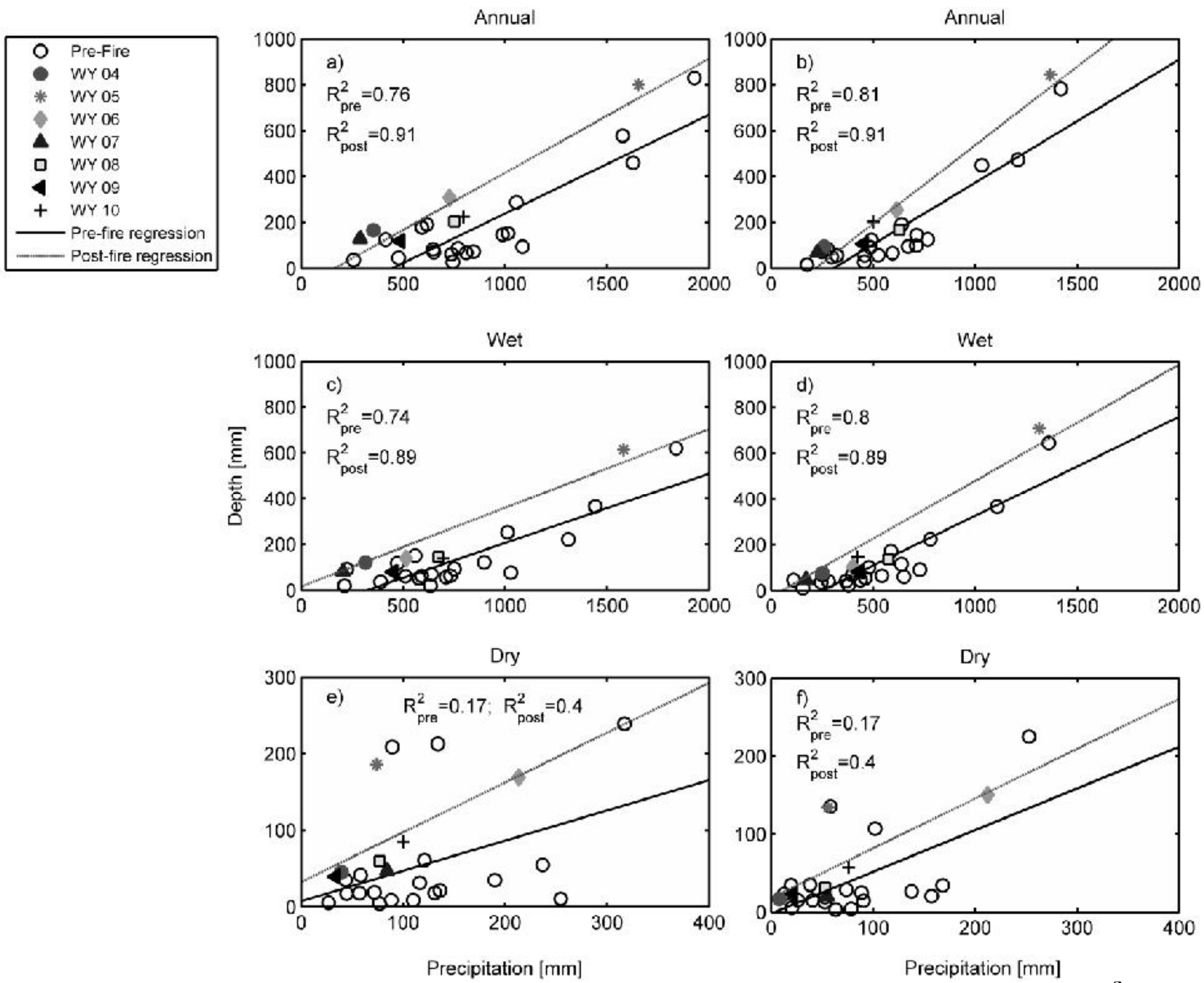

Figure 4-3: Runoff relationships, associated regression line, and correlation coefficient (R^2) for annual (WY 1985 –2008), wet (Oct – Mar), and dry (Apr – Sep) seasons for Devil Canyon (a, c, e) and City Creek (b, d, f).Pre-fire years and seasons are shown with open circles, while post-fire years and seasons are shown with filled symbols.

There is extra sensitivity to precipitation (increased runoff) during the extreme wet year (WY 2005), and then a gradual decrease in the runoff ratios to WY 2009. From 2009 to 2010 the runoff ratio for both watersheds show a slight increase from 0.25 to 0.28 (Devil Canyon) and

0.23 to 0.33 (City Creek). WY 2010 was generally wetter than the preceding years (Figure 4-2), which contributes to elevated runoff in Devil Canyon. City Creek exhibits a much larger increase in runoff, which is partly due to the increased precipitation but also attributed to the 2007 Slide Fire which occurred over a small portion of the basin. WYs 2007 through 2009 were relatively dry and the burned areas may not have contributed to increased runoff.

The post-fire trend line (annual response) shifts upward for both Devil Canyon (Figure 4-3a) and City Creek (Figure 4-3b). Investigation was also undertaken for both wet and dry seasons; with the wet season defined as fall and winter periods (October to March) and the dry season defined as spring and summer periods (April to September). During the wet season, the post-fire runoff ratio is higher than the pre-fire runoff ratio in both Devil Canyon (Figure 4-3c) and City Creek (Figure 4-3d). The post-fire regression line (relationship) is shifted up during the wet period and a slightly increased slope is seen at City Creek (Figure 4-3d), indicating increased discharge response for post-fire precipitation events that are similar to pre-fire levels. In both watersheds, there is also significantly more discharge present during the dry season (Figures 4-3e and 3f). Dry season runoff ratios are noticeably higher, especially in Devil Canyon (Figure 4-3e). Devil Canyon is smaller and steeper; hence a quicker (and elevated) response is reasonable. The highest runoff value in the post-fire study period is for WY 2005 (recorded as the second wettest year on record; NOAA, 2009a). In WY 2009, the runoff ratio values are near the pre-fire range and indicate the post-fire hydrologic response is returning to pre-fire conditions. These variations within the flow and precipitation regimes are further investigated with analyses of observed vegetation regrowth.

4.3.3 ANOVA and confidence intervals

As expected, during the pre-fire period, discharge is generally similar (within the average confidence interval) except for established El Nino years (WY 1993, 1995, 1997, 1998). Excess precipitation during El Nino years produces increased flow and shows a statistically different mean discharge from the pre-fire average. Annual and dry season confidence interval (CI) plots for EVI and Q are presented for each watershed (Figure 4-4). Pre-fire discharge is highly variable at the annual scale and wet season response tends to dominate the yearly trends. During the post-fire period, the dry season discharge values are elevated and significantly different than the estimated pre-fire average. This is especially evident during the extremely wet year (WY 2005) and the following year (WY 2006) which was influenced by residual moisture from the preceding year (Figures 4-4c and 4-4d). Dry season EVI for Devil Canyon (Figure 4-4a) and City Creek (Figure 4-4b) show an expected decrease in EVI values immediately post-fire, with a general progression towards pre-fire values. During the extremely wet year (WY 2005), vegetation responds to the high winter precipitation, means similar to pre-fire conditions. However, the EVI response is not sustained and recedes between 2006 and 2008. During the final year of the study period (WY 2010), Devil Canyon and City Creek's average EVI for the dry season are statistically similar to the pre-fire EVI.

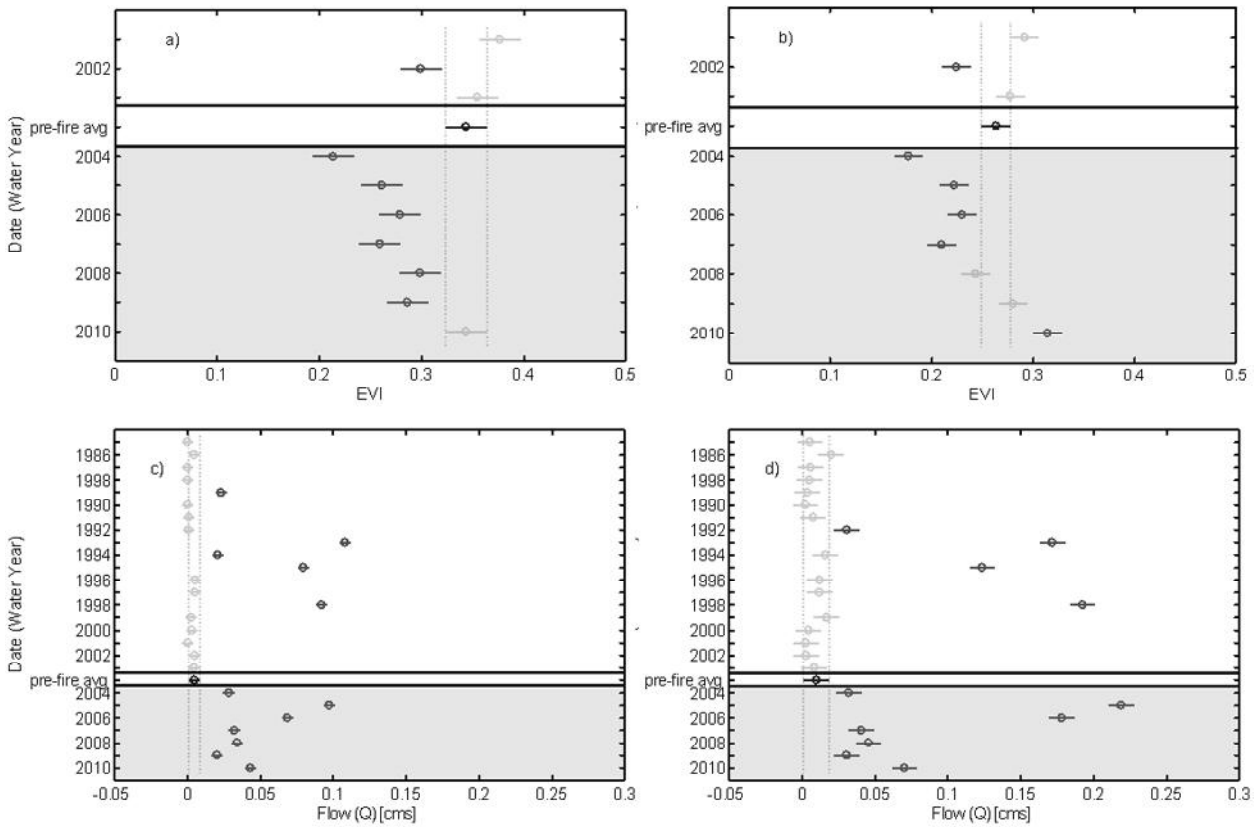

Figure 4-4: ANOVA (Confidence Intervals (CI)) results for the dry season period for Devil Canyon EVI (a) and discharge (c) and City Creek EVI (b) and discharge (d). The vertical lines around the pre-fire average represent the tested confidence interval. Post-fire years are shaded in grey. Bolded water years outside of the tested confidence interval represent a statistically different mean from the pre-fire period at a confidence level of α=0.05.

Table 4-2 highlights ANOVA results for each season; in general, the Devil Canyon post-fire EVI does not show statistically similar means compared to the pre-fire average. The vegetation and hydrology do show inter-relatedness; as demonstrated by the post-fire dry season flows in both watersheds. As the EVI values increase, the discharge values trend towards pre-fire values (Table 4-2), but still are not within the significance interval. Table 4-2 also shows that the annual EVI in both watersheds are statistically different from the pre-fire mean for five to six years.

Table 4-2: Average EVI annual and seasonal values for October through December (OND), January through March (JFM), April through June (AMJ), and July through September (JAS) and ANOVA results for the pre-fire and post-fire periods, including the 16-day EVI average and discharge (mean daily) for both Devil Canyon and City Creek

	Devil Canyon - Mean EVI				
	Annual	**OND**	**JFM**	**AMJ**	**JAS**
Pre-Fire Avg	3.42E-01	3.12E-01	3.25E-01	3.84E-01	3.43E-01
2004	2.02E-01	1.56E-01	1.80E-01	2.44E-01	2.14E-01
2005	2.63E-01	2.14E-01	2.45E-01	3.23E-01	2.61E-01
2006	2.62E-01	2.26E-01	2.19E-01	3.18E-01	2.79E-01
2007	2.67E-01	2.55E-01	2.49E-01	3.04E-01	2.59E-01
2008	2.83E-01	2.38E-01	2.53E-01	3.37E-01	2.98E-01
2009	2.96E-01	2.81E-01	2.79E-01	3.35E-01	2.86E-01
2010	3.31E-01	2.77E-01	2.92E-01	4.00E-01	3.44E-01
	Devil Canyon - Mean Flow				
	Annual	OND	JFM	AMJ	JAS
Pre-Fire Avg	4.80E-02	3.39E-02	1.18E-01	3.61E-02	4.80E-03
2004	8.03E-02	1.35E-01	1.20E-01	5.33E-02	2.82E-02
2005	3.61E-01	1.91E-01	9.29E-01	2.39E-01	9.72E-02
2006	1.39E-01	8.93E-02	1.62E-01	2.39E-01	6.84E-02
2007	5.84E-02	7.17E-02	7.67E-02	5.36E-02	3.20E-02
2008	9.18E-02	5.67E-02	2.04E-01	7.41E-02	3.41E-02
2009	5.38E-02	5.36E-02	9.11E-02	5.14E-02	2.02E-02
2010	1.01E-01	5.57E-02	1.97E-01	1.11E-01	4.31E-02
	City Creek - Mean EVI				
	Annual	OND	JFM	AMJ	JAS
Pre-Fire Avg	2.78E-01	2.43E-01	2.83E-01	3.16E-01	2.64E-01
2004	1.68E-01	1.14E-01	1.56E-01	2.05E-01	1.77E-01
2005	2.43E-01	2.04E-01	2.50E-01	2.89E-01	2.22E-01
2006	2.22E-01	1.89E-01	1.89E-01	2.73E-01	2.30E-01
2007	2.20E-01	2.01E-01	2.12E-01	2.54E-01	2.10E-01
2008	2.42E-01	1.92E-01	2.39E-01	2.83E-01	2.43E-01
2009	2.82E-01	2.71E-01	2.66E-01	3.11E-01	2.80E-01
2010	2.96E-01	2.59E-01	2.69E-01	3.35E-01	3.14E-01
	City Creek - Mean Flow				
	Annual	OND	JFM	AMJ	JAS
Pre-Fire Avg	1.36E-01	9.15E-02	3.33E-02	1.13E-01	9.70E-03
2004	1.61E-01	3.14E-01	2.64E-01	7.54E-02	3.20E-02
2005	1.36E+00	4.29E-01	4.20E+00	6.42E-01	2.19E-01
2006	4.09E-01	1.91E-01	4.92E-01	7.86E-01	1.78E-01
2007	1.11E-01	1.45E-01	1.69E-01	9.02E-02	4.06E-02
2008	2.71E-01	1.10E-01	7.80E-01	1.56E-01	4.55E-02
2009	1.71E-01	1.60E-01	3.77E-01	1.22E-01	3.06E-02
2010	3.26E-01	1.14E-01	8.36E-01	3.00E-01	7.03E-02

Devil Canyon EVI is the most statistically different from pre-fire, while City Creek seems to recover sooner. However, both Devil Canyon and City Creek streamflows during the summer (JAS) are not returned to pre-fire conditions. An analysis of controlling factors on vegetation recovery, including burn severity and aspect reveal that the EVI means are statistically different from pre-fire means in almost all scenarios, excluding Devil Canyon high burn north and City Creek low burn (Table 4-3). These observed EVI patterns prompt a more rigorous investigation as explored below.

Table 4-3: Average 16-day EVI values and ANOVA results for Devil Canyon and City Creek with respect to slope aspect and burn severity levels for the pre- and post-fire periods

		Devil Canyon Burn Severity			City Creek Burn Severity		
Aspect	**Water Year**	**Low**	**Moderate**	**High**	**Low**	**Moderate**	**High**
North	Pre-Fire Avg			2.74E-01	2.45E-01	2.58E-01	2.95E-01
	2004			1.30E-01	1.97E-01	1.81E-01	1.40E-01
	2005			2.40E-01	2.47E-01	2.37E-01	2.25E-01
	2006			2.41E-01	2.18E-01	2.14E-01	2.24E-01
	2007			2.44E-01	2.16E-01	2.19E-01	2.27E-01
	2008			2.64E-01	2.30E-01	2.29E-01	2.41E-01
	2009			2.64E-01	2.47E-01	2.41E-01	2.66E-01
	2010			2.94E-01	2.55E-01	2.58E-01	2.89E-01
East	Pre-Fire Avg		3.91E-01	4.02E-01	2.28E-01	2.61E-01	3.26E-01
	2004		2.29E-01	2.01E-01	1.78E-01	1.49E-01	1.45E-01
	2005		2.85E-01	2.73E-01	2.53E-01	2.32E-01	2.38E-01
	2006		2.94E-01	2.90E-01	1.90E-01	2.00E-01	2.56E-01
	2007		2.97E-01	2.96E-01	1.80E-01	1.99E-01	2.54E-01
	2008		3.13E-01	3.19E-01	2.23E-01	2.20E-01	2.65E-01
	2009		3.28E-01	3.40E-01	2.25E-01	2.41E-01	2.93E-01
	2010		3.63E-01	3.80E-01	2.31E-01	2.56E-01	3.07E-01
South	Pre-Fire Avg	3.34E-01	3.20E-01	3.54E-01	2.56E-01	3.05E-01	3.66E-01
	2004	2.31E-01	1.71E-01	1.54E-01	1.87E-01	1.66E-01	1.49E-01
	2005	2.79E-01	2.55E-01	2.44E-01	2.49E-01	2.44E-01	2.43E-01
	2006	2.65E-01	2.51E-01	2.51E-01	2.18E-01	2.30E-01	2.71E-01
	2007	2.70E-01	2.56E-01	2.56E-01	2.11E-01	2.36E-01	2.78E-01
	2008	2.86E-01	2.75E-01	2.82E-01	2.34E-01	2.54E-01	2.94E-01
	2009	2.92E-01	2.88E-01	3.01E-01	2.43E-01	2.75E-01	3.17E-01
	2010	3.20E-01	3.22E-01	3.40E-01	2.55E-01	2.93E-01	3.33E-01
West	Pre-Fire Avg	4.12E-01	3.23E-01	3.15E-01	2.43E-01	2.55E-01	3.39E-01
	2004	2.52E-01	1.66E-01	1.50E-01	1.96E-01	1.74E-01	1.39E-01
	2005	2.78E-01	2.28E-01	2.31E-01	2.47E-01	2.36E-01	2.22E-01
	2006	2.69E-01	2.31E-01	2.34E-01	2.12E-01	2.09E-01	2.42E-01
	2007	2.80E-01	2.35E-01	2.35E-01	2.06E-01	2.07E-01	2.47E-01
	2008	2.90E-01	2.55E-01	2.58E-01	2.24E-01	2.21E-01	2.62E-01
	2009	3.10E-01	2.65E-01	2.72E-01	2.30E-01	2.37E-01	2.87E-01
	2010	3.37E-01	2.96E-01	3.08E-01	2.38E-01	2.49E-01	3.02E-01

4.3.4 Post-fire EVI evolution

Annual total EVI values for each WY with respect to aspect and burn severity levels for both watersheds are highlighted in Figure 4-5 (the number of pixels for each aspect and burn severity are also shown). It is important to note that for all slope aspects, pixels associated with high burn severity (high burn pixels) show the highest pre-fire EVI (biomass) values and low burn pixels have the lowest pre-fire EVI (biomass) values. Generally, pre-fire pixels with larger total EVI values show the largest decrease in EVI immediately post-fire, with the exception of Devil Canyon, where inconsistencies may be due to the smaller sample size (number of pixels available). Devil Canyon shows the general trend of increasing post-fire annual total EVI and City Creek clearly illustrates the low burn severity stabilizing in Figure 4-5. The standard deviation is also estimated for each burn severity class. Devil Canyon has larger standard deviations, from 0.93 (low burn severity) to 1.63 (high burn severity) than City Creek (0.51 (low burn severity) to 1.56 (high burn severity)), also indicating increased variability in Devil Canyon. In both watersheds, the low severity burn has lower variability, while the high burn severities have more variability (larger standard deviation). The standard deviations for each aspect in Devil Canyon are 1.15 (north), 1.63 (east), 1.42 (south), and 1.51 (west).The standard deviations for each aspect in City Creek are 1.33 (north), 1.09 (east), 1.56 (south), and 1.35 (west).

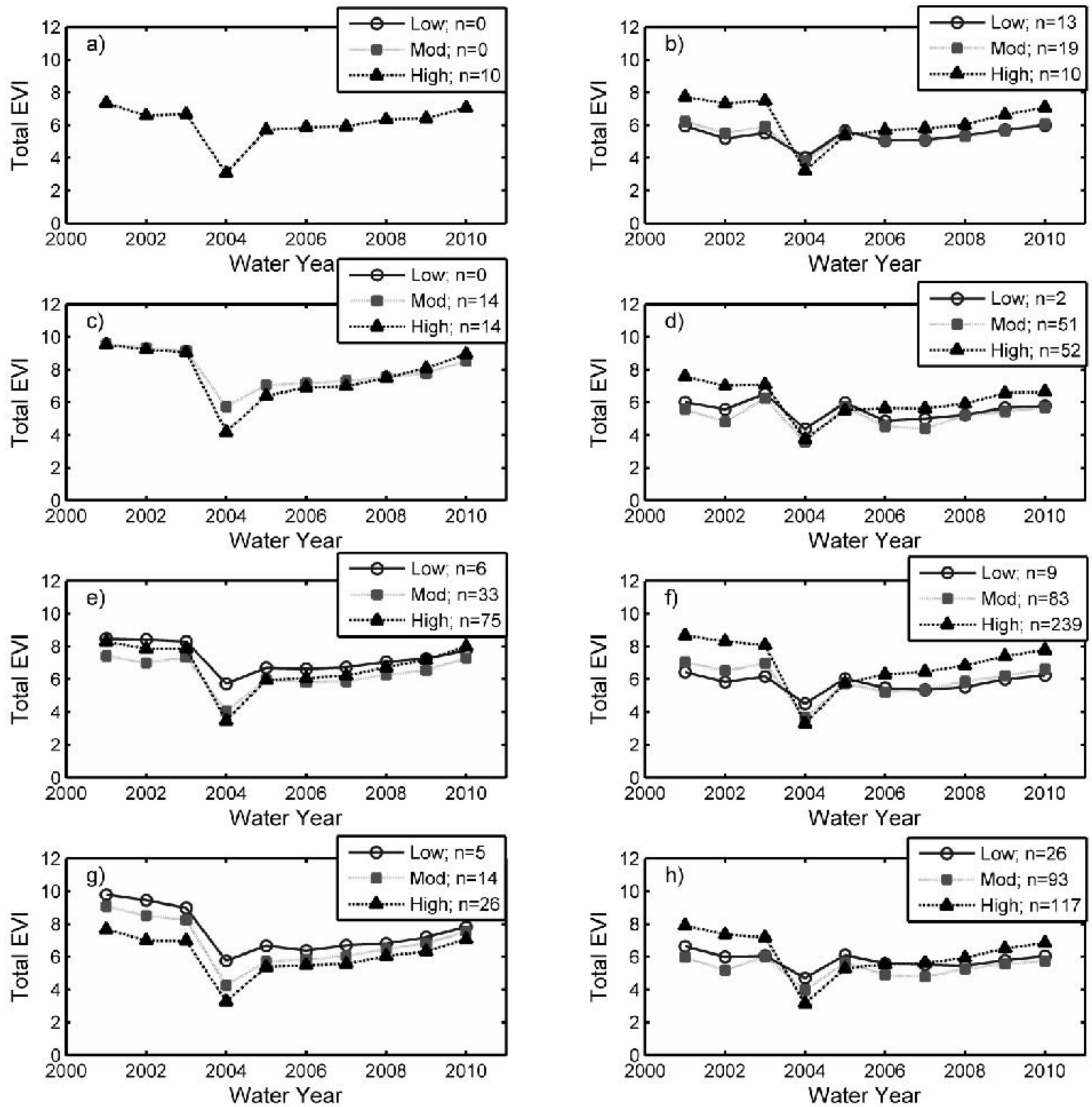

Figure 4-5: Annual total EVI for each year with respect to aspect and burn severity levels for Devil Canyon north aspect (a), east aspect (c), south aspect (e), and west aspect (g); and for City Creek north aspect (b), east aspect (d), south aspect (f), and west aspect (h). Numbers of pixels (n) is indicated for each burn severity level within each studied aspect.

Table 4-4 shows the percent recovery for each post-fire year for each aspect and burn severity relative to the pre-fire mean. We estimate a (subjective) threshold of ~90% as generally recovered, assuming some uncertainty in pre- and post-fire biomass estimates. The first post-fire year, WY 2004, indicates the initial recovery from the burn. Both watersheds experienced lower than average annual precipitation totals during this first wet season (260 mm and 355 mm for Devil Canyon and City Creek, respectively). Overall, recovery values range from 39% (south aspect, high burn in City Creek) to ~75% (west aspect, low burn in City Creek) during the first year. As expected, low burn pixels show the largest recovery during the first year (70% on average) and high burn pixels show the lowest recovery (43% average).

Table 4-4: Devil Canyon and City Creek percent annual total EVI recovery for each water year with respect to aspect and burn severity, where greater than 90% is assumed to be recovered to pre-fire vegetation conditions

		Devil Canyon % yearly EVI			City Creek % yearly EVI		
		Burn Severity			Burn Severity		
Aspect	**Water Year**	**Low**	**Moderate**	**High**	**Low**	**Moderate**	**High**
North	**2004**	---	---	45	73	64	43
	2005	---	---	83	102	94	71
	2006	---	---	85	91	86	76
	2007	---	---	86	92	86	77
	2008	---	---	92	97	90	80
	2009	---	---	93	103	96	89
	2010	---	---	103	108	103	94
East	**2004**	---	61	45	72	65	52
	2005	---	76	69	99	104	76
	2006	---	77	74	81	82	78
	2007	---	78	75	83	79	78
	2008	---	81	81	87	94	82
	2009	---	83	87	94	98	91
	2010	---	91	97	96	103	92
South	**2004**	68	56	43	73	53	39
	2005	80	83	74	98	84	69
	2006	79	80	76	89	76	75
	2007	80	81	78	87	78	77
	2008	84	86	84	90	86	82
	2009	86	90	90	97	91	89
	2010	92	100	100	102	97	93
West	**2004**	61	49	46	75	69	42
	2005	71	66	75	98	99	71
	2006	68	68	76	90	86	74
	2007	71	70	77	89	84	75
	2008	72	75	84	87	92	79
	2009	76	79	88	93	97	87
	2010	83	88	98	97	100	91

Moisture availability during the extremely wet second post-fire year (2005) accelerated vegetation activity in nearly all burn severity levels across all aspects, bringing biomass back up to 80-100% of pre-burn levels. In City Creek, the south low burn severity pixels are generally comparable to pre-fire values. However, the surge in vegetation activity is not sustained for the following post-fire years and after WY 2005, vegetation generally returns to a reduced recovery rate, with a slower increase of biomass through the next three study years (WY 2006 to 2010).

The majority of aspect and burn severities in both watersheds return to around 90% of the pre-fire vegetation by 2010, with the exception of Devil Canyon, where the limited number of pixels introduces more uncertainty in observed recovery trends. In City Creek, all aspects range from 91-107% recovered by the end of 2010, where the majority of observed pixels are in the south and west aspects (331 and 236 pixels, respectively; Figure 4-6). This indicates that detected vegetation biomass has met or exceeded the pre-fire amount. However, it is important to note that the high burn severity in all aspects just reach 90% by 2010. The north aspect pixels are back to pre-fire conditions in both watersheds and show at least 90% recovery a year or two earlier than the other aspects. All other aspects (south, west, east) appear, on average, about 75-85% recovered by WY 2008, with high burn severity pixels on the low end of this range. In Devil Canyon, the north high burn severity shows greater than 90% by 2008. The east and west aspects tend to recover by 2010, however, the west aspect does not appear to be recovered (83-98%) across the three burn severities.

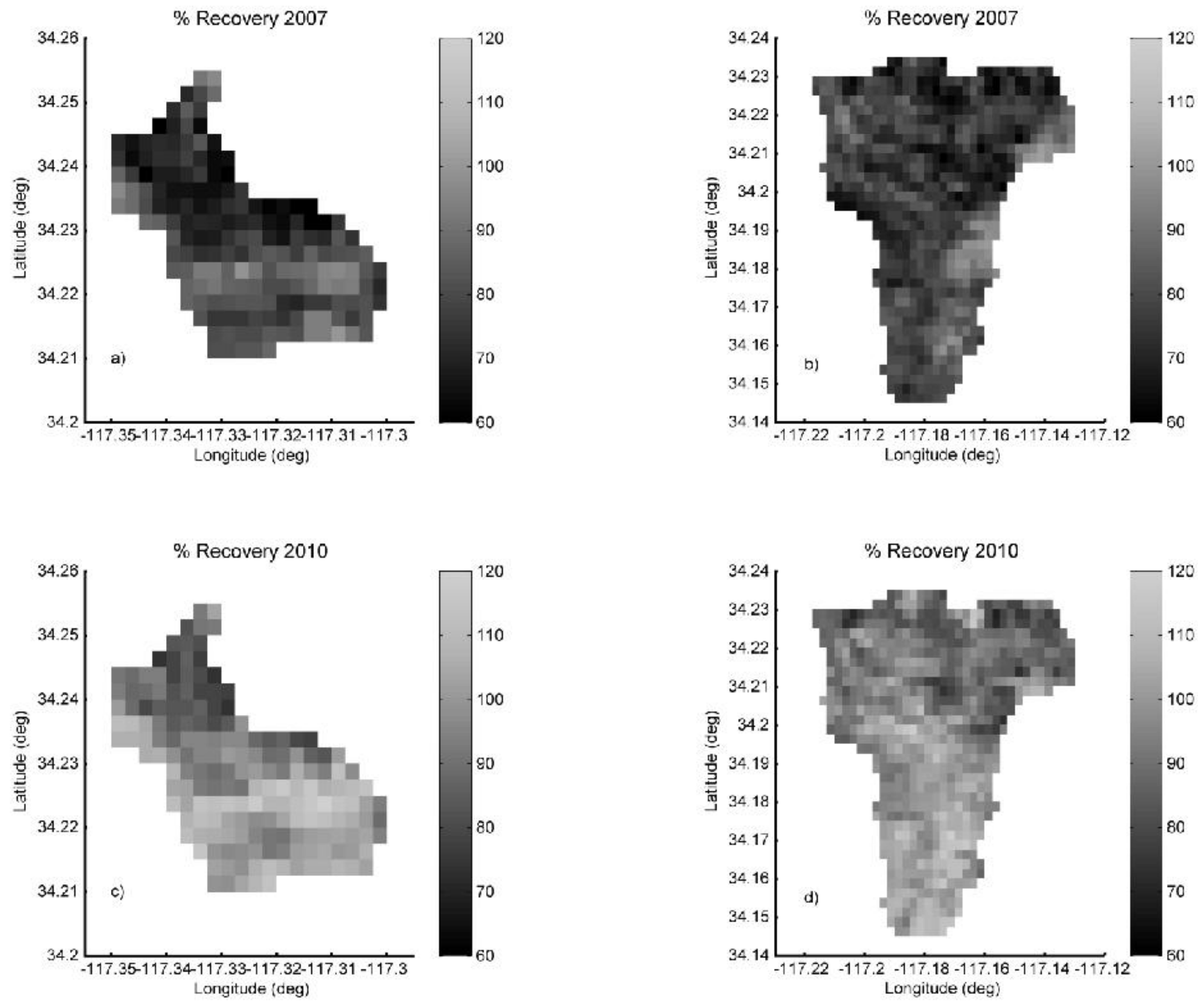

Figure 4-6: Percent spatial recovery for Devil Canyon for WY 2007 (a) and WY 2010 (c) and for City Creek for WY 2007 (b) and WY 2010 (d). Results are relative to the pre-fire mean. Pixels greater than 90% of the pre-fire average are considered recovered.

The recovery slopes (β_1 from Equation 3) for all aspects and burn severities are estimated and plotted for Devil Canyon and City Creek (Figure 4-7). The parameter β_1 represents the rate of biomass recovery relative to the initial loss (year 1). Overall recovery appears greatest (steeper slope) in the high burn pixels and lower in the moderate and low burn severities (Figure 4-7). The high burn pixels experience greater initial vegetation loss, which ultimately constrains recovery and suggests a pre-disposition to return to initial biomass conditions. Low and moderate burn severity pixels experience low and medium (respectively) recovery rates as the vegetation biomass begins to stabilize or reach pre-fire vegetation amounts. This observation is consistent across both watersheds. Established recovery rates (β_1) rates were analyzed with and without WY 2005 and minimal difference in overall recovery rates were noted. As highlighted previously in Figure 4-5, initial pre-fire biomass, and burn severity appear to dominate overall recovery rate in the two watersheds, and less long-term influence is noted from the observed variability in post-fire climatology.

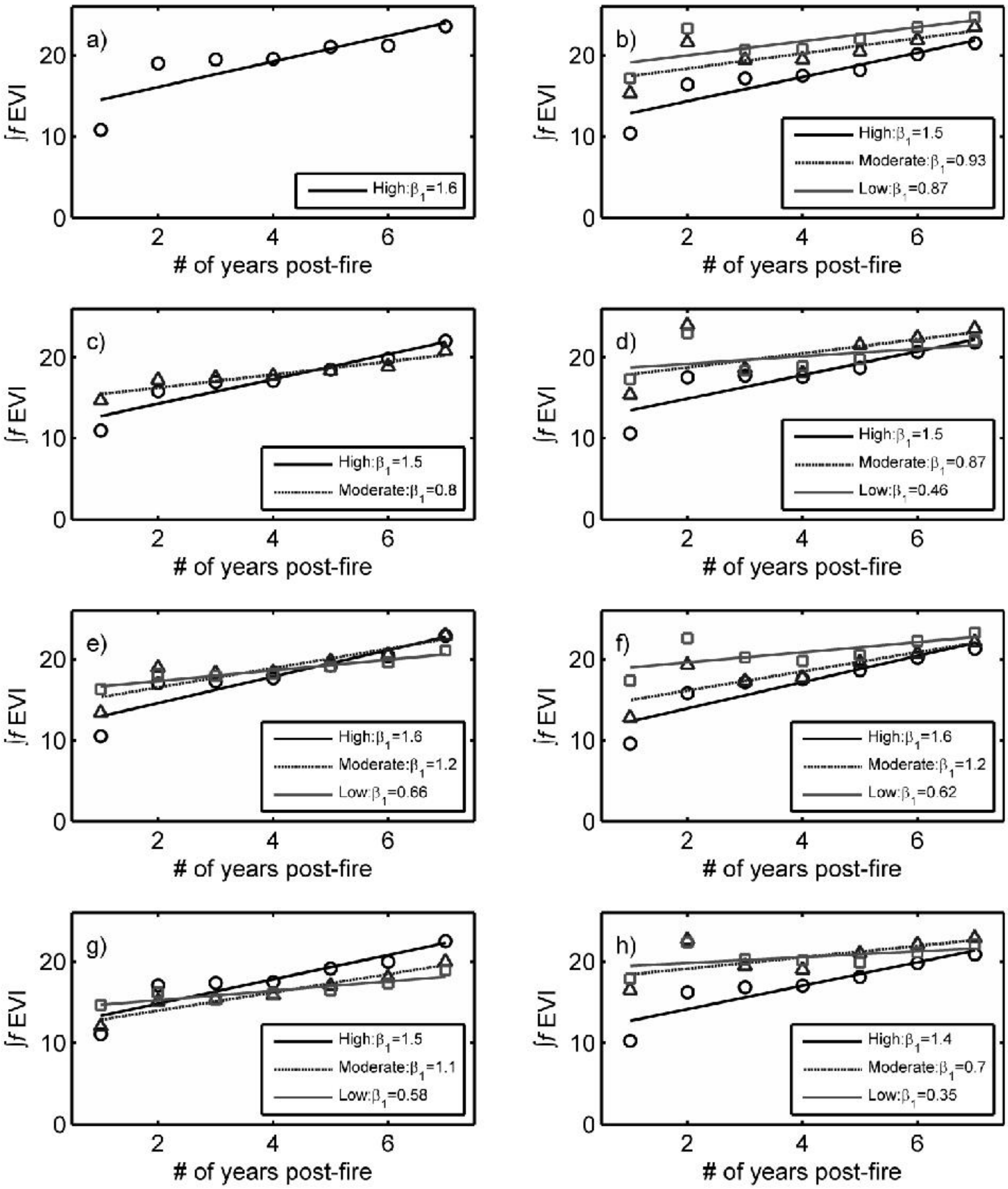

Figure 4-7: Recovery slopes (regression line, β1, from Equation 3) for the normalized EVI time series: Devil Canyon north (a), east (c), south (e), and west (g) and City Creek north (b), east (d), south (f), and west (h). Each burn severity level (low, moderate, high) is plotted for each aspect. Note: In Devil Canyon, EVI values do not exist for north low or moderate and east low burn pixels. The first post-fire year corresponds to WY 2004.

In addition to temporal EVI analysis, selected spatial recovery of EVI for both watersheds was analyzed (Figure 4-6). The percent recovery for each pixel is the total EVI for the year relative to the total pre-fire average (how the total EVI for each pixel has changed since pre-fire). For 2007, the percent recovery generally ranges from 60-80% in both watersheds. The lower recovery percentages align with the high burn areas and the mixed forest vegetation (Figures 4-6a and 4-6b). By 2010, the spatial percent recovery for both watersheds is dramatically different. The recovery percents are predominantly 90%, with the upper elevations (mixed conifer) still showing the lowest recovery. We hypothesize that the lower recovery at the top of the watershed, where steeper slopes and larger vegetation dominate (mixed forest versus chaparral), is contributing to prolonged increased runoff, especially during the summer period.

4.4 Conclusions

Evaluation of coupled ecologic and hydrologic recovery in post-fire systems over longer time periods in semi-arid regions has not been well-documented. The current study integrates a common vegetation index (EVI) and hydrologic data streams to simultaneously evaluate ecosystem and hydrologic dynamics for two burned watersheds affected by wildfire in October of 2003. The evaluation of vegetation biomass (EVI) in relation to factors such as slope aspect, burn severity and hydrologic timeseries over an extended period provides insight on the spatial variability of post-fire processes and ultimately, parameters controlling recovery patterns in each system. Primary findings from our investigations include:

- There is observed increase in discharge in both post-fire systems, especially in the dry season period. Distribution frequencies demonstrate that despite similar pre- and post-fire precipitation regimes, overall discharge patterns are significantly elevated over the seven-year study period, especially in the smaller, steeper Devil Canyon watershed. Similarly, the slower recovery of vegetation at the top of the watersheds (steeper) is contributing to prolonged increased runoff. The increased dry season flow supports our understanding that plant water consumption (ET) and flow pathways within the basin were significantly during the fire and are generally not back to pre-fire behavior by the end of WY 2010.

- The MODIS EVI product provides key information on pre-fire vegetation biomass and recovery cycles in post-fire watersheds, both temporally and spatially. In the studied systems, the south, east, and west facing slopes show higher pre-fire EVI values and annual totals, likely due to higher radiative forcing (conditions governed by solar radiation), facilitating increased plant growth during the growing season. In terms of recovery rates, higher pre-fire biomass appears correlated with larger EVI loss and significant initial deficits in vegetation mass. We advocate that this implies a longer return period for the original vegetation species (i.e. chaparral rather than short-term grass recovery). South (and west) slopes also show the lowest percent recovery by the end of the study period compared to pre-fire conditions. City Creek north and east slope aspects reach pre-fire conditions earlier than the south and west aspects, likely due to retained soil moisture (also noted in Casady et al., 2009).
- The low severity burn pixels for all aspects return to pre-fire levels relatively quickly, while high severity burn pixels show the lowest overall recovery by WY 2010 especially in City Creek (Table 4-4). High burn severities tend to show the largest recovery rates (β_1), attributed to the greater initial loss (Figure 4-7) and potential for biomass regrowth (available root structure, seed release for new plant growth, etc.) but are still not back to pre-fire conditions (Figure 4-5 and 4-7). Our results indicate that overall recovery in the

two watersheds is heavily influenced by the aspect and burn severity of each pixel, and less influenced by short-term climate conditions.

The extreme wet season during the post-fire period resulted in higher EVI values. However, vegetation response from precipitation spikes may not be conducive to, or representative of full or permanent recovery of the watershed vegetation. Shallow-rooted systems (e.g., grasses) likely appear after these heavy rain events in the immediate post-fire period and are detected by the MODIS EVI product, contributing to higher annual total EVI). However, vegetation behavior (i.e. ET response) is not similar to pre-fire conditions (evidenced by the EVI patterns/cycles and coupled hydrologic response). The growth of grasses is shown to alter the normal (pre-fire) water demand in a system (Prater and DeLucia, 2006; Schenk and Jackson, 2002). Grasses also have different spectral signatures, resulting in different EVI values (Huete et al., 2002). Despite the inability to document specific plant species, we advocate that the MODIS-based EVI adds significant insight into seasonal vegetation recovery and potential ET demand.

In summary, of the variables investigated in this study, longer-term hydrologic recovery appears more dependent on burn severity, slope aspect and vegetation type, and less dependent on short-term climatologic events. In addition, initial biomass appears to be the primary factor influencing burn severity, recovery potential, and overall recovery rates. Despite the general recovery of the north aspect and low burn severity areas, vegetation activity and hydrologic behavior are not back to pre-fire conditions after a seven-year period for the two systems studied. Although the difference in pixel numbers (significantly fewer observations in Devil Canyon) and slightly different fire history may influence comparisons between City Creek and Devil Canyon, recovery patterns are generally consistent in both watersheds, and significantly, high burn severity pixels (in any aspect in either watershed) just return within pre-fire ranges (~90%) by the end of the study period. Hydrologic behavior is still altered from pre-fire conditions, and it appears that the high burn pixels, particularly in the upper portion of the watershed, are exerting significant control on post-fire hydrologic recovery. Given the established recovery rates and observed patterns in both watersheds, we estimate that seasonal streamflow patterns will return to pre-fire levels when the high burn areas (across all aspects) have stabilized to pre-fire biomass conditions. Finally, the observed variability in post-fire discharge and precipitation demonstrates the importance of studying seasonal and sub-annual timescales over extended post-fire periods. The simultaneous exploration of vegetation biomass (EVI), slope-aspect, burn severity, and regional climate patterns provides insight on the spatial and temporal controls on hydrologic processes, and, ultimately, will assist in hydrologic predictions and watershed management over extended post-fire periods.

4.5 References

Box, G. E. P. and D.R. Cox, 1964. An analysis of transformations. Journal of the Royal Statistical Society, Series B26 (2): 211–252

Chen, X., Vierling, L., Deering, D., and Conley, A., 2005. Monitoring boreal forest leaf area index across a Siberian burn chronosequence: a MODIS validation study. International Journal of Remote Sensing 26(24): 5433-5451.

Casady, G.M., Leeuwen, W.J.D., Marsh, S.E., 2009. Evaluating Post-wildfire Vegetation Regeneration as a Response to Multiple Environmental Determinants. Environmental Model Assessment DOI: 10.1007/s10666-009-9210-x.

Cydzik, K. and T.S. Hogue, 2009. Modeling Post-fire Response and Recovery using the Hydrologic Engineering Center Hydrologic Modeling System (HEC-HMS), Journal of the American Water Resources Association, 45(3):702-714.

Debano, L.F., 2000. The role of fire and soil heating on water repellency in wildland environments: a review. Journal of Hydrology 231-232: 195-206.

Diaz-Delgado, R., Salvado, R, and Pons, X., 1998. Monitoring of plant community regeneration after fire by remote sensing. In: Traboud, L. (Ed.), Fire management and landscape ecology. International Association of Wildland Fire, Fairfield, WA, pp. 315-324.

Diaz-Delgado, R., Lloret, F., Pons, X., Terradas, J., 2002. Satellite evidence of decreasing resilience in Mediterranean plant communities after recurrent wildfires. Ecology 83(8): 2293-2303.

Duguy, B. and Vallejo, V.R., 2008. Land-use and fire history effects on post-fire vegetation dynamics in eastern Spain. Journal of Vegetation Science 19: 97-108.

Gao, X., Huete, A.R., Ni, W., and Miura, T., 2000. Optical-Biophysical Relationships of Vegetation Spectra without Background Contamination. Remote Sensing of Environment 74: 609-620.

Gitelson, A.A., Kaufman, Y.J., and Merzlyak, M.N., 1996. Use of a Green Channel in Remote Sensing of Global Vegetation from EOS-MODIS. Remote Sensing of Environment 58: 289-298.

Gonzalez-Pelayo, O., Andreu, V., Campo, J., Gimeno-Garcia, E., and Rubio, J.L., 2006. Hydrological properties of a Mediterranean soil burned with different fire intensities. Catena 68: 186-193.

Hogue, T.S., Sorooshian, S., and Gupta, H., 2000. A Multistep Automatic Calibration Scheme for River Forecasting Models. Journal of Hydrometeorology 1(6): 524-542.

Horton, J. S., and C. J. Kraebel. 1955. Development of Vegetation after Fire in the Chamise Chaparral of Southern California. Ecology 36:244–262.

Hromadka, T.V., 1986. San Bernardino County Hydrology Manual. San Bernardino Flood Control District, San Bernardino, California.

Huete, A., Didan, K., Miura, T., Rodriguez, E.P., Gao, X., and Ferreira, L.G., 2002. Overview of the radiometric and biophysical performance of the MODIS vegetation indices. Remote Sensing of Environment 83: 195-213.

Ice, G.G., Neary, D.G., and Adams, P.W., 2004. Effects of Wildfire on Soils and Watershed Processes. Journal of Forestry 16-20.

Jonsson, P. and Eklundh, L., 2004. TIMESAT – a program for analyzing time-series of satellite sensor data. Computers and Geosciences 30: 833-845.

Jung, H., Hogue, T.S., Rademacher, L., and Meixner, T., 2009. Impact of Wildfire on Source Water Contributions in Devil Creek, CA: Evidence from End-member Mixing Analysis. Hydrological Processes 23: 183 – 200.

Keeley, J.E., Sterling, C.K., 1981. Post-fire Regeneration of Southern California Chaparral. American Journal of Botany 68(4):524-530.

Keeley, J.E., Fotheringham, C.J., and Moritz, M.A., 2004. Lessons from the October 2003 Wildfires in Southern California. Journal of Forestry 102(7) 26-31.

Keeley, J.E., Fotheringham, C.J., and Baer-Keeley M., 2005. Determinants of Postfire Recovery and Succession in Mediterranean-Climate Shrublands of California. Ecological Applications 15(5): 1515-1534.

Keeley, J.E., Brennana, T., and Pfaff, A.H., 2008. Fire Severity and Ecosystem Responses Following Crown Fires in California Shrublands. Ecological Applications 18(6): 1530-1546.

Key C.H., Benson C.N., 2004. Landscape Assessment (LA) Sampling and Analysis Methods. FIREMON Landscape Assessment.

Matsushita, B., Yang, W., Chen, J., Onada, Y., and Qiu, G., 2007. Sensitivity of the Enhanced Vegetation Index (EVI) and Normalized Difference Vegetation Index (NDVI) to Topographic Effects: A Case Study in High-Density Cypress Forest. Sensors 7: 2636-2651.

Mays, L.W., 2001. Water Resources Engineering. John Wiley & Sons, Hoboken, New Jersey.

McMichael, C.E., Hope, A.S., and Loaiciga, H.A., 2006. Distributed hydrological modeling in California semi-arid shrublands: MIKE SHE model calibration and uncertainty estimation. Journal of Hydrology 317: 307-324.

McMichael, C.E., Hope, A.S., Roberts, D.A., and Anaya, M.R., 2004. Post-fire recovery of leaf area index in California chaparral: a remote sensing-chronosequence approach. International Journal of Remote Sensing 25(21): 4743-4760.

Meixner T., Wohlgemuth, P. 2003. Climate variability, fire, vegetation recovery, and watershed hydrology. In Proceedings of First Inter-Agency Conference on Research in the Watersheds, Benson, Arizona 651-656.

Minnich, R.A., 1988. The biogeography of fire in the San Bernardino Mountains of California: a historical study. University of California Publications in Geography 28:1-121.

Moody, J.A., Martin, D.A., Haire, S.L., and Kinner, D.A., 2007. Linking runoff response to burn severity after a wildfire. Hydrological Processes 22: 2063-2074.

Myneni, R.B., Maggion, S., Iaquinta, J., Privette, J.L., Gobron, N., Pinty, B., Kimes, D.S., Verstraete, M.M., and Williams, D.L., 1995. Optical Remote Sensing of Vegetation: Modeling, Caveats, and Algorithms. Remote Sensing of Environment 51: 169-188.

NOAA, 2003. National Oceanographic and Atmospheric Administration's Coastal Services Center. Southern California 2000-Era Land Cover/Land Use Metadata. http://www.csc.noaa.gov.

NOAA, 2009a. National Oceanic and Atmospheric Administration, The Second Wettest Rainfall Season in Los Angeles come to an End. Public Information Statement. National Weather Service, Oxnard, CA.

NOAA, 2009b. National Oceanic and Atmospheric Administration's National Weather Service. The Climate of Los Angeles, California.

NOAA, 2009c. National Oceanic and Atmospheric Administration's National Weather Service. Water Year Rainfall for Downtown Los Angeles (1877-78 thru 2005 Seasons).http://www.weather.gov/climate/.

Pierson, F.B., Robichaud, P.R., Moffet, C.A., Spaeth, K.E., Hardegree, S.P., Clark, P.E., Williams, C.J., 2008. Fire effects on rangeland hydrology and erosion in a steep sagebrush-dominated landscape. Hydrological Processes 22: 2916-2929.

Prater, M.R. and DeLucia, E.H., 2006. Non-native grasses alter evapotranspiration and energy balance in Great Basin sagebrush communities. Agricultural and Forest meteorology 139:154-163.

Pausas, J.G, 2003. The effect of landscape pattern on Mediterranean vegetation dynamics: A modeling approach using functional types. Journal of Vegetation Science 14: 365-374.

Riano, D., Chuvieco, E., Ustin, S., Zomer, R., Dennison, P., Roberts, D., and Salas, J., 2002. Assessment of vegetation regeneration after fire through multitemporal analysis of AVIRIS images in the Santa Monica Mountains. Remote Sensing of Environment 79: 60-71.

Roder, A., Hill, J., Duguy, B., Alloza, J.A., and Vallejo, R., 2008. Using long time series of Landsat data to monitor fire events and post-fire dynamics and identify driving factors. A case study in the Ayora region (eastern Spain). Remote Sensing of Environment 112(1): 259-273.

Schenk, H.J., Jackson, R.B., 2002. Rooting depths, lateral spreads, and below-ground/above-ground allometries of plans in water limited ecosystems. Ecology 90: 480-494.

USDA Forest Service, 2007. Slide Fire occurring on the San Bernardino National Forest – 2007 Geospatial_Data_Presentation_Form: raster digital data. http://activefiremaps.fs.fed.us/baer/download.php?year=2007

Wittenberg, L. and Inbar, M., 2009. The Role of Fire Disturbance on Runoff and Erosion Processes – a Long-Term Approach, Mt. Carmel Case Study, Israel. Geographical Research 47(1): 46-56.

Wittenberg, L., Malkinson, D., Beeri, O., Halutzy, A., and Tesler, N., 2007. Spatial and temporal patterns of vegetation recovery following sequences of forest fires in a Mediterranean landscape, Mt. Carmel Israel. Catena 71: 76-83.

Chapter 5. Investigating Triangle-Based ET Algorithms for Post-Fire Systems

5.1 Introduction

Increasing wildfires at the wildland-urban interface (WUI) are a concern to local populations and management communities. Post-fire consequences, such as debris flows, flooding, and degraded water quality, require accurate hydrologic modeling and prediction, especially in semi-arid regions, where water availability is already limited. Hydrologic systems affected by fire can be altered for more than eight years post-fire (Kinoshita and Hogue, 2011). Typical post-fire studies focus on vegetation or hydrologic recovery, and few examine the relationship between the two disciplines. Studies that concentrate on vegetation recovery generally utilize plot-scale or low temporal resolution remote sensing (Horton and Kraebel, 1955; Keeley and Sterling, 1981; McMichael et al., 2006; Keeley et al., 2008; Roder et al., 2008). Few studies have incorporated timeseries of remotely sensed vegetation indices in post-fire studies (Wittenberg, et al., 2007; Casady et al., 2009), but these data are necessary for understanding seasonal and annual variations in post-fire recovery (Kinoshita and Hogue, 2011).

Remote sensing variables enable continuous monitoring of ungaged or inaccessible watersheds at high spatial and temporal resolution and are well tested in unburned semi-arid regions. Incorporation of higher temporal and spatial resolution data streams will improve post-fire recovery models and predictions. NASA's Moderate Resolution imaging Spectrum (MODIS) has two satellites Aqua and Terra that capture images of the Earth with spatial resolutions that range from 250 meters to 1 kilometer and temporal resolutions that range from daily to 16-day averages. MODIS Aqua and Terra have 36 spectral bands from which land and cryosphere variables are estimated. Variables like evapotranspiration (ET) and soil moisture (SM) are important variables within the hydrological water budget, but are amongst the most difficult to retrieve. Traditionally, both variable measurements are ground-based and have limited coverage. Many studies have incorporated remote sensing for development of hydrological products over large spatial and ungaged areas (Jiang and Islam, 2003; Kim and Hogue, 2008; 2012; 2012b).Various studies have worked towards developing ET estimates based on remote sensing of land surface characteristics. The primary approaches to estimating ET are through the energy balance residual method or the evaporative fraction method. Key schemes that have been developed include the Surface Energy Balance Algorithm for Land (SEBAL) (Bastiaanssen et al., 1998; Kim and Hogue, 2012b), Mapping EvapoTranspiration at high Resolution with Internalized Calibration (METRIC) (Allen et al., 2007), Atmosphere-Land Exchange Inverse (ALEXI) (Norman et al., 1995) and the Triangle method (Gillies and Carlson, 1995; Nishida et al., 1995; Jiang and Islam, 2003). More recent models are moving away from integration of ground-based meteorological and remote sensing products towards purely remote sensing estimations (Gillies and Carlson, 1995; Nishida et al., 1995; Jiang et al., 2003, 2004; Nishida et al., 2003; Kim and Hogue, 2012). However, these models are calibrated for specific sites and not readily transferrable. To date, application of these models and products to post-fire sites has not been done, but these data have the potential to provide key information for post-fire water resource management.

After fire, affected areas experience significant loss in vegetation, altering evaporative fluxes and water budget dynamics until vegetation is recovered or replaced. Soil moisture is an important indicator of the water content of the soil and influences the exchange of water and heat energy between land and atmosphere. The relationship between ET and soil moisture and long-term hydrological recovery at high spatial and temporal resolution has not been explored and we advocate that remote sensing data streams using previously developed methods can provide estimation and monitoring of post-fire water budgets.

Prompted by the uncertainty in long-term, post-fire hydrologic response, Kinoshita and Hogue (2011) investigated controlling variables and establish a strong relationship between vegetation and hydrologic recovery using remote sensing. The current study seeks to incorporate more remote sensing variables and products in the post-fire setting for continuous monitoring of hydrologic recovery. Our work will build upon previously developed methods for estimating high resolution ET (Kim and Hogue, 2008, 2012) and soil moisture (Kim and Hogue, 2012). Many triangle methods have been developed and applied to hydrological variables such as ET and soil moisture. A key component of these methods is defining an appropriate triangle and related parameters over the chosen study domain to reflect variations in temperature for a range of vegetation to establish evaporative cooling. The semi-arid climate and homogenous vegetation type (mostly chaparral) of southern California presents a relatively insensitive triangle over the region. We hypothesize that the triangle method will need enhancement and calibration for utilization in the region, and especially over burned watersheds. The goals of this preliminary work include determining an appropriate triangle method that will provide a representative evaporative fraction for the Arroyo Seco, a southern California watershed affected by the 2009 Station Fire and estimating pre- and post-fire ET for the study period. Findings from this study will be used to develop longer-term timeseries of ET (2002-2012) and to develop a timeseries of downscaled soil moisture(AMSR-MODIS product), which will enable us to develop improved estimates of pre- and post-fire water balance for disturbed systems in southern California.

5.2 Methods

5.2.1 Study Area

We investigate hydrologic and ecologic recovery in Arroyo Seco, an urban-fringe watershed located in the Angeles National Forest in the San Gabriel Mountains of southern California, northeast of downtown Los Angeles (Figure 5-1). The hydrology and vegetation of southern California are influenced by periodic El Nino events. El Nino typically brings cooler, wetter weather, and encourages vegetation growth. Southern California also experiences hot and dry Santa Ana Winds in the fall, which move air from the desert to the ocean. The cyclical vegetation growth and drying out make southern California one of the worst fire regimes in the country. The Station Fire (26 September 2009 – 16 October 2009) in 2009 is the largest fire in Los Angeles County record. It burned over 160,000 acres and caused over a billion dollars in suppression and damage. The Arroyo Seco was completely burned (mostly moderate severity) by the Station Fire.

The Arroyo Seco is approximately 41 km^2 and receives an average of 760 mm of precipitation a year (Los Angeles County). The Arroyo Seco is a steep watershed with an elevation range from approximately 430 m to 1877 m and a watershed slope of 6% (USGS Digital Elevation Map).The Arroyo Seco consists of a mixture of hydrologic soil groups A (1%), B (29%), C (34%), and D (36%) (USDA Natural Resources Conservation Service). The Arroyo Seco is primarily shrubland (71%) and forest (23%), with a mix of developed, barren, and herbaceous land cover (6%) (National Land Cover Database, 2006).

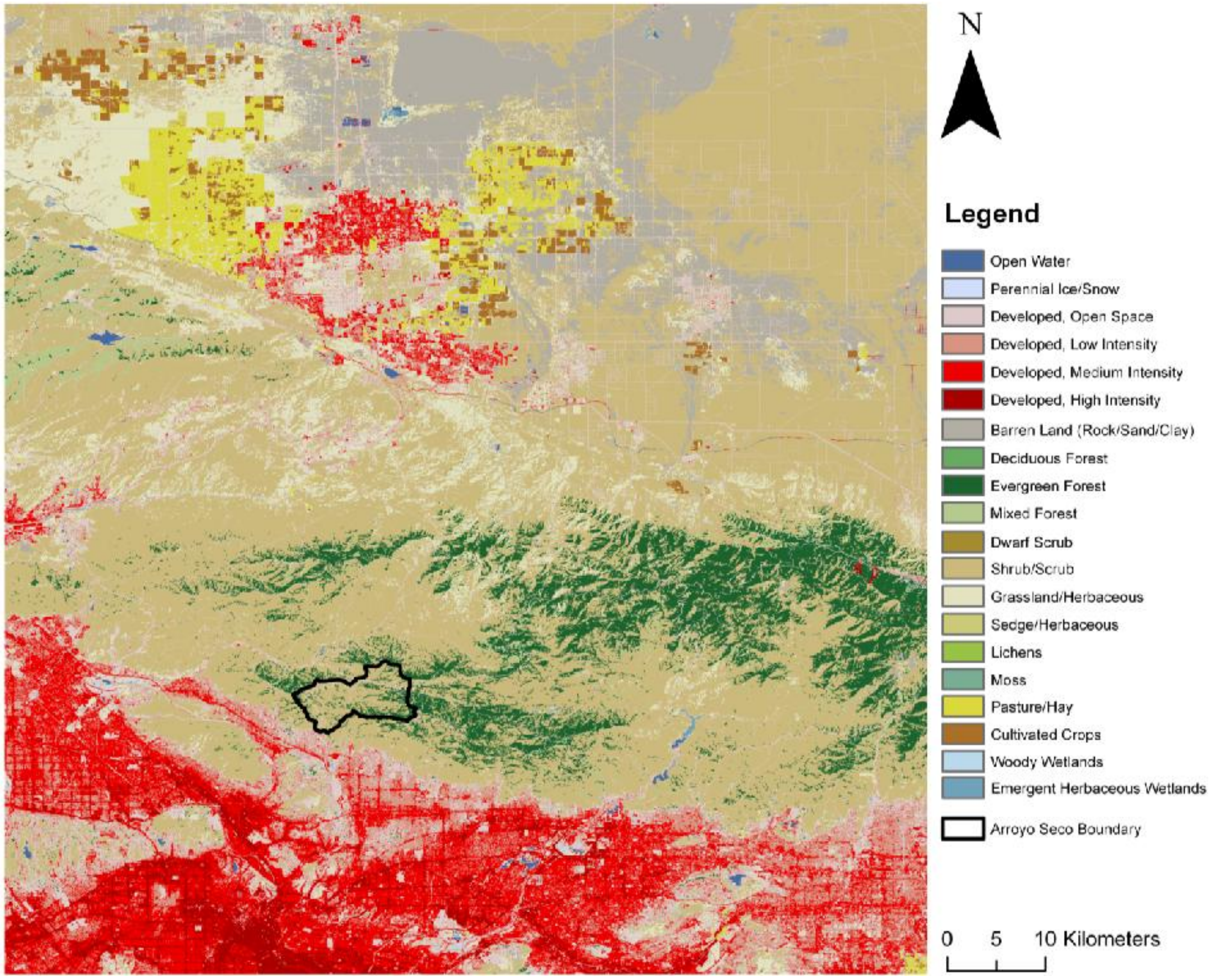

Figure 5-1: Landcover for the Arroyo Seco watershed and surrounding areas. The domain of landcover shown is 1º by 1.5º (34 to 35ºand -118.5º to -117) and is used for the triangle method.

5.2.2 In situ variables

Observed Hydrology

Precipitation data for Arroyo Seco is estimated from three Los Angeles County gages (280c, 47d, and 56b) distributed just outside the basin, but representing low, middle, and high elevations for water years 2006 to 2010. USGS discharge data is available at the outlet of Arroyo Seco (gage 11098000) at 426 meters. Mean daily averages are used for the study period 2006-

2010. The discharge values are transformed using the Box-Cox transformation for visualization of low and high flows. The transformed flow is estimated as follows (Box and Cox, 1964):

$$Q_t = \frac{(Q+1)^{\lambda} - 1}{\lambda}$$

Equation 5-1

where

λ= 0.3 (Hogue et al., 2000)

California Irrigation management Information System

The California Irrigation management Information System (CIMIS) manages a network of over 120 weather stations in California. CIMIS weather stations collect and record seven meteorological variables (solar radiation, air temperature, soil temperature, relative humidity, wind speed, wind direction, and precipitation) and calculate six variables (net radiation, reference evapotranspiration, wind rose, wind cubed, vapor pressure, and dew point temperature). Reference ET (ET_o) is the evapotranspiration from standardized well-watered maintained grass or alfalfa surfaces. The CIMIS ET_o values are based on a modified Penman-Monteith equation (Equation 5-2):

$$ET_o = \frac{\Delta(R_n - G)}{\lambda\left[\Delta + \gamma(1 + C_d U_2)\right]} + \frac{\gamma \frac{37}{T_a + 237.16} U_2 (e_s - e_a)}{\Delta + \gamma(1 + C_d U_2)}$$

Equation 5-2

where:

ET_o= grass reference evapotranspiration [mm h^{-1}]

Δ = slope of saturation vapor pressure curve [kPa $^{\circ}C^{-1}$] at mean air temperature (T) in ºC

R_n = net radiation [MJ m^{-2} h^{-1}]

G = soil heat flux density [MJ m^{-2} h^{-1}]

γ = psychrometric constant [kPa $^{\circ}C^{-1}$]

T_a = mean hourly air temperature [ºC]

U_2 = wind speed at 2 meters [m s^{-1}]

e_s = saturation vapor pressure [kPa] at the mean hourly air temperature (T) in ºC

e_a = actual vapor pressure [kPa] at the mean hourly air temperature (T) in ºC

λ = latent heat of vaporization in [MJ kg^{-1}]

C_d = bulk surface resistance and aerodynamic resistance coefficient

The Glendale CIMIS station's (#133) net radiation and ETo (grass surface) is used for comparison with the Arroyo Seco. The Glendale station is located at an elevation of 388 meters southwest of the Arroyo Seco watershed outlet (426 meters).

5.2.3 Remote sensing variables

Enhanced vegetation index

To detect the amount of vegetation present during pre- and post-fire periods, MOD13Q1 is acquired from NASA's Earth observing System Data and Information System (EOSDIS) Reverb, whose database consists of various atmospheric, hydrologic, and energy variables that can be applied to global vegetation observations, hydrologic modeling, and other management applications. EVI measures the greenness of vegetation and is used as an indicator of the amount of vegetation biomass present. The MOD13Q1 product has a temporal resolution of 16 days and a spatial resolution of 250 meters and contains the red, near infrared, blue, mid-infrared, view zenith angle, sun zenith angle, relative azimuth, and calculated NDVI, EVI, and relevant QA (quality analysis) data (Huete et al., 2002; Chen et al., 2005). EVI data is collected from 2006-2010 and the equation used to derive the EVI product from MOD13Q1 is noted as:

$$EVI = 2.5\left[\frac{\rho_{NIR} - \rho_{RED}}{\rho^*_{NIR} + C_1\rho^*_{NIR} - C_2\rho^*_{BLUE} + L}\right]$$

Equation 5-3

where ρ^*_{NIR} is the near infrared reflectance, ρ^*_{RED} is the red channel reflectance, ρ^*_{BLUE} is the blue channel reflectance, C_1andC_2 are the red and blue correction coefficients for atmospheric resistance, and L is the canopy background brightness correction factor (Huete et al., 2002; Chen et al., 2005).

Evapotranspiration

There are nine MODIS products used to estimate ET, based on Kim and Hogue (2012) (Figure 5-2). These products include: solar zenith angle, relocation, aerosol optical depth, angstrom exponent, water vapor, albedo, total ozone, air temperature, dewpoint temperature, emissivity, surface temperature (LST), enhanced vegetation index, cloud fraction, and cloud optical thickness. The previously developed ET scheme is a combination of MODIS products that incorporates daily available energy (Net Radiation – Ground Heat Flux ($R_n - G$) and an evaporative fraction (EF) based on a triangle method to estimate a daily actual evapotranspiration (Gillies et al., 1995; Jiang and Islam, 2003; Bisht and Bras, 2010; Kim and Hogue, 2008; 2012).

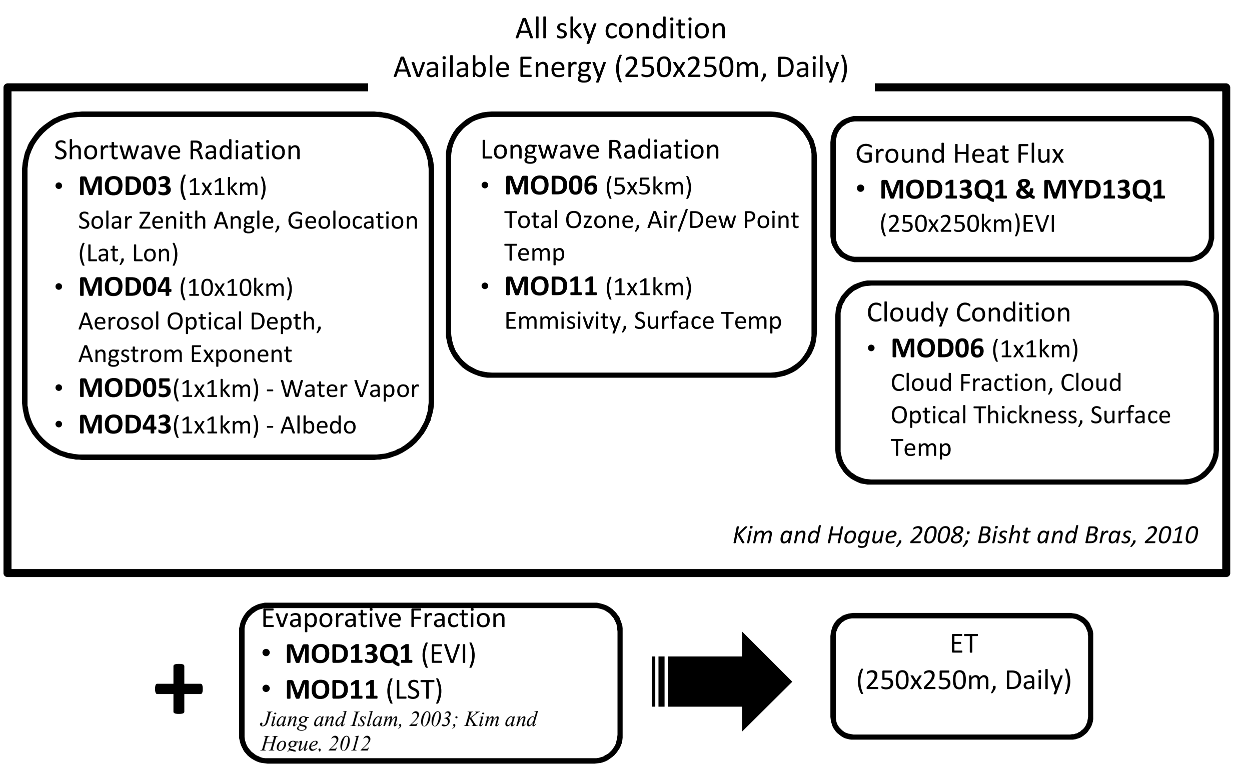

Figure 5-2: MODIS variables used in the ET scheme

Net radiation

Net radiation, the residual of the total incoming and outgoing radiation, is estimated by the combination of various MODIS products (Kim and Hogue, 2008; Bisht and Bras, 2010). It utilizes eight MODIS products to develop net radiation for clear sky conditions (Figure 5-2). Clear sky radiation is estimated as follows:

$$R_{n_{clear}} = (1-\alpha)R_s \downarrow_{clear} + R_l \downarrow_{clear} - R_l \uparrow_{clear}$$

Equation 5-4

Cloudy sky radiation is estimated as follows (Bisht and Bras, 2010; Kim and Hogue, 2012b)

$$R_{n_{cloudy}} = (1-\alpha)R_s \downarrow_{cloudy} + R_l \downarrow_{cloudy} - R_l \uparrow_{cloudy}$$

Equation 5-5

where: α is the surface albedo

$R_s\downarrow_{clear}$ is downward shortwave radiation from a PS (Paulescu and Schlett, 2003) parametric model for clear sky conditions

$R_l\downarrow_{clear}$ is downward longwave radiation from a scheme developed by Brutsaert (1975), using MOD07 (Air Temp) for clear sky conditions

$R_l\uparrow_{clear}$ is upward longwave radiation derived from the Stefan-Boltzmann equation, using MOD11 (LST) for clear sky conditions

$R_s\downarrow_{cloudy}$ is downward shortwave radiation derived using cloud fraction and optical thickness to interpolate between adjacent clear days for cloudy sky conditions (Bisht and Bras, 2010)

$R_l\downarrow_{cloudy}$ is downward longwave radiation derived using the Brutsaert (1975) equation and an inverse distance weighting relationship to back-calculate air temperature from MOD06 for cloudy conditions (Kim and Hogue, 2012b)

$R_l\uparrow_{cloudy}$ is upward longwave radiation derived using the Stefan-Boltzmann equation, by substituting MOD06 (LST) and surface emissivity for daily values for cloudy sky conditions

The net radiation for all sky conditions at satellite overpass time is used to develop a daily average net radiation based on the following sinusoidal function:

$$\overline{R}_n = R_{ni} \times \frac{2}{\pi \sin\left[\left(\frac{t_i - t_{sunrise}}{t_{sunset} - t_{sunrise}}\right)\pi\right]}$$

Equation 5-6

Where $\overline{R}_n$ is daily net radiation and R_i is instantaneous net radiation ($R_{ncloudy}$ *or* R_{nclear}). The sunrise ($t_{sunrise}$) and sunset (t_{sunset}) are obtained from the U.S. Naval Observatory and t_i is the satellite over-passing time.

Ground Heat Flux

To estimate the ground heat flux for semi-arid regions, we use the Moran et al. (1994) relationship, modified by Kim and Hogue (2012b) as follows:

$$\overline{G} = 0.22 \cdot \exp(-1.4EVI) \cdot \overline{R}_n$$

Equation 5-7

Evaporative Fraction

The EF is the ratio of latent heat flux to the available energy at the surface and measures the amount of available energy contributing to latent heat flux. The EF can be written as (Jiang and Islam, 2003):

$$EF = \frac{\lambda E}{R_n - G} = 1 - \frac{\rho C_p}{R_n - G}\frac{1}{r_a}\Delta T$$

Equation 5-8

Where λ is the latent heat of evaporation, E is the evaporation, R_n is the net radiation, and G is the ground heat flux. ρ is the density of air, C_p is the heat capacity of air at constant pressure, r_a is the aerodynamic resistance for heat and momentum transfer, and ΔT is the difference between surface and air temperature. There is small variation in the $\frac{\rho C_p}{R_n - G}\frac{1}{r_a}$ term, so it can be assumed constant and we are able to develop a linear relationship between EF and ΔT (for specific vegetation class). Constructing a trapezoidal space of vegetation index to temperature (Figure 5-3), we can obtain the EF for any point (*i*) within the bounding triangle using the following equation based on Jiang and Islam (2003):

$$EF = 1 - \frac{(1 - \beta EVI)\Delta T}{(1 - EVI)\Delta T_{\max} + EVI \Delta T_e}$$

Equation 5-9

where $\Delta T = T_{MODIS} - T_{min}$, $\Delta T_{max} = T_{max} - T_{min}$, and $\Delta T_e = T_e - T_{min}$ (all temperatures are MODIS surface temperature). The water stress parameter, $\beta = 1 - (\Delta T_e / \Delta T_{max})$ and theoretically ranges from 0 to 1. When β is approximately 0, it is unstressed conditions, and when β is approximately 1, there are fully stressed conditions (Jiang and Islam, 2003). The temperature parameters T_{max}, T_{min}, and T_e are determined from the EVI and temperature triangle/trapezoidal space (Figure 5-3). T_{max} is the maximum MODIS surface temperature within the triangle domain. T_{min} is the minimum MODIS surface temperature within the triangle domain. T_e is the maximum MODIS surface temperature at maximum vegetation coverage (EVI is approximately 1).

The triangle method uses the relationship between vegetation coverage and land surface temperature to estimate EF (Jiang and Islam, 2003). It is based on the concept that bare ground is warmer and as ground cover (vegetation) increases, temperature linearly decreases (Figure 5-3).

The cold edge, where $\Delta T = 0$ (EF = 1), the triangle represents maximum evapotranspiration for all vegetation cover classes. The warm edge (linear regression from minimum evaporation to minimum transpiration) includes dry pixels over the study domain (minimum evapotranspiration for all vegetation cover). There are four vertices, 1) minimum vegetation coverage and maximum temperature (minimum evaporation), 2) minimum vegetation coverage and minimum temperature (max evaporation), 3) maximum vegetation coverage and temperature (minimum transpiration or water stress), and 4) maximum vegetation coverage and minimum temperature (maximum transpiration).

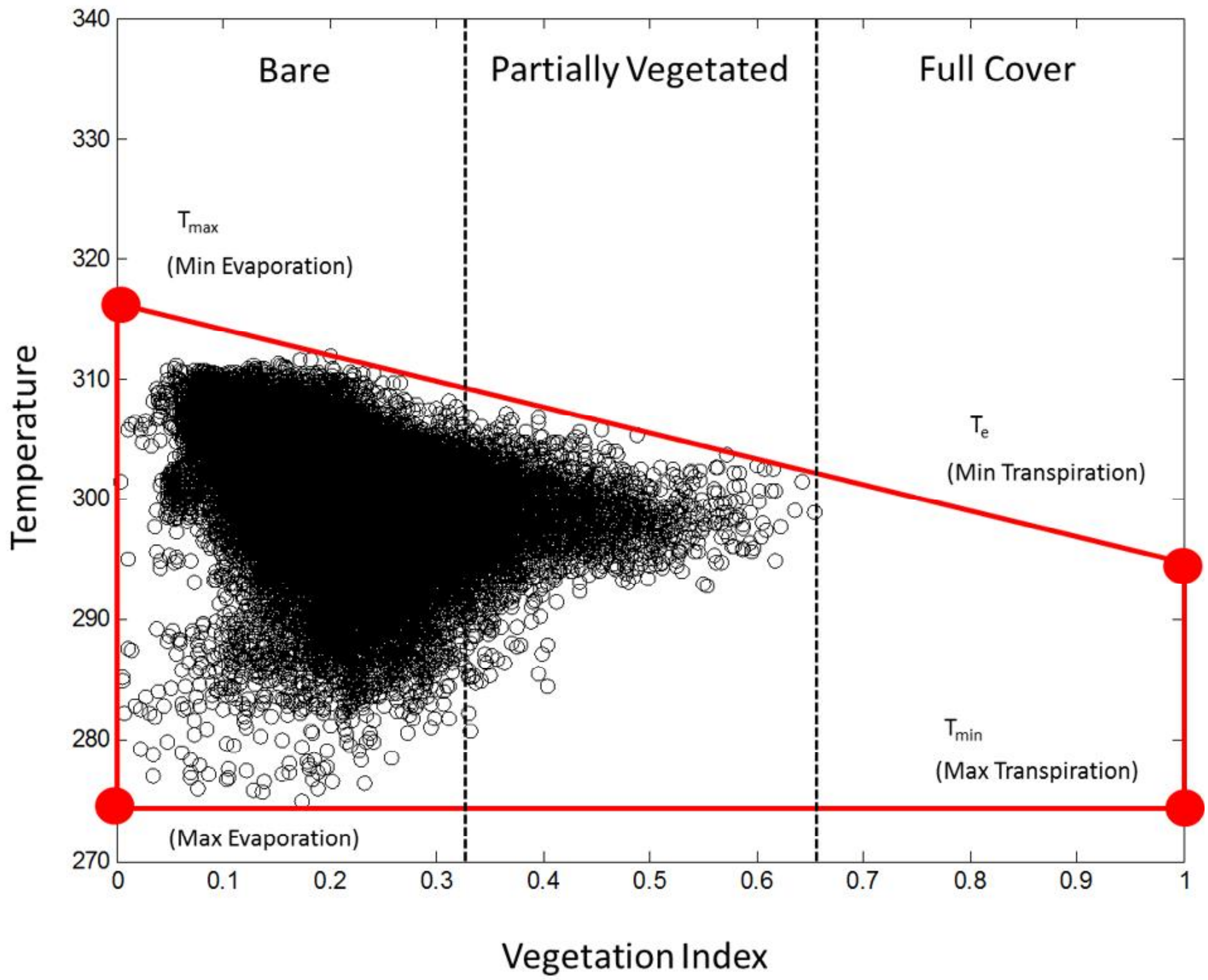

Figure 5-3: EF concept (for the large domain surrounding and including the Arroyo Seco) using vegetation index and temperature spaces for 1 January 2009

The EF triangle must be constructed with a large enough domain that can capture the variability in vegetation coverage and temperature. This study develops a triangle over a large domain (1º by 1.5º) that includes the Arroyo Seco watershed (Figure 5-1). The temperature is a daily MOD11 product and the EVI is an 8-day composite. Initial trials (not shown) find that the EVI and LST domain limited to the Arroyo Seco is not large enough or sensitive enough for the triangle method, thus the domain is expanded appropriately. Clouds (present in daily MOD11 product) and outliers contribute to error in the triangle method. Outliers skew the shape of the triangle. To develop the warm edge of the triangle, we establish a constant interval (approximately 10 intervals) for EVI and find the maximum temperature of each interval and calculate the deviation between the interval maximum and the line. A threshold is set and standard deviations that exceed this threshold are considered outliers and deleted. The new set of maximum temperatures is used to re-develop the linear regression line (warm edge). For days where the triangle is not well defined, we manually estimated the triangle vertices.

5.3 Preliminary Results

Hydrology and vegetation index

The annual precipitation and discharge show cyclical trends, increased precipitation and discharge during the winter seasons (Figure 5-4). The annual precipitation and discharge for the Arroyo Seco is used to estimate annual runoff ratios. Pre-fire the ratios are 0.21 (2006), 0.05 (2007), 0.19 (2008), and 0.15 (2009). The post-fire runoff ratio is 0.42 (2010), highlighting the immediate effect of wildfire on discharge. The EVI shows seasonal trends, with more vegetation after precipitation and less vegetation during the summer. Immediately following the fire, the amount of vegetation detected significantly decreases (Figure 5-4).

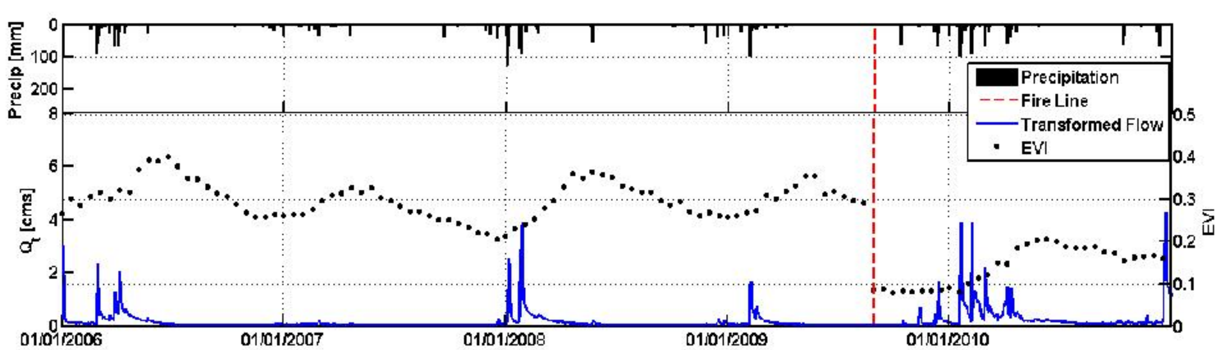

Figure 5-4: Arroyo Seco hydrology (precipitation and transformed discharge) and EVI for 2006-2010. The red dashed vertical line indicates the date the Arroyo Seco is completely burned by the Station Fire.

Net radiation

The MODIS net radiation for the Arroyo Seco is larger than the CIMIS net radiation (Figure 5-5). The Arroyo Seco net radiation is the average over the entire watershed, which includes an elevation range of 431-1877 meters, while the CIMIS station is located at 388 meters. The difference in elevation affects the estimated temperature; given that temperature linearly decreases with increasing elevation. The temperature at the CIMIS station is greater than the average temperature at the Arroyo Seco (adiabatic cooling). On cloudy sky conditions, the 8-day composite MYD06 product is used as substitution for the daily MOD11 surface temperature and emissivity. This affects the outgoing longwave radiation and influences the net radiation over the Arroyo Seco watershed. It is important to note that the Arroyo Seco watershed is naturally vegetated and will tend to have a lower LST, which will decrease the longwave radiation and increase the net radiation. Whereas, the CIMIS station estimates net radiation over well maintained grass surface, which will have a different LST than the natural vegetation of the Arroyo Seco.

Despite the discrepancies between the two net radiation timeseries for 2009, the patterns appear generally similar. The MODIS net radiation is able to capture the “June Gloom” (phenomenon typical in southern California, an inversion brings marine layer to the coast), where the net radiation is much lower than the surrounding months (Figure 5-5).

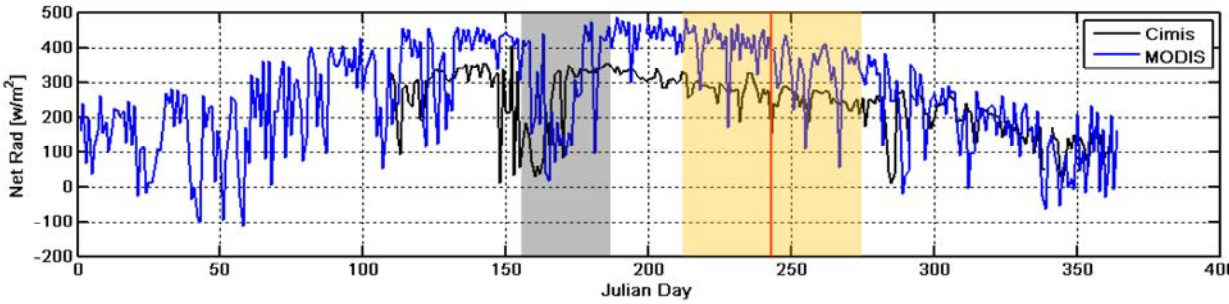

Figure 5-5: Average net radiation over the Arroyo Seco (elevation: 426m with mainly chaparral) compared to estimated net radiation at the Glendale CIMIS station (elevation: 300 m over well-maintained grass). The red vertical line represents the date where the Arroyo Seco is completely burned. The grey box shows the approximate dates of "June Gloom" and the orange box shows the approximate dates of the Station Fire.

Triangle method

As previously described, the triangle method is adjusted specifically for our study area to include a larger domain, but we highlight the pixels from within the Arroyo Seco (red circles; Figure 5-6).Triangles are developed for fifteen days in 2009 to evaluate variability in EVI and LST space from month to month; days are chosen where the Arroyo Seco MODIS data is cloud-free (49 pixels represented). We also highlight the day before the fire (25 August 2009) and the day after fire containment (17 October 2009). The large domain chosen is not affected by the fire (too few pixels), but the Arroyo Seco (49 pixels) is affected. The EVI for the Arroyo Seco is generally around 0.2-0.4 until the fire. During the fire the EVI decreases to less than 0.2, except for a few pixels that are unburned or have low burn severity. By early December, the spread of the EVI seems to increase, indicating some vegetation regrowth, but not back to pre-fire conditions. The temperature is generally between 280 and 300ºK except 25 August – 1 November 2009, where the temperature increases to 300 to 320ºK.

To highlight the triangle parameters, June 2, 2009 vertices are estimated. The sparse EVI (0.4 to 0.5) to LST (300 to 320ºK) pixels skew the triangle vertex estimations and are manually modified. This causes inconsistencies in the estimated triangle and final ET product.

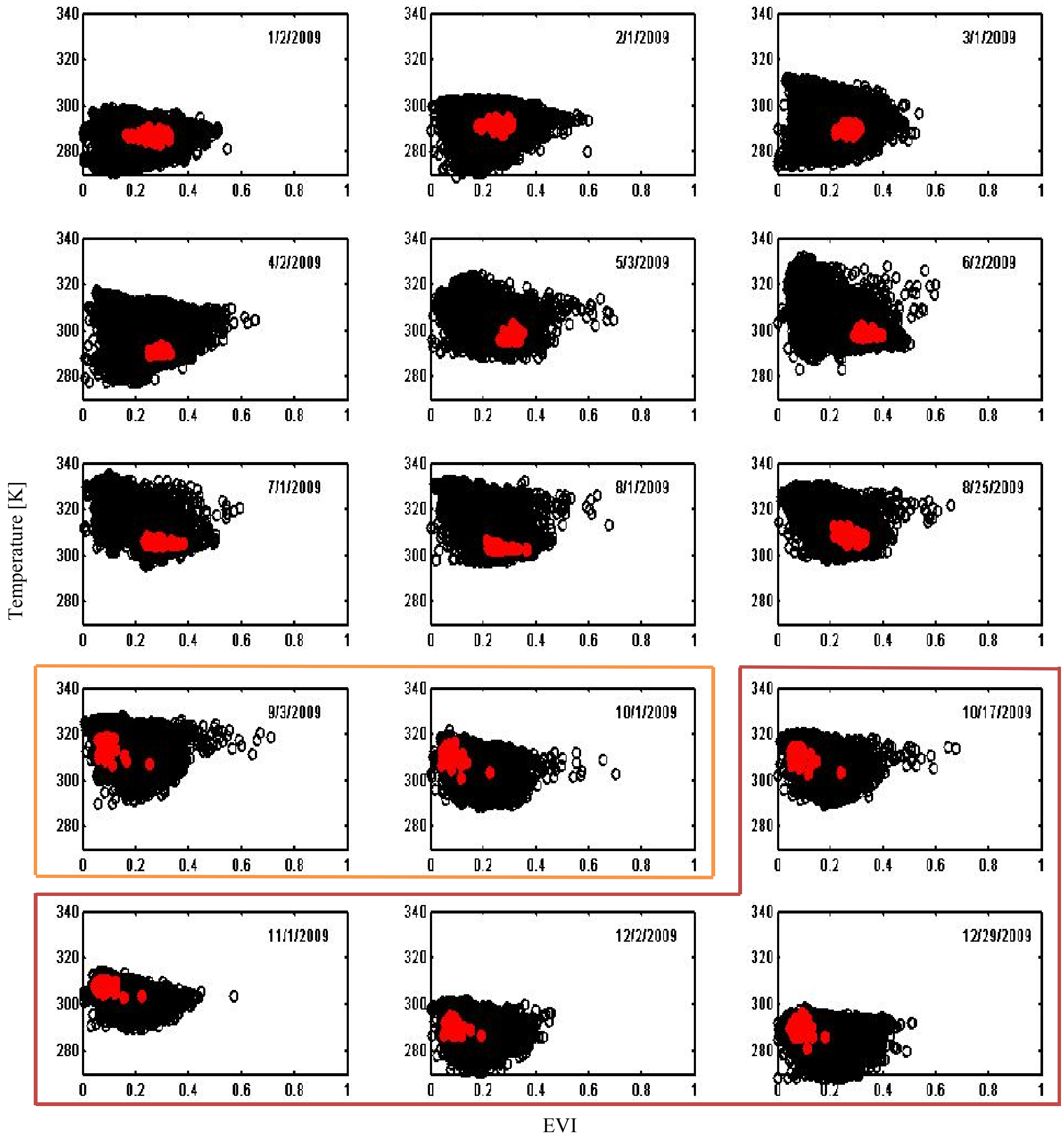

Figure 5-6: Select triangles constructed for the large domain (black open circles) and the Arroyo Seco (red filled circles) during 2009. The Orange box includes two days during the fire (3

September 2009 and 1 October 2009). The red box includes four days post-fire (17 October 2009 (immediately post fire), 1 November 2009, 2 December 2009, and 29 December 2009).

We incorporate the temperature parameters from the 2009 triangle models into daily ET estimates (Figure 5-7). The triangle boundary conditions, MODIS surface temperatures for the domain, vary daily and influence the ET estimates.

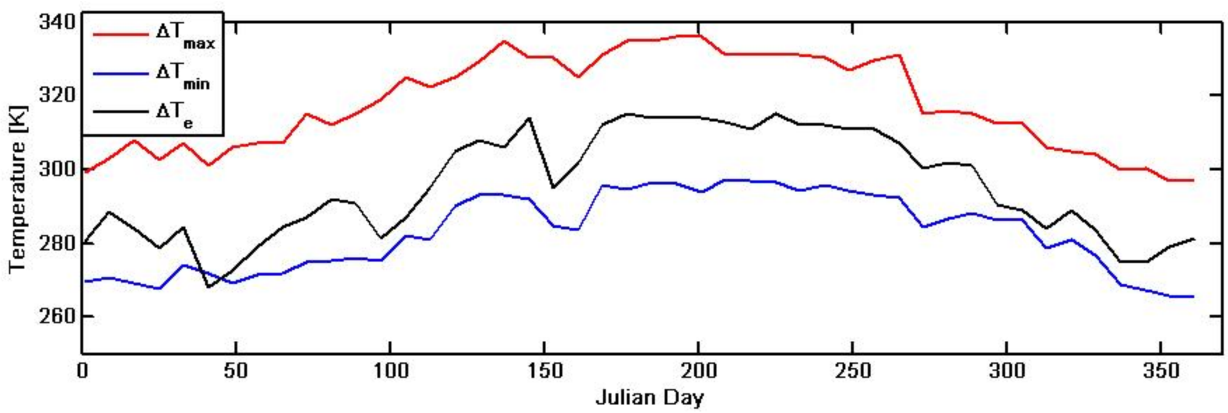

Figure 5-7: Daily MODIS surface temperatures, T_{max}, T_{min}, and T_e, for the large domain over the Arroyo Seco for 2009.

2009 ET for Arroyo Seco

We calculate the 2009 ET timeseries for the Arroyo Seco using the developed triangle method (Figure 5-7 parameters). The CIMIS ETo from approximately Julian day 0 to 100 (January to mid-April) seem to have missing data and the daily data is interpolated (smoothed line). The MODIS ET is generally lower than the CIMIS ETo and follows the same seasonal patterns. Both ET and ET_o are affected by the "June Gloom" and show a decrease around Julian day 150 (end of May and early June). After the watershed is completely burned, the MODIS ET decreases more than the CIMIS ET_o, which would correspond to loss in vegetation (decreased EVI).

As discussed above, the temperature of the CIMIS station is generally higher than the temperature over the Arroyo Seco. Generally, the net radiation over the Arroyo Seco is also higher than the CIMIS station, likely due to elevation and atmospheric conditions, resulting in a higher ET. Despite CIMIS ET_o being characterized as a potential ET (maximum evapotranspiration), we cannot assume the CIMIS ET_o as the upper limit of evaporative flux in our watershed (different vegetation pattern and soil conditions).

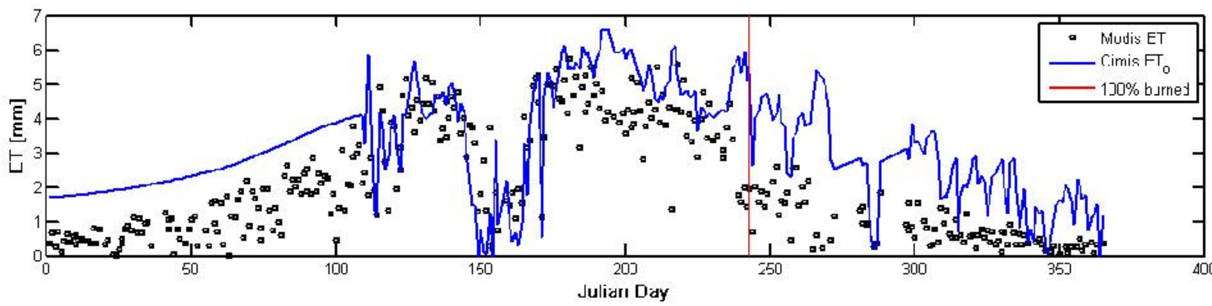

Figure 5-7: Estimated ET using MODIS products and triangle method for the Arroyo Seco, 2009 (black filled circles). Daily ET_o estimated at the Glendale CIMIS Station (blue line). The day the Arroyo Seco is completely burned is shown as a vertical red line.

Challenges with the triangle method application

The triangle method is based on many assumptions that increase uncertainties in the ET algorithm. A summary of uncertainties in the application of the triangle method to our post-fire area is outlined below:

- Cloudy days obstruct reliable LST (MOD11) acquisition and significantly affect net radiation and evaporative fraction estimates.
- The Arroyo Seco study domain is too small and the EVI and LST space is insensitive. A large domain used for the triangle method incorporates a 1° by 1.5° domain around the Arroyo Seco. This assumes that the varying landcover within this domain is representative of our watershed. However, the domain in this study includes different landcover classes than just the natural landcover found in the Arroyo Seco (Figure 5-1).
- Temperature and elevation assumptions. The large domain covers urban and mountainous areas, which affect the shape and vertices of the triangle, used for the Arroyo Seco. The

vegetation in the Arroyo Seco is different from the grass at the CIMIS station and affects the temperature, net radiation, and ET. We will further explore the triangle domain and sensitivity to land cover types in upcoming work.

5.4 Summary

Remote sensing is critical for post-fire monitoring and recovery because it is able to capture seasonal and annual trends at spatial resolutions critical for resource management. This preliminary study investigates application and sensitivity of a triangle-based method for estimating the ET over a post-fire system. The triangle method is sensitive to the study domain and variability in the EVI and temperature that are necessary to define the triangle vertices. In semi-arid regions such as southern California, where there is more bare ground and homogenous chaparral vegetation coverage, the necessary spread in EVI values is difficult to obtain. To address this limitation, we enlarge the triangle space to include a larger domain. Although the domain creates more defined triangles, there is large uncertainty associated with this method. The vegetation type represented in the triangle domain may significantly influence the EF and ultimately ET. We will re-develop the triangle to include more natural vegetation (similar to that found in the Arroyo Sec) to test the sensitivity of the triangle method. In this way, we will understand the limitations of the triangle method and acceptable landcover types to incorporate into the triangle space.

The triangle is the basis for developing the current ET algorithm over the burned system in this study and is also the basis for a soil moisture product developed by Kim and Hogue (2012). This soil moisture product improves the spatial resolution of Advanced Microwave Scanning Radiometer (AMSR-E) from the NASA Earth Observing System's Aqua Satellite. The

Aqua satellite is capable of retrieving soil moisture using the C-band microwave channel (6.9 GHz) that is approximately 60 km mean spatial resolution and is resampled to global cylindrical 25 km Equal-Area Scalable Earth Grid (EASE-Grid) cell spacing (Njoku et al., 2003). The AMSR-E soil moisture only represents the upper soils (approximately 1 cm for bare soil). The Kim and Hogue (2012) downscaled soil moisture is a computationally fast and based purely on remote sensing data. It uses a modified Jiang and Islam (2003) triangle to derive soil wetness (SW) index with higher resolution at 1 km spatial resolution. The MODIS SW index is used to scale the AMSR-E (25 km) soil moisture product.

Future work will also include validation of the remotely sensed ET product for burned surfaces. A coarse validation will include using a disaggregated MOD16 ET product to compare with our triangle-based ET product. We will also include the comparison of a higher spatial resolution (MODIS plus Landsat combined products), 30m daily ET product using the SEBAL method to our triangle-based ET method to determine the best algorithm for post-fire systems in semi-arid climates. The preliminary determination of an appropriate triangle method over our study domain is the first step towards estimating hydrological variables such as evapotranspiration and soil moisture. Ultimately we will incorporate these hydrologic variables and other key controlling parameters that affect recovery into a simple multi-variable predictive model for estimating daily discharge in ungaged and post-burn systems.

5.5 References

Allen, R.G., Tasumi, M., Morse, A., Trezza, T., 2007. Satellite-Based Energy Balance for Mapping Evapotranspiration with Internalized Calibration (METRIC) – Model. Journal of Irrigation and Drainage Engineering, 133(4): 380-394.

Bastiaanssen, W.G.M., Menenti, M., Feddes, R.A., and Holtslag, A.A.M., 1998. A remote sensing surface energy balance algorithm for Land (SEBAL), Part 1: Formulation. Journal of Hydrology 212-213: 198–212.

Bisht, G. and Bras, R.L., 2010. Estimation of net radiation from the MODIS data under all sky conditions: Southern Great Plains case study. Remote Sensing of Environment 114(7): 1522-1534.

Box, G. E. P. and D.R. Cox, 1964.An analysis of transformations. Journal of the Royal Statistical Society, Series B26 (2): 211–252

Brutsaert, W., 1975. On a derivable formula for long-wave radiation from clear skies, Water Resources Research, 11, 742– 744.

Casady, G.M., Leeuwen, W.J.D., Marsh, S.E., 2009. Evaluating Post-wildfire Vegetation Regeneration as a Response to Multiple Environmental Determinants. Environmental Model Assessment DOI: 10.1007/s10666-009-9210-x.

Chen, X., Vierling, L., Deering, D., and Conley, A., 2005.Monitoring boreal forest leaf area index across a Siberian burn chronosequence: a MODIS validation study. International Journal of Remote Sensing 26(24): 5433-5451.

Gillies, R.R. and Carlson, T.N., 1995. Thermal remote sensing of surface soil water content with partial vegetation cower for incorporation into mesoscale prediction models. Journal of Applied Meteorology: 34, 745−756.

Hogue, T.S., Sorooshian, S., and Gupta, H., 2000. A Multistep Automatic Calibration Scheme for River Forecasting Models. Journal of Hydrometeorology 1(6): 524-542.

Horton, J. S., and C. J. Kraebel. 1955. Development of Vegetation after Fire in the Chamise Chaparral of Southern California. Ecology 36:244–262.

Huete, A., Didan, K., Miura, T., Rodriguez, E.P., Gao, X., and Ferreira, L.G., 2002. Overview of the radiometric and biophysical performance of the MODIS vegetation indices. Remote Sensing of Environment 83: 195-213.

Jiang, L. and Islam, S., 2003. An intercomparison of regional latent heat flux estimation using remote sensing data International Journal of Remote Sensing 24(11): 261-274.

Jiang, L., Islam, S., and Carlson, T., 2004.Towards the uncertainty of surface fluxes estimation and implications for using a simplified approach with remote sensing data, Canadian Journal of Remote Sensing30 (5:769–787.

Keeley, J.E., Sterling, C.K., 1981. Post-fire Regeneration of Southern California Chaparral. American Journal of Botany 68(4):524-530.

Keeley, J.E., Brennana, T., and Pfaff, A.H., 2008. Fire Severity and Ecosystem Responses Following Crown Fires in California Shrublands. Ecological Applications 18(6): 1530-1546.

Kim, J. and T.S. Hogue, 2008: Evaluation of a MODIS-based Potential Evapotranspiration Product at the Point-scale, Journal of Hydrometeorology, 9, 444-460.

Kim, J., and Hogue, T.S., 2012. Improving Spatial Soil Moisture Representation Through Integration of AMSR-E and MODIS Products. IEEE Transactions on Geoscience and Remote Sensing 50(2):446-460.

Kim, J., and Hogue, T.S., 2012b. Development of an actual evapotranspiration estimation algorithm for semi-arid environments using satellite-based data. *In review*

McMichael, C.E., Hope, A.S., and Loaiciga, H.A., 2006. Distributed hydrological modeling in California semi-arid shrublands: MIKE SHE model calibration and uncertainty estimation. Journal of Hydrology 317: 307-324.

Merlin, O., Walker, J.P., Chenbouni, A., and Kerr, Y.H., 2008. Towards deterministic downscaling of SMOS soil moisture using MODIS derived soil evaporative efficiency. Remote Sensing of Environment 112: 3935-3946.

Moran, M.S., Clarke, T.R., Inoue, Y., and Vidal, A., 1994. Estimating crop water deficit using the relation between surface-air temperature and spectral vegetation index. Remote Sensing of Environment 49(3): 246-263.

Nishida, K., Nemani, R., Glassy, J.M., and Running, S.W., 2003. Development of an evapotranspiration index from Aqua/MODIS for monitoring surface moisture status. IEEE Transactions on Geoscience and Remote Sensing, 41(2): 493-501.

Njoku, E., Jackson, T.J., Lakshmi, V., Chane, T., and Nghiem, 2003. Soil moisture retrieval from AMSR-E. IEEE Trans. Geosci. Remote Sens., 41(2):215-299.

Norman, J.M., Kustas, W.B., and Humes, K.S., 1995. Source approach for estimating soil and vegetation energy fluxes in observations of directional radiometric surface temperature. Agricultural and Forest Meteorology, 77: 263−293.

Paulescu, M. and Schlett, Z., 2004. Performance assessment of global solar irradiation models under Romanian climate, Renew. Energy29, pp. 767–777.

Roder, A., Hill, J., Duguy, B., Alloza, J.A., and Vallejo, R., 2008. Using long time series of Landsat data to monitor fire events and post-fire dynamics and identify driving factors. A case study in the Ayora region (eastern Spain). Remote Sensing of Environment 112(1): 259-273.

Tang, R., Li, Z., and Tang, B., 2010. An application of the T_s-VI triangle method with enhanced edges determination for evapotranspiration estimation from MODIS data in arid and semi-arid regions: Implementation and validation. Remote Sensing of Environment 114:540-551.

Wittenberg, L., Malkinson, D., Beeri, O., Halutzy, A., and Tesler, N., 2007. Spatial and temporal patterns of vegetation recovery following sequences of forest fires in a Mediterranean landscape, Mt. Carmel Israel. Catena 71: 76-83.

Chapter 6. Contributions and Continuation of Work

Communicating the ongoing hazards associated with wildfires during and after a post-fire event to the public is necessary and our work has shown that there is a significant need for more post-fire research to guide cost-effective and efficient management decisions. Post-fire policies, models, and recovery predictions depend on accurate data and the increased usage of remote sensing in post-fire environments require uncertainty assessments. Vegetation indices are important variables of post-fire recovery and ongoing work includes collaboration with the USFS to validate remotely sensed vegetation with ground-based observations in post-fire systems (Section 6.1). Accurate detection of vegetation and other post-fire variables can be included in models to improve post-fire recovery predictions (Section 6-2).

6.1 Remotely sensed post-fire vegetation regeneration and prediction

Post-fire watershed response is influenced by numerous variables and establishment of vegetative cover is often used to determine when watersheds return to pre-fire response behavior. BAER teams, along with other agencies that have jurisdictional responsibility to prescribe and implement post-fire treatments based on expected hydrologic response and associated threats to life, property, and resources. Remote sensing technologies can be utilized to assess the rate of natural vegetative regeneration after wildfire and evaluate the risk for continued increased post-fire watershed response. The following sections summarizes preliminary methods, findings, and future needs for the development of a decision support tool that will give land managers and emergency response teams guidance on the level of risk relative to pre-fire or immediate post-fire levels (Clark et al., 2012).

The presence of ground cover is the governing factor of post-fire erosion. Hillslope treatments, such as mulching with agricultural straw, are most effective at reducing rill development and sediment transportation when applied at 60% or greater cover (Robichaud et al., 2010). This is critical especially during the first post-fire year, when the highest risk of erosion exists (DeBano et al., 1998). As natural vegetation begins to recover, more protection to the soil is provided, decreasing erosion risks. Material such as downed woody debris, sloughed tree bark, and needle cast provide ground cover and intercept precipitation, but are not easily discernible using common remote sensing data sets, thus living plant material is classified in the following photo interpretation method. Remotely sensed vegetation indices measure the amount of "green" cover present. The vegetation index, EVI is an important indicator of post-fire recovery and serves as an indicator of post-fire hydrology (Kinoshita and Hogue, 2011). As more studies utilize remotely sensed products such as vegetation indices, it becomes necessary for an uncertainty assessment with the remotely sensed products and ground-based observations. The ultimate goal of this work is to correlate commonly used vegetation indices (EVI and normalized differenced vegetation index (NDVI)) from remote sensing platforms with hydrologic and geomorphologic response and provide predictive tools for mitigation strategies (Clark et al., 2012).

Initial research of in situ and remote sensing post-fire vegetation shows discrepancies between the amount of cover estimated by remote sensing and present in situ. Burned surfaces, dead vegetation, and rock outcrops skew the amount of vegetation detected by satellites. An ongoing project, in collaboration with the U.S. Forest Service, provides a ground-based opportunity to collect in situ post-fire vegetation data across many wildfires to improve the relationship between remotely sensed EVI and NDVI and the actual vegetation biomass present.

This study consists of the following tasks: 1) ground-based vegetation data acquisition, 2) comparison of ground-based and remotely sensed products, and 3) regression analysis and validation of regression model. Ultimately, this study will develop a decision support tool that incorporates geospatial inputs to assist monitoring watershed recovery.

6.1.1 Ground-based vegetation data acquisition

Ground-based vegetation sampling and images are acquired from six fires in California (Table 6-1) covering a variety of vegetation types, elevation, and recovery stages. These six sites are used to document the percent cover that exists within the burned area. This study uses pole-mast photography (down-looking camera attached to the top of a telescoping monopod) to take pictures of the ground from an elevated height, about 25-30 feet (Gilbert et al 2009, Smith et al. 2000, Vanha-Majamaa et al. 2000). The ground locations must consist of homogeneous vegetation type and include a variety of spatial coverage (full to no coverage). Four to ten photos are taken along a defined transect (transects endpoints are flagged and GPS locations recorded). The number of photos taken will depend on the homogeneity of the ground coverage (no less than 4 photos should be taken) and more photos should be taken as the landscape changes. This is necessary as these homogeneous areas of data will be correlated to remote sensing products (i.e. Landsat or MODIS products).

Table 6-1: Summary of fire sites with photo data and validation sites, where NF is National Forest

Fire	National Forest	Year of fire	Years visited
Old	San Bernardino NF	2003	2011
American River Complex	Tahoe NF	2008	2011
La Brea	Los Padres NF	2009	2011
Station	Angeles NF	2009	2010; 2011
Bull	Sequoia NF	2010	2010; 2011
Canyon	Sequoia NF	2010	2010; 2011
Validation			
Monument	Coronado NF	2011	N/A
Horseshoe2	Coronado NF	2011	N/A
Sagehen treatments	Tahoe NF	N/A	N/A

6.1.2 Comparison of ground-based and remotely sensed products

Ground-based photo interpretation

Photos are interpreted with Esri's ArcGIS ArcMap as a simple binary (cover-no cover) classification using a random dot grid sampling approach (Figure 6-1). The number of photo points (n) needed per transect is at least 400 (regardless of the number of photos acquired along a transect) for a 95% confidence interval (CI) (Equation 6-1). The number of photo points, n, is calculated using the equation below. 600 points are initially collected so points that captured anomalies in the photos (humans, monopod, etc.) can be ignored or thrown out. Finally, a binary photo interpretation will estimate percent cover.

$$95\%CI = 2 * \sqrt{\frac{p*(1-p)}{n}}$$

Equation 6-1

where: 95% CI = +/- 0.05 and p = 0.5 (worst case scenario; equal chance of the ground exhibiting cover or bare ground).

Figure 6-1: In situ pole-mast photography and photo interpretation using random dot grid and binary classification of percent ground cover.

Remote sensing observations

Landsat 5 Thematic Mapper (TM) imagery is used for fire severity mapping (Clark and Bobbe, 2006) and vegetation regeneration monitoring (Diaz-Delgado et al., 1998, Clark and Kuyumjian, 2006, Wittenberg et al., 2007), and many other resource applications. To leverage the spectral richness of Landsat, this study creates vegetation indices that are used for vegetation regeneration monitoring. Three common indices are the normalized difference vegetation index (NDVI; Equation6-2), enhanced vegetation index (EVI; Equation 6-3), and normalized burn ratio (NBR; Equation 6-4) (Chen et al., 2011). NDVI and EVI measure the chlorophyll activity and content in plant material (Huete et al., 2002), while NBR is influenced by chlorophyll activity and soil moisture content (presence or absence of dry, bare soil) (Lòpez Garcia and Caselles, 1991).

$$NDVI = (B4 - B3) / (B4 + B3)$$

Equation 6-2

$$EVI = 2.5 * ((B4 – B3) / (B4 + 6 * B3 – 7.5 * B1 + 1))$$

Equation 6-3

$$NBR = (B4 – B7) / (B4 + B7)$$

Equation 6-4

where B is the top of atmosphere (TOA) reflectance of the specified Landsat TM/ETM+ band.

The photo interpretation includes only living plant material (green and brown), similarly, satellite imagery will only capture green-up cycles. Cloud-free Landsat imagery is acquired for the entire growing season or seasons after the fire to create the vegetation indices for each image, then the indices are composited based on their maximum value (Sousa et al., 2003). This approach sufficiently highlights grasses or other vegetation that are green in the spring but brown in August.

6.1.3 Regression analysis and validation

Regression analysis

Geospatial analysis creates a predictive model that computes ranges of percent ground cover from a composite vegetation index. This process based on data that represents areas burned by wildfire. Regression models produce an acceptable model fit for NDVI (N = 53, R2 = 0.65, p = 0.038) and EVI (N = 53, R2 = 0.63, p = 0.019), but not for NBR (N = 53, R2 = 0.17, p = 0.004). The following equations are fitted for NDVI (6-5) and EVI (6-6):

$$Predicted\ cover = 221.18*MaxNDVI - 26.273$$

Equation 6-5

$$Predicted\ cover = -455.22*MaxEVI2 + 519.99*MaxEVI - 47.508$$

Equation 6-6

Validation of regression model

Equations 6-5 and 6-6 are applied to the Monument and Horseshoe2 fires (southern Arizona, 2011). Class thresholds of 0-30%, 30-60%, 60-100% are applied to the continuous data for interpretation. An initial qualitative assessment of the classification for the Monument Fire showed strong potential for predicting current percent ground cover. The data used to create the regression analysis are from one sampling period and result in a single snapshot in time with respect to vegetation conditions. To address this, only live material is included in the field photos for comparison. The areas also vary in years following the fire (i.e. the Old Fire is about eight years recovered and the Bull Fire is only one year recovered). Ongoing photographs are being acquired for the Bull Fire as they recover over time (photos taken approximately every 112 days) to better develop a model that sufficiently matches observed ground cover over time. Also, the Sagehen Experimental Watershed in the Tahoe National Forest will undergo forest management treatments in 2013 and will present an opportunity for further analysis. Sagehen will provide pre- and post-treatment remote sensing validation. Coordination between federal agencies and non-federal agencies must continue beyond containment of the fire for efficient implementation of protection treatments. The in situ observations and geospatial technologies from this study will help land managers make more informed decisions regarding watershed recovery.

6.2 Application of remote sensing algorithms for post-fire systems

Prompted by previous work, further investigation of watershed recovery and ecosystem resilience will expand the analysis to include more watersheds across various regional fires. It will also include a more rigorous hydrological application of remote sensing in post-fire environments. An important hydrological variable that is affected by vegetation is evapotranspiration and is arguably the most difficult variable to retrieve in the water balance equation, yet is an important parameter for water resources management, ecology, and climate change studies (Huxman et al., 2004; Kim and Hogue, 2008; 2012b). A UCLA-developed remotely sensed evapotranspiration (ET) product that uses MODIS and Landsat will estimate an independent satellite-based ET time series over various burned watersheds (Kim and Hogue, 2012b). The ET variable can be monitored at high spatial and temporal resolution for pre-fire seasonal patterns and also response to burned areas. Monitoring post-fire soil moisture recovery will provide insight to post-fire water balances. Remote sensing algorithms investigated by this work are applicable to post-fire systems from the watershed to regional scale. Dependency on remote sensing data provides convenient and large coverage for post-fire monitoring, which will provide significant benefit for predicting consistent and high-resolution hydrologic response over large burn areas.

6.3 Summary and Contributions

The overarching goal of this project is to assess current post-fire modeling techniques and develop tools using remote sensing products that can improve our understanding of post-fire hydrologic behavior and ultimately be utilized across the western United States for post-fire predictions. The major contributions of this research are presented in response to the guiding questions posed in Chapter 1.

- *What are current hydrological post-fire management protocols in the western U.S. and how are communities affected by both pre- and post-fire management and policy decisions?*

  Current post-fire management consists of BAER teams that assess immediate values at risk and implement decisions and treatments to mitigate threats. Downstream communities are immediately at risk to increased flooding, debris flows, and degraded water quality. BAER teams focus on estimating potential increases in post-fire runoff and sediment that place downstream values at risk or threaten human life and natural resources. Mitigation efforts include closures of public areas, k-rails, or ground treatment (i.e. mulching or seeding to protect the ground surface and deter erosion).

A federally funded NFIP is available to property owners and renters that live in qualifying communities, but there is a probationary period of 30-days. Analytical tools and incorporation into polices should be further investigated to provide policies that encourage minimizing development or better homeowner preparation in fire-prone areas.

- *What are commonly used models in post-fire assessments and how do these models perform across diverse hydroclimatic regimes? What models are optimal for post-fire hydrologic predictions?*

  Hydrologic models incorporated in BAER hydrologic assessments vary by region, fire, modeler, accessibility, and ease of use. A lack of consistency in model parameter acquisition contributes to uncertainty in post-fire peak discharge estimates. A study of a suite of hydrologic models used by BAER hydrologists tests multiple models over diverse pre- and post-fire sites in California, Colorado, and Montana. Hydrologic soil group and rainfall distributions (based on site location and region) significantly affect model predictions. Model results for each site are highly variable and demonstrate inconsistencies based on model selection. The HEC-HMS is the most robust model if users have time to incorporate many parameters and calibrate the model. The Wildcat5 provides a simpler model that estimates peak discharge well without calibration, if the area of interest meets size requirements.
- *Does the integration of remote sensing products improve post-fire modeling and management, especially in semi-arid regions? Can current remote sensing algorithms be*

adapted for post-fire systems? What key variables can be used to assess post-fire hydrologic behavior?

Remote sensing provides convenient access to continuous data streams that cover large regions. Remote sensing provides many variables for post-fire systems that are often isolated and ungaged. Specifically, remote sensing can provide insight to hydrological variables that are important in estimating water availability in semi-arid regions. Post-fire ecology and hydrology are strongly related and ecosystem dynamics largely affect system recovery. Key controlling parameters of post-fire hydrologic recovery include slope aspect, burn severity, and MODIS EVI (proxy for vegetation biomass). Despite the general recovery of the north aspect and low burn severity areas, vegetation activity and hydrologic behavior are not back to pre-fire conditions after a seven-year period for the two southern Californian systems.

Methods to estimate evapotranspiration and soil moisture from purely remote sensing data is available. These methods can be modified for post-fire systems to provide details for a water balance. A triangle method used for ET and SM has been validated in semi-arid regions and is a promising selection for ET and SM algorithms in burned systems. The triangle-based ET is undergoing more validation, but will ultimately provide a key component of the water balance, essential in water limited regions such as southern California.

- *How do we utilize answers to the above questions to inform future modeling, prediction, and post-fire response efforts, especially for responsible agencies such as the USFS or the National Weather Service (NWS)?*

The ability to accurately model and predict post-fire hydrological consequences with improved confidence is critical for agencies such as the USFS or NWS for forecasting and reducing management costs and improving regional resource allocation. Including remote sensing data streams will provide higher spatial and temporal resolutions to current models and predictions. Better resolution will enhance post-fire monitoring and encourage more efficient post-fire management.

This study evaluate models used for post-fire decisions and encourage more accurate and confident models that have important implications for mitigation treatments and costs. This study provides new tools and methods that can be integrated into post-fire policies to improve management and preparation at the WUI, specifically with remote sensing methods. This study also establishes collaboration with the USFS to validate and improve post-fire models and remote sensing products.

6.4 References

Chen, X., Vogelmann, J., Rollins, M., Ohlen, D., Key, C., Yang, L., Huang, C., Shi, H. 2011. Detecting post-fire burn severity and vegetation recovery using multitemporal remote sensing spectral indices and field-collected composite burn index data in a ponderosa pine forest. International Journal of Remote Sensing 32(23): 7905-7927.

Clark, J., Bobbe, T. 2006. Using remote sensing to map and monitor fire damage in forest ecosystems. In Understanding forest disturbance and spatial pattern: Remote sensing and GIS approaches. (Eds. M. Wulder, S. Franklin). Boca Raton, FL: Taylor and Francis. Pp. 113-131.

Clark, J., Kuyumjian, G. 2006. Landscape-scale postfire vegetative condition monitoring using multi-temporal Landsat imagery on the Cerro Grande Fire. In 'Proceedings of the eleventh biennial forest service remote sensing applications conference.' (CD-ROM) USDA Forest Service RSAC: Salt Lake City, UT.

Clark, J., Stamer, M., Cooper, K., Napper, C., Hogue, T., and Kinoshita, A., 2012.Evaluating Post-fire Vegetation Regeneration with Remote Sensing and Predicting Out-year Post-fire Watershed Response. Madrean Conference, Tucson, Arizona, May 1-5, 2012.

Diaz-Delgado, R., Salvador, R., Pons, X. 1998.Monitoring of plant community regeneration after fire by remote sensing. In: L. Traboud (Ed.), Fire management and landscape ecology (pp. 315 - 324). Fairfield, WA: International Association of Wildland Fire.

Gilbert, J., Butt, K. 2009. Evaluation of digital photography as a tool for field monitoring in potentially inhospitable environments. Mires and Peat. 5(5): 1-6.

Huete, A., Didan, K., Miura, T., Rodriguez, E., Gao, X., Ferreira, L., 2002. Overview of the radiometric and biophysical performance of the MODIS vegetation indices. Remote Sensing of Environment. 83: 195-213.

Huxman, T.E., Cable, J.M., Ignace, D.D., Eilts, A.J., English, N.B., Weltzin, J., and Williams, D.G., 2004. Response of net ecosystem gas exchange to a simulated precipitation pulse in a semi-arid grassland: the role of native versus non-native grasses and soil texture. Oecologia 141: 295-305.

Kim, J. and T.S. Hogue, 2008: Evaluation of a MODIS-based Potential Evapotranspiration Product at the Point-scale, Journal of Hydrometeorology, 9, 444-460.

Kim, J., and Hogue, T.S., 2012. Improving Spatial Soil Moisture Representation Through Integration of AMSR-E and MODIS Products. IEEE Transactions on Geoscience and Remote Sensing 50(2):446-460.

Kim, J., and Hogue, T.S. 201b2. Development of an actual evapotranspiration estimation algorithm for semi-arid environments using satellite-based data. In review

Kinoshita, A., Hogue, T. 2011: Spatial and temporal controls on post-fire hydrologic recovery in Southern California watersheds. Catena. 87: 240-252.

Lòpez Garcia, M., Caselles, V. 1991. Mapping burns and natural reforestation using Thematic Mapper data. Geocarta International. 1: 31-37.

Smith, Stephen M., Garrett, P. Brian, Leeds, Jennifer A., McCormick, Paul V. 2000. Evaluation of digital photography for estimating live and dead aboveground biomass in monospecific macrophyte stands. Aquatic Botany. 67: 69-77.

Sousa, A., Pereira, J., Silva, J. 2003. Evaluating the performance of multitemporal image compositing algorithms for burned area analysis. International Journal of Remote Sensing. 24(6): 1219-1236.

Vanha-Majamaa, I., Salemaa, M., Tuominen, S., Mikkola, K. 2000.Digitized photographs in vegetation analysis – a comparison of cover estimates. Applied Vegetation Science. 3: 89-94.

Wittenberg, L. and Inbar, M., 2009. The Role of Fire Disturbance on Runoff and Erosion Processes – a Long-Term Approach, Mt. Carmel Case Study, Israel. Geographical Research 47(1): 46-56.

Appendix A. Publication of Chapter 4

Catena 87 (2011) 240–252

Contents lists available at ScienceDirect

Catena

journal homepage: www.elsevier.com/locate/catena

Spatial and temporal controls on post-fire hydrologic recovery in Southern California watersheds

Alicia M. Kinoshita, Terri S. Hogue *

Department of Civil and Environmental Engineering, University of California, Los Angeles, California, USA

ARTICLE INFO

Article history:
Received 24 March 2010
Received in revised form 29 May 2011
Accepted 4 June 2011

Keywords:
Wildfire
Hydrology
Recovery
EVI
Streamflow
Semi-arid

ABSTRACT

The current study investigates the spatial and temporal dynamics of post-fire vegetation and the subsequent influence on seasonal and annual hydrologic responses in chaparral-dominated watersheds. Post-fire climatology, burn severity, slope aspect, and vegetation behavior are evaluated for two basins burned during the 2003 Old Fire in the San Bernardino Mountains in Southern California. Climate and discharge data are used to evaluate seasonal and annual variability of post-fire hydrologic fluxes. Data obtained from the Moderate Resolution Imaging Spectroradiometer (MODIS) are used to estimate Enhanced Vegetation Index (EVI) and differenced Normalized Burn Ratio (dNBR). A Savitzky–Golay filtering technique and an integrated EVI annual fraction are utilized to assess vegetation recovery under a range of potential controls. Vegetation recovery is highly variable in both watersheds and is related to slope aspect (solar and water availability), initial biomass levels, and burn severity. South and west facing slopes show higher pre-fire EVI (biomass) and significant loss of vegetation cover after fire. Vegetation in both watersheds responds to an extreme wet season during the second post-fire year, however recovery rates are not sustained. North and east aspects show the quickest biomass gain relative to pre-fire conditions by the end of the study period (WY 2010), while the west and south slopes show lower biomass recovery. High burn severity areas show the slowest recovery across all slope aspects, with these regions just approaching 90% of pre-fire biomass by the end of the seven-year post-fire period. The variable rate of vegetation recovery across the watersheds results in significant changes in annual and seasonal discharge throughout the post-fire period. Runoff ratios remain elevated in both systems and there is increased dry season flow for much of the study period, indicating that plant water consumption and flowpaths are not back to pre-fire behavior by the end of WY 2010.

1. Introduction

Fire dramatically alters watershed processes. Loss of vegetation and soil transformation alters normal flow patterns and disrupts expected hydrologic behavior for years after fire (Cydzik and Hogue, 2009; Debano, 2000; Ice et al., 2004; Jung et al., 2009; McMichael et al., 2004; Pierson et al., 2008). Mediterranean systems are generally resilient to fire and have been noted to exhibit fairly quick recovery (Horton and Kraebel, 1955; Wittenberg et al., 2007). However, non-native plants can invade post-fire landscapes and alter water and energy balances in semi-arid regions (Prater and DeLucia, 2006). Succession of vegetation or type conversion due to fire may also result in decreased evaporation and may be partly responsible for increased summer streamflow in post-fire semi-arid systems (Meixner and Wohlgemuth, 2003). Although ecosystem behavior and hydrologic recovery are linked, few studies have explicitly coupled investigation of both processes in post-fire systems. Typical studies of post-fire dynamics in chaparral dominated systems include field observations of vegetation recovery and resilience (Horton and Kraebel, 1955; Keeley et al., 2008; Keeley and Sterling, 1981). Studies in post-fire chaparral shrublands demonstrate that parameters such as slope aspect and stand age (last fire event) are important determinants of burn severity; older vegetation implies more biomass, ground litter and fallen debris available to burn (Keeley et al., 2008). However, fire history, pre-fire land attributes (i.e. plant species and land-use history), and event-dependent characteristics such as fire severity and post-fire precipitation complicate predictions of post-fire vegetation recovery (Duguy and Vallejo, 2008; Keeley et al., 2005; Pausas, 2003; Roder et al., 2008).

Various studies have utilized remotely-sensed data to link burn or fire severity to hydrologic or soil behavior (Gonzalez-Pelayo et al., 2006; Moody et al., 2007). Vegetation regeneration after fire has also been evaluated in Mediterranean systems using a range of vegetation indices (Diaz-Delgado et al., 2002; McMichael et al., 2004; Roder et al., 2008; Wittenberg et al., 2007; Wittenberg and Inbar, 2009). Many remotely-sensed vegetation indices are available, with most studies

* Corresponding author at: Department of Civil and Environmental Engineering, 5731F Boelter Hall, University of California, Los Angeles, CA 90095-1593, USA. Tel.: +1 310 794 4239.
E-mail address: thogue@seas.ucla.edu (T.S. Hogue).

0341-8162/$ – see front matter © 2011 Elsevier B.V. All rights reserved.
doi:10.1016/j.catena.2011.06.005

utilizing Leaf Area Index (LAI) or Normalized Difference Vegetation Index (NDVI) (i.e. Landsat-TM or spectral mixture analysis (SMA) from Airborne Visible/Infrared Imaging Spectrometer (AVIRIS)) as a proxy of green biomass or vegetation activity present in post-fire systems (Diaz-Delgado et al., 1998, 2002; McMichael et al., 2004, 2006; Riano et al., 2002; Roder et al., 2008).

LAI is the leaf area per unit ground area and estimates the structural property of vegetation canopy (Myneni et al., 1995). LAI is estimated through the inversion of a canopy radiative transfer model that simulates radiative absorption and vegetation scattering (Myneni et al., 1995). Uncertainties in the LAI product include background interference and atmospheric scattering at the top of the atmosphere and top of the canopy (Myneni et al., 1995). NDVI uses the normalized difference between red and near-infrared channels. The product is sensitive to vegetation fraction and the rate of absorption of photosynthetic solar radiation (Gitelson et al., 1996). NDVI is noted to be adequate for monitoring plant recovery processes, but has drawbacks due to atmospheric and soil reflectance interference (McMichael et al., 2004; Wittenberg et al., 2007). For example, darker soils result in higher NDVI values (Gao et al., 2000) and there are non-linear relationships between NDVI and other vegetation variables, particularly under increasing biomass conditions. NDVI reaches a saturation level before the maximum is reached and may be most useful during initial post-fire conditions (Diaz-Delgado et al., 2002). Vegetation indices used in post-fire recovery studies typically have high spatial resolution (e.g. 30 m), but the number of images utilized over study sites has been limited (McMichael et al., 2006; Roder et al., 2008).

Investigators have also worked toward improving vegetation indices and validating new observations (Chen et al., 2005; Gao et al., 2000; Huete et al., 2002). The difference between the reflectance of the blue and red bands can be used to correct the atmospheric influences afflicting the NDVI parameter (Chen et al., 2005). The result is an Enhanced Vegetation Index (EVI) that is less sensitive to atmospheric influences and contains a blue band correction factor (Chen et al., 2005; Gao et al., 2000). EVI effectively monitors plant resilience, while reducing the effect of soil and atmospheric background interference. Unlike NDVI, EVI remains sensitive to vegetation at high biomass levels due to its sensitivity to canopy structure (Chen et al., 2005; Gao et al., 2000; Huete et al., 2002; Matsushita et al., 2007). EVI has been shown to detect variations in LAI, canopy type and architecture, plant structure, seasonal vegetation patterns, land cover, and biophysical variations (Gao et al., 2000; Wittenberg et al., 2007).

Despite the extensive literature on the application of remote-sensing products to study vegetation behavior, there is a lack of studies evaluating coupled ecosystem and hydrologic response in burned watersheds – especially integrating data from advanced satellite platforms. Several recent studies utilize field observations and five LANDSAT-based EVI images to evaluate the resilience of vegetation in semi-arid (Mediterranean) systems and the long-term effects of repeat fires on plant recovery (Wittenberg et al., 2007; Wittenberg and Inbar, 2009). The authors conclude that north facing slopes tend to return to pre-fire conditions faster than south facing slopes (in the northern hemisphere) and that remotely-sensed EVI helps detect pre- and post-fire vegetation cover but does not provide information on specific vegetation species. A recent study by Casady et al. (2009) also utilizes MODIS EVI time series (every 16 days for 5 years) as a proxy for green biomass recovery with respect to slope aspect and burn severity and develops a decision tree model to predict post-fire vegetation behavior.

The segregation of hydrologic or ecosystem recovery in previous post-fire studies highlights the need for investigation of coupled ecohydrologic response in fire altered systems. We advocate that simultaneous evaluation of EVI, burn severity, slope aspect and post-fire climatology will improve our understanding of the dynamics of ecosystem regeneration in burned watersheds and the corresponding seasonal and annual hydrologic responses. Similar to previous studies, our work focuses on the amount of post-fire green biomass detected as a proxy of vegetation recovery and does not specifically identify plant species recovery (Casady et al., 2009; Keeley et al., 2008; Wittenberg, et al., 2007). The objectives of the current study are to: 1) investigate the influence of aspect, burn severity and precipitation patterns on post-fire vegetation response (using EVI as a proxy), 2)

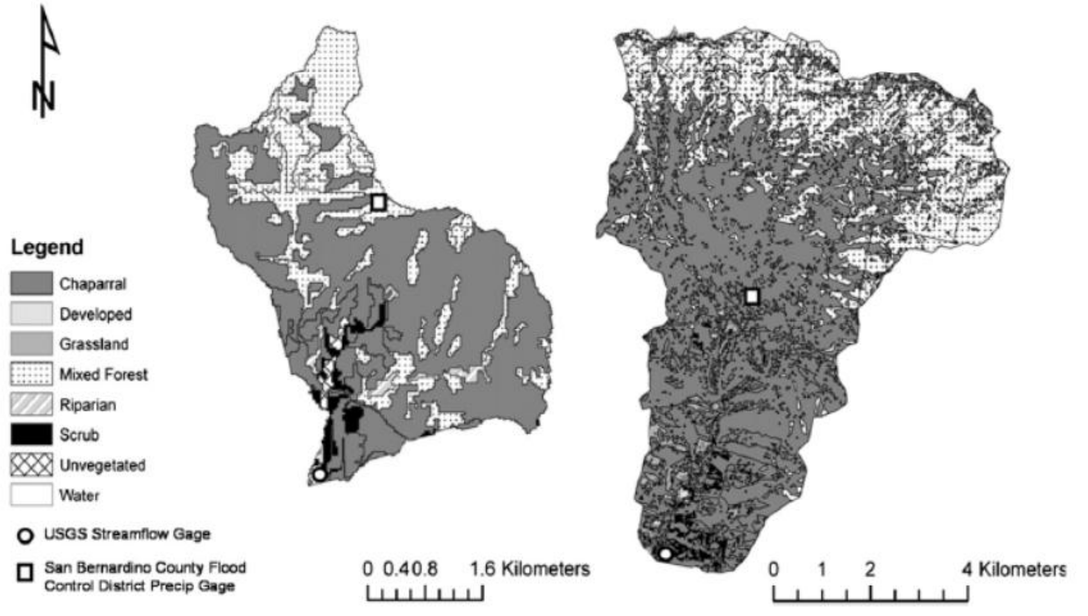

Fig. 1. Pre-fire vegetation for Devil Canyon (left) and City Creek (right) retrieved from the Landsat Thematic Mapper layer (30 m; NOAA C-CAP, 2000). Gage locations are also plotted.

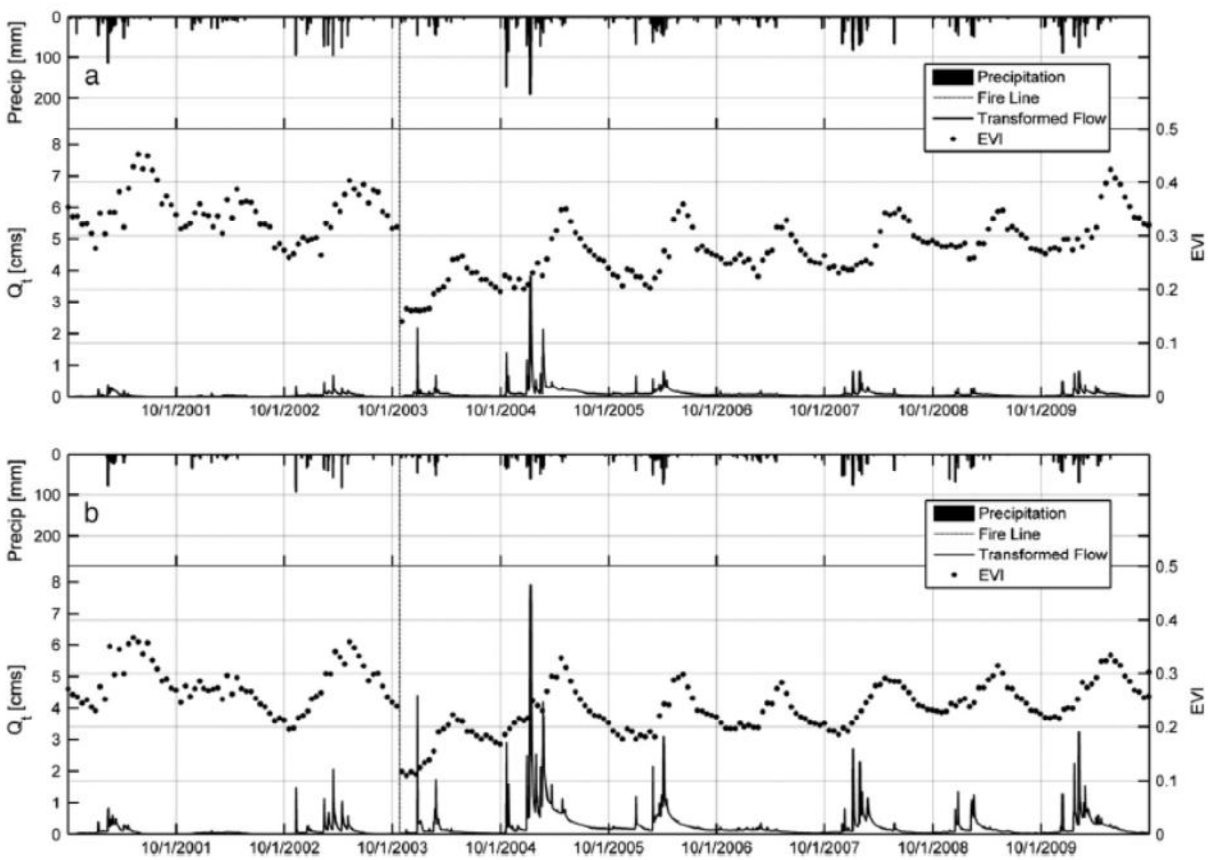

Fig. 2. Observations for Devil Canyon (a) and City Creek (b) including precipitation, discharge (transformed) and 16-day EVI. The dark gray line indicates the start date of the Old Fire (23 October 2003).

determine the impact of selected determinants (vegetation, burn severity, aspect, and climate) on post-fire hydrologic variability, and 3) establish recovery patterns and trends of both vegetation and discharge in post-fire chaparral systems.

2. Methods

We investigate hydrologic and ecologic recovery in two watersheds located in the San Bernardino Mountains of Southern California that were burned during the Old Fire of 2003 (26 October 2003–06 November 2003). Both watersheds are predominantly covered by chaparral with mixed forests in the higher elevations of the watersheds. To evaluate pre-and post-fire vegetation activities, we utilize MODIS EVI (MOD13Q1), a 16-day product with 250 m spatial resolution (Huete et al., 2002). Burn severity and slope aspect of each watershed are also extracted and aggregated to 250 m resolution using MODIS and USGS Digital Elevation Models (DEMs). Estimates of EVI (16-day), burn severity, and slope aspect are then evaluated as to their influence and control on post-fire hydrologic response in each watershed system.

2.1. Study areas

Southern California has a semi-arid, Mediterranean climate, including a relatively short precipitation season (generally December to March) and an extended dry period over the summer and fall season (NOAA, 2009a). Vegetation is primarily chaparral, sage, and scrub, with mixed conifer in the upper elevations. Chaparral typically have deep rooted systems necessary for obtaining water and surviving in hot dry climates (Schenk and Jackson, 2002), while shallow-rooted vegetation (grasses) cannot access deeper water stores and are senescent when moisture at the surface is depleted (Prater and DeLucia, 2006). The hydrology and vegetation of Southern California are heavily influenced by periodic El Nino events (NOAA, 2009b),

Table 1
Devil Canyon and City Creek watershed characteristics with pre- and post-fire runoff ratios.

		Devil Canyon (DC)	City Creek (CC)
Watershed size		14.2 km^2	50.8 km^2
Watershed slope		15%	10%
USGS gage #		11063680	11055800
San Bernardino precipitation gage #		2840	2860 and 3377
% Burned		97%	94%
Pre-fire vegetation (%)	Chaparral	55%	72%
	Mixed forest	29%	20%
Average runoff ratio	Pre-fire (WY85-03)	0.19	0.22
	Post-fire (WY04-10)	0.37	0.36
Yearly post-fire runoff ratio	WY 2004	0.47	0.36
	WY 2005	0.48	0.62
	WY 2006	0.42	0.41
	WY 2007	0.45	0.3
	WY 2008	0.27	0.27
	WY 2009	0.25	0.23
	WY 2010	0.28	0.33

which typically result in cooler, wetter conditions, and enhance vegetation growth. During the dry (fall) season, the region experiences Santa Ana Winds where hot, dry air is moved west from the desert towards the ocean, drying out vegetation and encouraging ignited fires to spread (Keeley et al., 2004).

The Devil Canyon watershed (Fig. 1) is approximately 14 km^2 and receives an average of 840 mm of precipitation each year (San Bernardino County Flood Control District (SBCFCD), 2008; data period from 1985 to 2010). Pre-fire vegetation for Devil Canyon watershed was retrieved from Landsat Thematic Mapper and consists primarily of chaparral (55%) and mixed forest at higher elevations (29%); the remaining 16% consists of a mixture of coastal sagescrub, developed areas, riparian zones, unvegetated areas, water, and woodlands (Minnich, 1988; NOAA, 2003). Devil Canyon exhibits vegetation, soil, relief, and atmospheric conditions typical to Southern Californian urban-fringe watersheds. The watershed was 97% burned during the Old Fire. A historical fire perimeter data set provided by the California Department of Forestry and Fire Protection (from ~1900 to 2010) reveals notable fire events in Devil Canyon during 1918 (24% burned), 1924 (27% burned), and 1980 (28% burned). The last major fire event was over fifty years ago in 1954 (92% burned). Keeley et al. (2004) note that Southern California chaparral systems generally have a natural frequency rate of 30–40 years, indicating that Devil Canyon is generally close to a natural fire regime. The elevation range in Devil Canyon is 500 to 1700 m and the overall watershed slope is 15% (USGS 7.5 min, Quadrangle Map; Silverwood Lake and San Bernardino North). The soil in Devil Canyon is associated with gravelly loamy sand, loamy sand, coarse loamy sand, sandy loam, and clay loam (Hromadka, 1986; Mays, 2001).

The City Creek watershed (Fig. 1) is approximately 51 km^2 and is located just southeast of the Devil Canyon catchment. The basin receives an average of 600 mm of precipitation a year (San Bernardino County Flood Control District (SBCFCD), 2010; data period from 1985 to 2010). City Creek consists primarily of chaparral (72%) and mixed evergreen and mixed conifer forests (20%) at higher elevations; the remaining 8% consists of a mixture of coastal sagescrub, developed areas, riparian zones, unvegetated areas, water, and woodlands (Minnich, 1988; NOAA, 2003). The watershed was estimated as 94% burned by the Old Fire. The California Department of Forestry and Fire Protection's historic fire perimeter set reveals notable fire events in City Creek in 1922 (53% burned), 1956 (61% burned), and 1970 (28% burned). In 2007, the Slide Fire burned less than five percent of

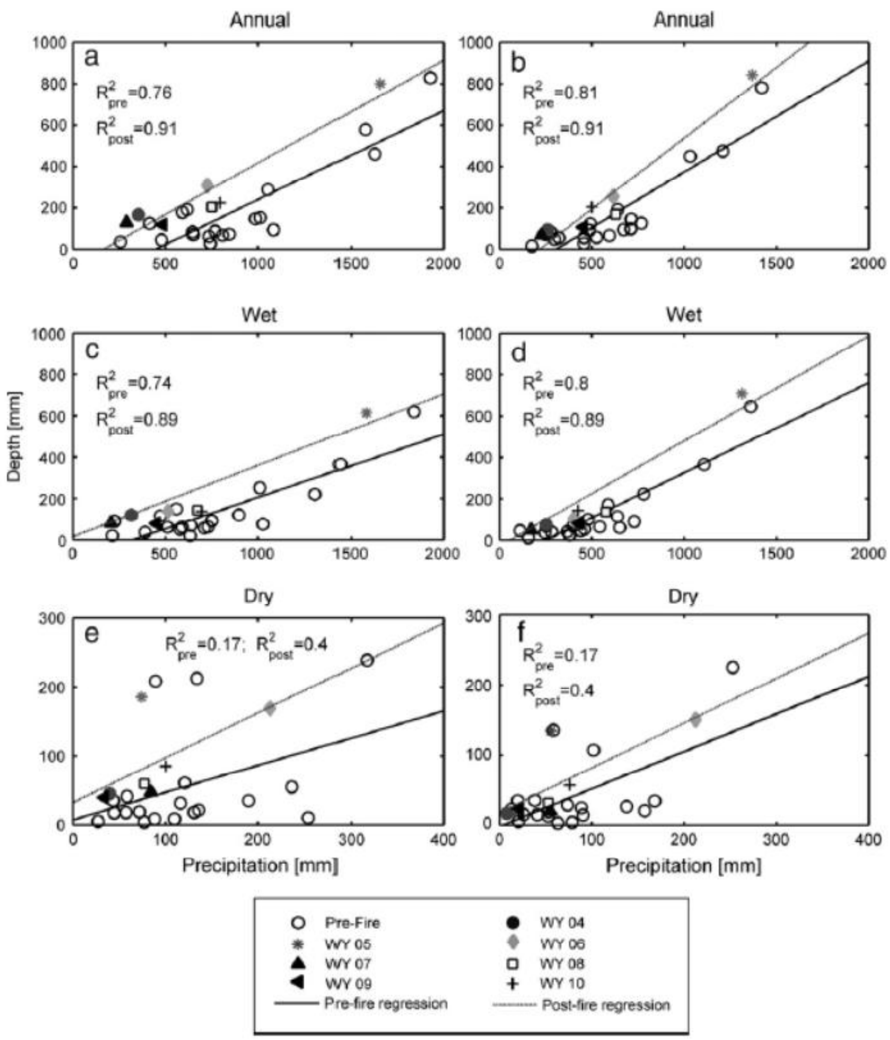

Fig. 3. Runoff relationships, associated regression line, and correlation coefficient (R^2) for annual (WY 1985–2008), wet (Oct–Mar), and dry (Apr–Sep) seasons for Devil Canyon (a, c, e) and City Creek (b, d, f). Pre-fire years and seasons are shown with open circles, while post-fire years and seasons are shown with filled symbols.

the northeast corner of City Creek (predominantly mixed forest). The portion of City Creek re-burned during the 2007 fire was classified by the USDA Forest Service Remote Sensing Applications Center as mostly unchanged/very low and low burn severity (USDA Forest Service, 2007). City Creek's elevation range is 300 to 2100 m and the overall watershed slope is estimated at 10% (USGS 7.5 min, Quadrangle Map Harrison). The soil in City Creek is associated with clay loams, shallow sandy loam, soils with low organic content, and soils higher in clay content (Hromadka, 1986; Mays, 2001).

2.2. Data and analysis

2.2.1. Hydrologic data

Precipitation data for the two watersheds are available from the San Bernardino County Flood Control District for water years (WY) 1985 to 2010 (01 October 1984 to 30 September 2010). The Devil Canyon rain gage (Gage 2840) is located at the top of the watershed, while the City Creek rain gage (Gage 3377) is more centrally located in the middle elevation of the basin. There were about 160 days of missing data for the study period for the City Creek gage and additional gages (5140 and 5339) outside (5 and 5.5 miles respectively) of the watershed were used to estimate missing values (filled by the inverse-distance weighting method). Daily precipitation data for Devil Canyon contained 373 days of missing data. Gage 3377 in City Creek is approximately 13 km directly south of the Devil Canyon gage, hence a linear regression was developed between the two gages to establish a relationship and estimate missing precipitation at the Devil Canyon gage. During the study period, WY 2005 is noted as the second wettest year on record (NOAA, 2009a) and WY 2002 is noted as the driest year on record (NOAA, 2009c).

USGS discharge data are available at the outlet of both watersheds (gages 11055800 (City Creek) and 11063680 (Devil Canyon)). Hydrologic observations (discharge, runoff depth, and precipitation) were aggregated to various timescales, including monthly, seasonal and yearly totals for water years 1986 to 2010 to evaluate pre- and post-fire behaviors of the watersheds. Additionally, discharge (Q) values were transformed to provide improved visualization of the full range of flows. In particular, transformed flows are more ideal for observing baseflow, where the transformation expands the recessions (Hogue et al., 2000). Transformed flow, Q_t, is similar to a Box–Cox transformation (Box and Cox, 1964) and is calculated as follows:

$$Q_t = \frac{(Q+1)^{\lambda}-1}{\lambda} \tag{1}$$

where $\lambda = 0$ equates to a log transformation and $\lambda = 1$ implies no transformation. In the current study, we set $\lambda = 0.3$ (Hogue et al., 2000). Annual and seasonal discharge values are compared with corresponding EVI values for both pre- and post-fire periods. Each 250 m EVI is further classified by aspect and level of burn severity.

2.2.2. Aspect

Aspect is defined as the compass direction of the slope face in the watershed and is classified using a Digital Elevation Model (DEM). Slope aspect influences the amount of radiative forcing that a respective land surface receives, facilitating or deterring growth rates. USGS DEMs were obtained for each watershed with a 10 m resolution as Spatial Data Transfer Standard (SDTS) and aggregated to a 250 m × 250 m resolution to match the remote sensing data utilized in this study. Devil Canyon requires two DEM tiles (Silverwood Lake

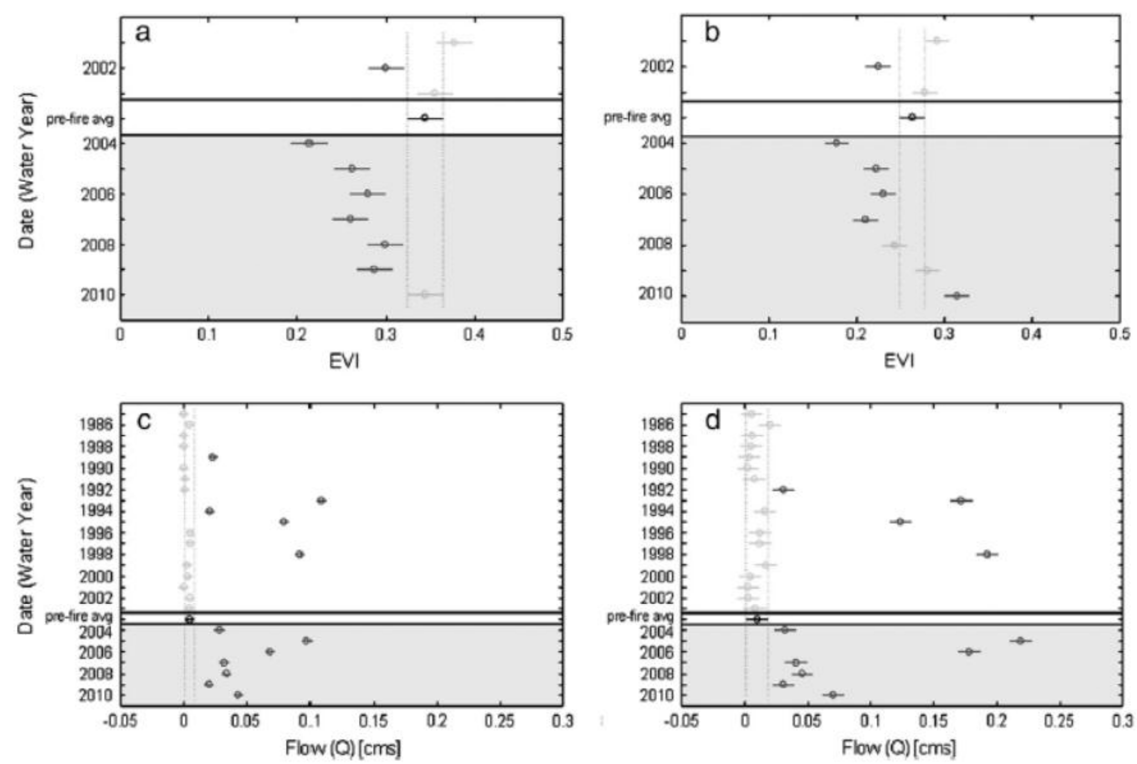

Fig. 4. ANOVA (Confidence Intervals (CI)) results for the dry season period for Devil Canyon EVI (a) and discharge (c) and City Creek EVI (b) and discharge (d). The vertical lines around the pre-fire average represent the tested confidence interval. Post-fire years are shaded in gray. Bolded water years outside of the tested confidence interval represent a statistically different mean from the pre-fire period at a confidence level of $\alpha = 0.05$.

and San Bernardino North) and City Creek requires the Harrison Mountain tile. Similar to Wittenberg et al. (2007), each grid is categorized into four primary aspects: north (315° to 45°), east (45° to 135°), south (135° to 225°), and west (225° to 315°).

2.2.3. Differenced Normalized Burn Ratio (dNBR)

MODIS is a multi-spectral sensor onboard the Aqua and Terra satellite platforms containing 36 spectral bands with wavelengths between 0.4 and 14.4 μm. Spatial resolutions include 250 m, 500 m, and 1000 m and temporal resolutions include daily, 8-day, 16-day, monthly, quarterly, or yearly. Normalized Burn Ratio (NBR) is derived from remotely-sensed near infrared (NIR) and mid-infrared (MIR) MODIS bands and provides an estimate of the burn severity level (loss of vegetation) of a patch of land surface (Key and Benson, 2006). In the current study, NIR and MIR bands from the MOD13Q1 tile are used to derive NBR images for pre-fire (30 September 2003) and post-fire (17 November 2003) dates. The developed pre- and post-fire NBR images are differenced to create a differenced NBR (dNBR) image, which differentiates between burned and unburned areas (Key and Benson, 2006) and approximates the amount of vegetation density lost directly from wildfire. Based on Key and Benson's (2006) definition of severity levels, dNBR images were classified into the following categories: unburned (<+100), low severity (+100 to +269), moderate severity (+270 to +659), and high severity (+660 to +1300). The relative amount of vegetation biomass lost during the wildfire (burn severity) provides insight on post-fire soil conditions (hydrophobicity, structure, etc.).

2.2.4. Vegetation indices (MODIS, MOD13Q1)

MOD13Q1 is acquired from the EROS Data Center, whose database consists of various atmospheric, hydrologic, and energy variables that can be applied to global vegetation observations, hydrologic modeling, and other management applications. MOD13Q1 contains vegetation parameters such as NDVI, EVI, and relevant QA (quality analysis) data (Chen et al., 2005; Huete et al., 2002). The MOD13Q1 EVI data are utilized with a temporal resolution of 16 days and a spatial resolution of 250 m. EVI data were collected from WY 2001 to 2010 (01 October 2000–30 September 2010). The equation used to derive MOD13Q1 (EVI) is noted as:

$$\mathrm{EVI} = 2.5\left[\frac{\rho^{*}_{\mathrm{NIR}} - \rho^{*}_{\mathrm{RED}}}{\rho^{*}_{\mathrm{NIR}} + C_1\rho^{*}_{\mathrm{NIR}} - C_2\rho^{*}_{\mathrm{BLUE}} + L}\right] \tag{2}$$

where ρ^{*}_{NIR} is the near infrared reflectance, ρ^{*}_{RED} is the red channel reflectance, ρ^{*}_{BLUE} is the blue channel reflectance, C_1 and C_2 are the red and blue correction coefficients for atmospheric resistance, respectively, and L is the canopy background brightness correction factor (Huete et al., 2002; Chen et al., 2005). Spatial and temporal EVI values were extracted and visualized, and various spatial aggregations are undertaken (per aspect type, per burn severity group, per basin area, etc.). The extracted EVI time series values are used to quantify the total annual EVI detected (summation of each 16-day EVI value per determinant over the entire water year) in order to represent the total vegetation biomass (dead or living) for each pre- and post-fire year. A single image or "snapshot" of EVI values will miss the variability present in vegetation, while the accumulation of EVI detected over the course of a year will capture the vegetation activity and variability. We also estimate a percent recovery for each post-fire year, relative to the three-year pre-fire average, with respect to each burn severity and aspect.

2.2.5. Savitzky–Golay analysis

EVI data are filtered using the Savitzky–Golay (S–G) least squares polynomial filter (Jonsson and Eklundh, 2004). An unfiltered EVI time series contains "noise" or small scale temporal variations and, similar to previous studies, steps are taken to filter this "noise" out to create a smoother signal for analysis. The EVI time series for each aspect for each burn severity level is smoothed using the S–G method where the degree of the polynomial regression is 1. After filtering, the Casady et al. (2009) method is used to develop a relationship between post-fire years. The EVI time series is normalized by the pre-fire EVI mean (f EVI); making the post-fire EVI a fraction of the pre-fire EVI, also allowing for evaluation of the post-fire EVI vegetation relative to pre-fire EVI levels. For each succeeding post-fire year (WY 2004–2010), the f EVI is summed to derive the integrated annual EVI. The annual integral is subsequently fit with a regression line using the least squares method, using the following equation:

$$\int f\,\mathrm{EVI} = \beta_0 + \beta_1(Year) \tag{3}$$

where $\int f$ EVI is the annual integration of the fraction of EVI for each successive post-fire year, β_1 is the slope that represents the recovery from year to year, and β_0 is the slope intercept. The derived regression provides an estimate of the annual progression (rate) of vegetation recovery throughout the study period for each slope aspect and burn severity level pair.

2.2.6. Analysis of Variance (ANOVA)

An Analysis of Variance (ANOVA) is employed to determine the significance of relationships between study parameters. Discharge and EVI are separated annually and seasonally (OND (Oct to Dec–fall), JFM (Jan to Mar–winter), AMJ (Apr to Jun–spring), and JAS (Jul to Sep–summer)) and evaluated for statistical differences from the pre-fire

Table 2
Average annual and seasonal EVI and discharge (cms) values for October through December (OND), January through March (JFM), April through June (AMJ), and July through September (JAS) for the pre-fire and post-fire periods for Devil Canyon and City Creek. ANOVA results are highlighted (shaded) for various seasonal and annual periods.

	Annual	OND	JFM	AMJ	JAS
			Devil Canyon – mean EVI		
Pre-fire Avg	3.42E-01	3.12E-01	3.25E-01	3.84E-01	3.43E-01
2004	2.02E-01	1.56E-01	1.80E-01	2.44E-01	2.14E-01
2005	2.63E-01	2.14E-01	2.45E-01	3.23E-01	2.61E-01
2006	2.62E-01	2.26E-01	2.19E-01	3.18E-01	2.79E-01
2007	2.67E-01	2.55E-01	2.49E-01	3.04E-01	2.59E-01
2008	2.83E-01	2.38E-01	2.53E-01	3.37E-01	2.98E-01
2009	2.96E-01	2.81E-01	2.79E-01	3.35E-01	2.86E-01
2010	3.31E-01	2.77E-01	2.92E-01	4.00E-01	3.44E-01
			Devil Canyon – mean flow		
Pre-fire Avg	4.80E-02	3.39E-02	1.18E-01	3.61E-02	4.80E-03
2004	8.03E-02	1.35E-01	1.20E-01	5.33E-02	2.82E-02
2005	3.61E-01	1.91E-01	9.29E-01	2.39E-01	9.72E-02
2006	1.39E-01	8.93E-02	1.62E-01	2.39E-01	6.84E-02
2007	5.84E-02	7.17E-02	7.67E-02	5.36E-02	3.20E-02
2008	9.18E-02	5.67E-02	2.04E-01	7.41E-02	3.41E-02
2009	5.38E-02	5.36E-02	9.11E-02	5.14E-02	2.02E-02
2010	1.01E-01	5.57E-02	1.97E-01	1.11E-01	4.31E-02
			City Creek – mean EVI		
Pre-fire Avg	2.78E-01	2.43E-01	2.83E-01	3.16E-01	2.64E-01
2004	1.68E-01	1.14E-01	1.56E-01	2.05E-01	1.77E-01
2005	2.43E-01	2.04E-01	2.50E-01	2.89E-01	2.22E-01
2006	2.22E-01	1.89E-01	1.89E-01	2.73E-01	2.30E-01
2007	2.20E-01	2.01E-01	2.12E-01	2.54E-01	2.10E-01
2008	2.42E-01	1.92E-01	2.39E-01	2.83E-01	2.43E-01
2009	2.82E-01	2.71E-01	2.66E-01	3.11E-01	2.80E-01
2010	2.96E-01	2.59E-01	2.69E-01	3.35E-01	3.14E-01
			City Creek – mean flow		
Pre-fire Avg	1.36E-01	9.15E-02	3.33E-02	1.13E-01	9.70E-03
2004	1.61E-01	3.14E-01	2.64E-01	7.54E-02	3.20E-02
2005	1.36E+00	4.29E-01	4.20E+00	6.42E-01	2.19E-01
2006	4.09E-01	1.91E-01	4.92E-01	7.86E-01	1.78E-01
2007	1.11E-01	1.45E-01	1.69E-01	9.02E-02	4.06E-02
2008	2.71E-01	1.10E-01	7.80E-01	1.56E-01	4.55E-02
2009	1.71E-01	1.60E-01	3.77E-01	1.22E-01	3.06E-02
2010	3.26E-01	1.14E-01	8.36E-01	3.00E-01	7.03E-02

Note: Shading highlights statistically different means from the pre-fire period ($\alpha = 0.05$).

period. We test the null hypothesis that the mean of each discharge time series (WY 1986–2010; seasonal and annual periods) is similar to the mean from the pre-fire data period (WY 1986–2003) ($\alpha = 0.05$). For consistency, pre-fire discharge average is calculated by excluding El Nino years (given that no El Nino years were noted in the post-fire period). We also evaluate the null hypothesis that the mean of each seasonal and annual EVI time series (WY 2001–2010) is similar to the mean of the same pre-fire EVI period (WY 2001–2003). We perform a multiple ANOVA comparison (pair-wise design) and evaluate successive pairs of post-fire means to the pre-fire average. This step-wise comparison allows us to evaluate when pre-fire conditions (behavior) are generally restored.

3. Results and discussion

3.1. General watershed behavior

Relevant characteristics, including precipitation, discharge, and average (basin-scale) EVI values are evaluated for each watershed for WY 2001–2010 (Fig. 2). Both watersheds show a distinct (pulse) response to precipitation events during the winter season and minimal but consistent baseflow response in the summer period. Post-fire, discharge is significantly elevated for precipitation events that are of similar (or lower) amounts to pre-fire storms. In addition, baseflow values are heightened during the post-fire summer periods, especially after WY 2005 and WY 2006 winter seasons. Vegetation (EVI) in both basins shows a prolonged and increased response to precipitation events, with an extended sinusoidal seasonal pattern, peaking after the peak rainfall/discharge flux in each basin. Devil Canyon (Fig. 2a) also shows a slightly higher basin-average EVI than City Creek (Fig. 2b). We attribute this to the initial difference in vegetation distributions (Devil Canyon has a higher percentage of mixed forest and smaller percentage of chaparral than City Creek). Immediately post-fire (right of the vertical dashed line), the EVI of both watersheds shows a sharp decline, with EVI values decreasing by more than half. Significant winter rainfall during WY 2005 increases the EVI to near pre-fire levels in both Devil Canyon and City Creek; however the EVI response is dampened again during the next and subsequent seasons. This implies that the rainfall during WY 2005 resulted in a brief "green-up" of watershed vegetation; however the green-up was not sustained for either watershed. Discharge values remain elevated during the following summer period, and we hypothesize that mature (deeper) root systems, which can tap into deeper soil water stores, were not yet developed (Jung et al., 2009). Finally, the aggregate EVI signal of both watersheds does not appear to be back to pre-fire levels (maximum values are significantly lower) in the last year of the study period (WY 2010).

3.2. Seasonal runoff ratios

Annual and seasonal (wet and dry) runoff ratios (depth runoff: depth precipitation) are highlighted in Table 1 and Fig. 3. In general, City Creek and Devil Canyon exhibit fairly similar runoff ratios over the pre-fire period, including 0.19 for Devil Canyon and 0.22 for City Creek. After fire, the average annual runoff ratios are significantly higher for both basins, with Devil Canyon having a runoff ratio of 0.37 and City Creek having a runoff ratio of 0.36 for the entire post-fire study period (Table 1). A cumulative distribution analysis also

Table 3
Average 16-day EVI values and ANOVA results for Devil Canyon and City Creek with respect to slope aspect and burn severity levels for the pre- and post-fire periods.

Aspect	Water year	Devil Canyon			City Creek		
		Burn severity			Burn severity		
		Low	Moderate	High	Low	Moderate	High
North	Pre-fire avg			2.74E-01	2.45E-01	2.58E-01	2.95E-01
	2004			1.30E-01	1.97E-01	1.81E-01	1.40E-01
	2005			2.40E-01	2.47E-01	2.37E-01	2.25E-01
	2006			2.41E-01	2.18E-01	2.14E-01	2.24E-01
	2007			2.44E-01	2.16E-01	2.19E-01	2.27E-01
	2008			2.64E-01	2.30E-01	2.29E-01	2.41E-01
	2009			2.64E-01	2.47E-01	2.41E-01	2.66E-01
	2010			2.94E-01	2.55E-01	2.58E-01	2.89E-01
East	Pre-fire avg		3.91E-01	4.02E-01	2.28E-01	2.61E-01	3.26E-01
	2004		2.29E-01	2.01E-01	1.78E-01	1.49E-01	1.45E-01
	2005		2.85E-01	2.73E-01	2.53E-01	2.32E-01	2.38E-01
	2006		2.94E-01	2.90E-01	1.90E-01	2.00E-01	2.56E-01
	2007		2.97E-01	2.96E-01	1.80E-01	1.99E-01	2.54E-01
	2008		3.13E-01	3.19E-01	2.23E-01	2.20E-01	2.65E-01
	2009		3.28E-01	3.40E-01	2.25E-01	2.41E-01	2.93E-01
	2010		3.63E-01	3.80E-01	2.31E-01	2.56E-01	3.07E-01
South	Pre-fire avg	3.34E-01	3.20E-01	3.54E-01	2.56E-01	3.05E-01	3.66E-01
	2004	2.31E-01	1.71E-01	1.54E-01	1.87E-01	1.66E-01	1.49E-01
	2005	2.79E-01	2.55E-01	2.44E-01	2.49E-01	2.44E-01	2.43E-01
	2006	2.65E-01	2.51E-01	2.51E-01	2.18E-01	2.30E-01	2.71E-01
	2007	2.70E-01	2.56E-01	2.56E-01	2.11E-01	2.36E-01	2.78E-01
	2008	2.86E-01	2.75E-01	2.82E-01	2.34E-01	2.54E-01	2.94E-01
	2009	2.92E-01	2.88E-01	3.01E-01	2.43E-01	2.75E-01	3.17E-01
	2010	3.20E-01	3.22E-01	3.40E-01	2.55E-01	2.93E-01	3.33E-01
West	Pre-fire avg	4.12E-01	3.23E-01	3.15E-01	2.43E-01	2.55E-01	3.39E-01
	2004	2.52E-01	1.66E-01	1.50E-01	1.96E-01	1.74E-01	1.39E-01
	2005	2.78E-01	2.28E-01	2.31E-01	2.47E-01	2.36E-01	2.22E-01
	2006	2.69E-01	2.31E-01	2.34E-01	2.12E-01	2.09E-01	2.42E-01
	2007	2.80E-01	2.35E-01	2.35E-01	2.06E-01	2.07E-01	2.47E-01
	2008	2.90E-01	2.55E-01	2.58E-01	2.24E-01	2.21E-01	2.62E-01
	2009	3.10E-01	2.65E-01	2.72E-01	2.30E-01	2.37E-01	2.87E-01
	2010	3.37E-01	2.96E-01	3.08E-01	2.38E-01	2.49E-01	3.02E-01

Note: Shading highlights statistically different means from the pre-fire period ($\alpha = 0.05$).

indicates that post-fire precipitation patterns are generally similar to the pre-fire cumulative precipitation patterns. However, the post-fire runoff depth is significantly altered (larger) in both watersheds relative to the pre-fire period (Table 1).

There is extra sensitivity to precipitation (increased runoff) during the extreme wet year (WY 2005), and then a gradual decrease in the runoff ratios to WY 2009. From 2009 to 2010 the runoff ratio for both watersheds shows a slight increase from 0.25 to 0.28 (Devil Canyon) and 0.23 to 0.33 (City Creek). WY 2010 was generally wetter than the preceding years (Fig. 2), which contributes to elevated runoff in Devil Canyon. City Creek exhibits a much larger increase in runoff, which is partly due to the increased precipitation but also attributed to the 2007 Slide Fire which occurred over a small portion of the basin. WYs 2007 through 2009 were relatively dry and the burned areas may not have contributed to increased runoff.

The post-fire trend line (annual response) shifts upward for both Devil Canyon (Fig. 3a) and City Creek (Fig. 3b). Investigation was also undertaken for both wet and dry seasons; with the wet season defined as fall and winter periods (October to March) and the dry season defined as spring and summer periods (April to September). During the wet season, the post-fire runoff ratio is higher than the pre-fire runoff ratio in both Devil Canyon (Fig. 3c) and City Creek (Fig. 3d). The post-fire regression line (relationship) is shifted up during the wet period and a slightly increased slope is seen at City Creek (Fig. 3d), indicating increased discharge response for post-fire precipitation events that are similar to pre-fire levels. In both watersheds, there is also significantly more discharge present during the dry season (Fig. 3e and f). Dry season runoff ratios are noticeably higher, especially in Devil Canyon (Fig. 3e). Devil Canyon is smaller and steeper; hence a quicker (and elevated) response is reasonable. The highest runoff value in the post-fire study period is for WY 2005 (recorded as the second wettest year on record; NOAA, 2009a). In WY 2009, the runoff ratio values are near the pre-fire range and indicate the post-fire hydrologic response is returning to pre-fire conditions. These variations within the flow and precipitation regimes are further investigated relative to of observed vegetation regrowth.

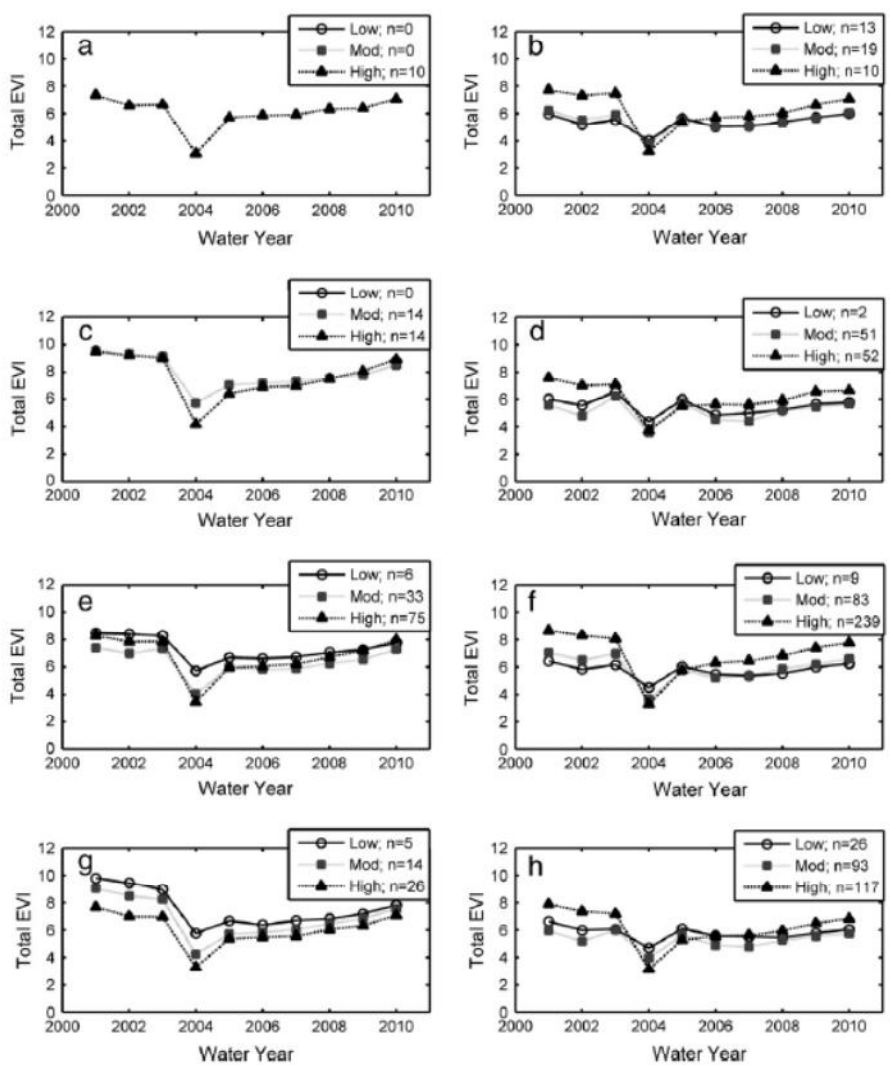

Fig. 5. Annual total EVI for each year with respect to aspect and burn severity levels for Devil Canyon north aspect (a), east aspect (c), south aspect (e), and west aspect (g); and for City Creek north aspect (b), east aspect (d), south aspect (f), and west aspect (h). Numbers of pixels (n) is indicated for each burn severity level within each studied aspect.

3.3. ANOVA and Confidence Intervals (CI)

As expected, during the pre-fire period, discharge is generally similar (within the average confidence interval) except for established El Nino years (WY 1993, 1995, 1997, 1998). Excess precipitation during El Nino years produces increased flow and results in a statistically different mean discharge from the pre-fire average. Dry season confidence interval (CI) plots for EVI and Q are presented for each watershed (Fig. 4). Pre-fire discharge is highly variable at the annual scale and wet season response tends to dominate the yearly trends. During the post-fire period, the dry season discharge values are elevated and significantly different than the estimated pre-fire average. This is especially evident during the extremely wet year (WY 2005) and the following year (WY 2006) which was influenced by residual moisture from the preceding year (Fig. 4c and d). Dry season EVI for Devil Canyon (Fig. 4a) and City Creek (Fig. 4b) show an expected decrease in EVI values immediately post-fire, with a general progression towards pre-fire values. During the extremely wet year (WY 2005), vegetation responds to the high winter precipitation, means similar to pre-fire conditions. However, the EVI response is not sustained and recedes between 2006 and 2008. During the final year of the study period (WY 2010), Devil Canyon and City Creek's average EVI for the dry season are statistically similar to the pre-fire EVI.

Table 2 highlights seasonal and annual results. In general, the Devil Canyon post-fire EVI does not show statistically similar means compared to the pre-fire average. The vegetation and hydrology do show inter-relatedness; as demonstrated by the post-fire dry season flows in both watersheds. As the EVI values increase, the discharge values trend towards pre-fire values (Table 2), but still are not within the significance interval. Table 2 also shows that the annual EVI in both watersheds are statistically different from the pre-fire mean for five to six years after fire. Devil Canyon EVI is the most statistically different from pre-fire, while City Creek seems to recover sooner. However, both Devil Canyon and City Creek streamflows during the summer (JAS) are not returned to pre-fire conditions. An analysis of controlling factors on vegetation recovery, including burn severity and aspect reveals that the EVI means are statistically different from pre-fire means in almost all scenarios, excluding Devil Canyon high burn north and City Creek low burn (Table 3). These observed EVI patterns prompt a more rigorous spatial investigation as explored below.

3.4. Post-fire EVI evolution

Annual total EVI values for each WY with respect to aspect and burn severity levels for both watersheds are highlighted in Fig. 5 (the number of pixels for each aspect and burn severity is also shown). For all slope aspects, pixels associated with high burn severity (high burn pixels) show the highest pre-fire EVI (biomass) values and low burn pixels have the lowest pre-fire EVI (biomass) values. Generally, pre-fire pixels with larger total EVI values show the largest decrease in EVI immediately post-fire, with the exception of Devil Canyon, where inconsistencies are noted that may be due to the smaller sample size (number of pixels available). Devil Canyon shows the general trend of increasing post-fire annual total EVI and City Creek clearly illustrates the low burn severity stabilizing (Fig. 5). The standard deviation is also estimated for each burn severity class. Devil Canyon has larger standard deviations, from 0.93 (low burn severity) to 1.63 (high burn severity) than City Creek (0.51 (low burn severity) to 1.56 (high burn severity)), also indicating increased variability in Devil Canyon. In both watersheds, the low severity burn has lower variability, while the high burn severities have more variability (larger standard deviation). The standard deviations for each aspect in Devil Canyon are 1.15 (north), 1.63 (east), 1.42 (south), and 1.51 (west). The standard deviations for each aspect in City Creek are 1.33 (north), 1.09 (east), 1.56 (south), and 1.35 (west).

Table 4 shows the percent recovery for each post-fire year for each aspect and burn severity relative to the pre-fire mean. We set a (subjective) threshold of ~90% as generally recovered, assuming some uncertainty in pre- and post-fire biomass estimates. The first post-fire year, WY 2004, indicates the initial recovery from the burn. Both watersheds experienced lower than average annual precipitation totals during this first wet season (260 mm and 355 mm for Devil Canyon and City Creek, respectively). Overall, recovery values range from 39% (south aspect, high burn in City Creek) to ~75% (west aspect, low burn in City Creek) during the first year. As expected, low burn pixels show the largest recovery during the first year (70% on average) and high burn pixels show the lowest recovery (43% average).

Moisture availability during the extremely wet second post-fire year (2005) accelerated vegetation activity in nearly all burn severity levels across all aspects, bringing biomass back up to 80–100% of pre-burn levels. In City Creek, the south low burn severity pixels are generally comparable to pre-fire values. However, the surge in vegetation activity is not sustained for the following post-fire years and after WY 2005, vegetation generally returns to a reduced recovery rate, with a slower increase of biomass through the next four study years (WY 2006 to 2010).

The majority of aspect and burn severities in both watersheds return to around 90% of the pre-fire vegetation by 2010, with the exception of Devil Canyon, where the limited number of pixels introduces more uncertainty in observed recovery trends. In City Creek, all aspects range from 91 to 107% recovered by the end of 2010, where the majority of observed pixels are in the south and west aspects (331 and 236 pixels, respectively; Fig. 7). This indicates that detected vegetation biomass has met or exceeded the pre-fire amount. However, it is important to note that the high burn severity in all aspects just reach 90% by 2010. The north aspect pixels are back to pre-fire conditions in both watersheds and show at least 90% recovery a year or two earlier than the other aspects. All other aspects

Table 4
Devil Canyon and City Creek percent annual total EVI recovery for each water year with respect to aspect and burn severity, where greater than 90% is assumed to be recovered to pre-fire vegetation conditions.

		Devil Canyon % yearly EVI			City Creek % yearly EVI		
Aspect	Burn severity	Low	Moderate	High	Low	Moderate	High
North	2004	–	–	44.7	72.6	64.5	42.8
	2005	–	–	83.0	101.6	94.2	71.5
	2006	–	–	85.3	90.9	86.1	75.7
	2007	–	–	86.1	91.6	86.2	77.2
	2008	–	–	92.1	96.6	90.1	80.0
	2009	–	–	93.1	103.0	96.2	88.5
	2010	–	–	102.9	107.9	102.9	94.2
East	2004	–	61.2	45.2	72.4	64.6	51.7
	2005	–	75.6	69.1	99.1	103.6	76.3
	2006	–	76.7	74.5	80.5	81.6	78.2
	2007	–	78.2	75.3	82.8	79.4	77.7
	2008	–	80.6	80.9	86.5	93.8	81.9
	2009	–	83.2	87.2	93.8	98.0	90.8
	2010	–	91.2	96.6	95.8	102.5	91.9
South	2004	68.1	55.7	43.4	73.2	53.2	39.4
	2005	79.8	82.7	74.3	98.5	84.0	68.9
	2006	78.9	80.1	75.7	89.0	76.1	75.5
	2007	80.2	81.0	77.8	87.2	78.1	77.3
	2008	84.1	86.4	84.1	89.9	85.8	81.8
	2009	86.5	90.3	89.7	97.5	90.8	88.7
	2010	92.5	100.4	100.0	101.7	96.7	93.3
West	2004	61.2	49.5	45.7	75.5	69.2	42.1
	2005	71.0	66.5	74.6	98.0	98.7	70.7
	2006	67.8	67.7	76.1	89.6	85.6	74.1
	2007	71.2	70.1	77.2	88.8	83.7	75.1
	2008	72.5	75.1	83.8	87.5	92.0	79.5
	2009	76.4	79.3	87.8	92.9	97.0	87.0
	2010	83.2	87.6	98.2	97.0	100.1	91.4

(south, west, east) appear, on average, about 75–85% recovered by WY 2008, with high burn severity pixels on the low end of this range. In Devil Canyon, the north high burn severity shows greater than 90% by 2008. The east and west aspects tend to recover by 2010, however, the west aspect does not appear to be recovered (83–98%) across the three burn severities.

The recovery slopes (β_1 from Eq. (3)) for all aspects and burn severities are estimated and plotted for Devil Canyon and City Creek (Fig. 6). The parameter β_1 represents the rate of biomass recovery relative to the initial loss (year 1). Overall recovery appears greatest (steeper slope) in the high burn pixels and lower in the moderate and low burn severities (Fig. 6). The high burn pixels experience greater initial vegetation loss, which ultimately constrains recovery and suggests a pre-disposition to return to initial biomass conditions. Low and moderate burn severity pixels experience low and medium (respectively) recovery rates as the vegetation biomass begins to stabilize or reach pre-fire vegetation amounts. This observation is consistent across both watersheds. Established recovery rates (β_1) rates were analyzed with and without WY 2005 and minimal difference in overall recovery rates were noted. As highlighted previously (Fig. 5), initial pre-fire biomass, and burn severity appear to dominate overall recovery rate in the two watersheds, and less long-term influence is noted from the observed variability in post-fire climatology.

Selected spatial maps of recovery for both watersheds were analyzed (Fig. 7). The percent recovery for each pixel is the total EVI for the year relative to the total pre-fire average. For 2007, the percent recovery generally ranges from 60 to 80% in both watersheds. The lower recovery percentages align with the high burn areas and the mixed forest vegetation (Fig. 7a and b). By 2010, the spatial percent recovery for both watersheds is dramatically different. The recovery percents are predominantly 90%, with the upper elevations (mixed conifer) still showing the lowest recovery. We hypothesize that the lower recovery at the top of the watershed, where steeper slopes and

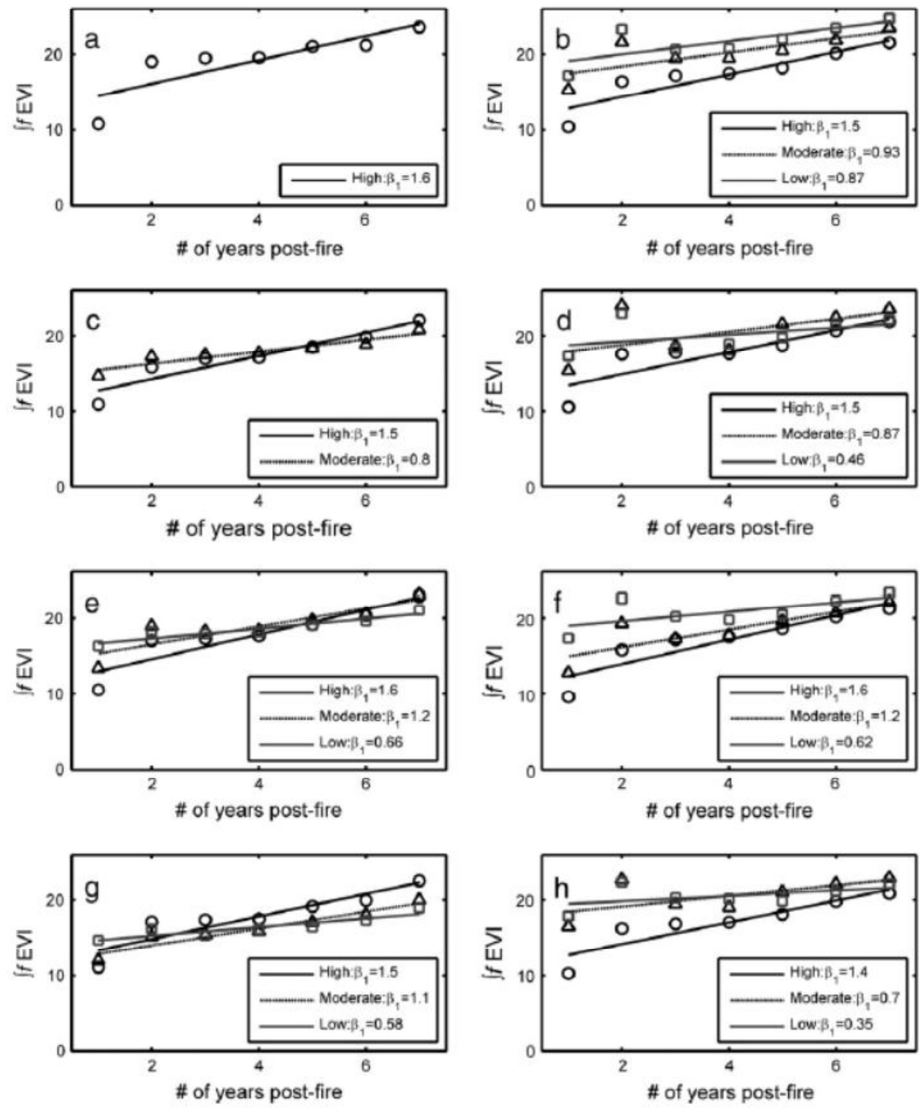

Fig. 6. Recovery slopes (regression line, β_1, from Eq. (3)) for the normalized EVI time series: Devil Canyon north (a), east (c), south (e), and west (g) and City Creek north (b), east (d), south (f), and west (h). Each burn severity level (low, moderate, high) is plotted for each aspect. Note: In Devil Canyon, EVI values do not exist for north low or moderate and east low burn pixels. The first post-fire year corresponds to WY 2004.

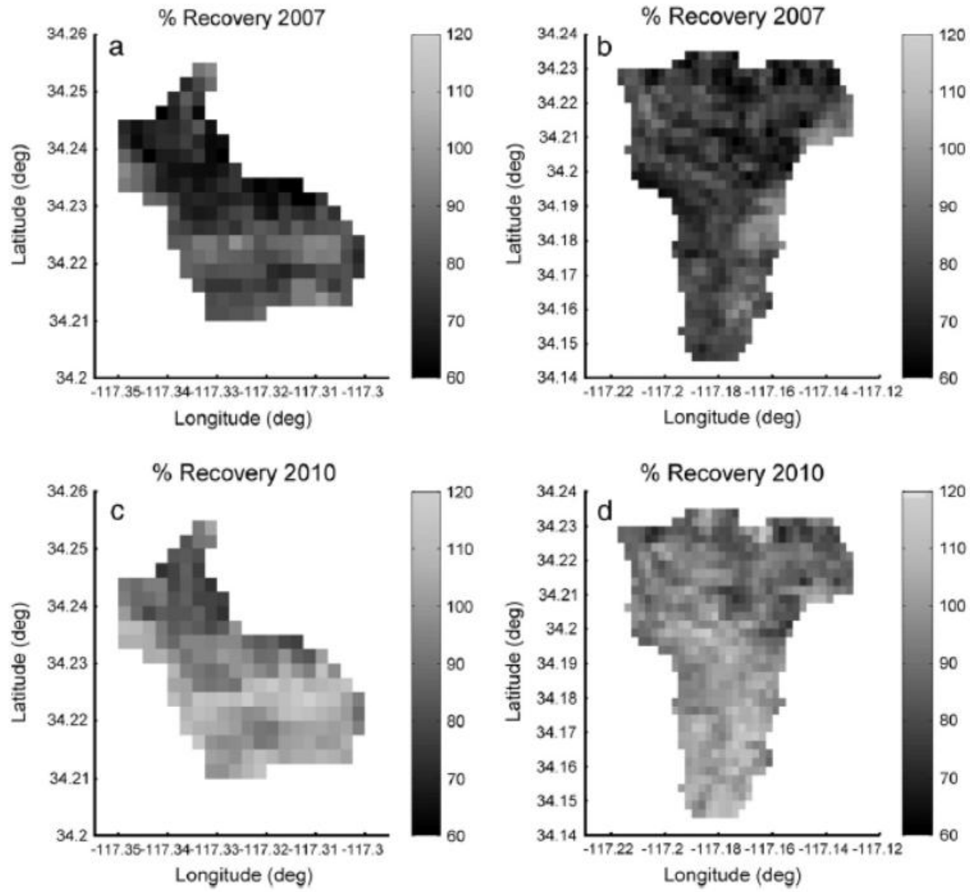

Fig. 7. Percent spatial recovery for Devil Canyon for WY 2007 (a) and WY 2010 (c) and for City Creek for WY 2007 (b) and WY 2010 (d). Results are relative to the pre-fire mean. Pixels greater than 90% of the pre-fire average are considered recovered.

larger vegetation dominate (mixed forest versus chaparral), is contributing to prolonged increased runoff, especially during the dry season period.

4. Conclusions

Evaluation of coupled ecologic and hydrologic recovery in post-fire systems over longer time periods in semi-arid regions has not been well-documented. The current study integrates a common vegetation index (EVI) and hydrologic data streams to simultaneously evaluate ecosystem and hydrologic dynamics for two burned watersheds affected by wildfire in October of 2003. The evaluation of vegetation biomass (EVI) in relation to factors such as slope aspect, burn severity and hydrologic time series over an extended period provides insight on the spatial variability of post-fire processes and ultimately, parameters controlling recovery patterns in each system. Primary findings from our investigations include:

- There is observed increase in discharge in both post-fire systems, especially in the dry season period. Distribution frequencies demonstrate that despite similar pre- and post-fire precipitation regimes, overall discharge patterns are significantly elevated over the seven-year study period, especially in the smaller, steeper Devil Canyon watershed. Similarly, the slower recovery of vegetation at the top of the watersheds is likely contributing to prolonged increased runoff. The increased dry season flow supports our understanding that plant water consumption (ET) and flow pathways within the basin were significantly during the fire and are generally not back to pre-fire behavior by the end of WY 2010.
- The MODIS EVI product provides key information on pre-fire vegetation biomass and recovery cycles in post-fire watersheds, both temporally and spatially. In the studied systems, the south, east, and west facing slopes show higher pre-fire EVI values and annual totals, likely due to higher radiative forcing (conditions governed by solar radiation), facilitating increased plant growth during the growing season. In terms of recovery rates, higher pre-fire biomass appears correlated with larger EVI loss and significant initial deficits in vegetation mass. We advocate that this implies a longer return period for the original vegetation species (i.e. chaparral rather than short-term grass recovery). South (and west) slopes also show the lowest percent recovery by the end of the study period compared to pre-fire conditions. North and east slope aspects reach pre-fire conditions earlier than the south and west aspects, likely due to retained soil moisture (also noted in Casady et al., 2009).
- The low severity burn pixels for all aspects return to pre-fire levels relatively quickly, while high severity burn pixels show the lowest overall recovery by WY 2010 especially in City Creek (Table 4). High burn severities tend to show the largest recovery rates (β_1), attributed to the greater initial loss (Fig. 6) and potential for

biomass regrowth (available root structure, seed release for new plant growth, etc.) but are still not back to pre-fire conditions (Figs. 5 and 6). Our results indicate that sustainable recovery in the two watersheds is heavily influenced by the aspect and burn severity of each pixel, and less influenced by short-term climate conditions.

The extreme wet season during the post-fire period resulted in higher EVI values. However, vegetation response from precipitation spikes may not be conducive to, or representative of full or permanent recovery of the watershed vegetation. Shallow-rooted systems (e.g., grasses) likely appear after these heavy rain events in the immediate post-fire period and are detected by the MODIS EVI product, contributing to higher annual total EVI. However, vegetation behavior (i.e. ET response) is not similar to pre-fire conditions (evidenced by the EVI patterns/cycles and coupled hydrologic response). The growth of grasses is shown to alter the normal (pre-fire) water demand in a system (Prater and DeLucia, 2006; Schenk and Jackson, 2002). Grasses also have different spectral signatures, resulting in different EVI values (Huete et al., 2002). Despite the inability to document specific plant species, we advocate that the MODIS-based EVI adds significant insight into seasonal spatial vegetation recovery and potential ET demand.

In summary, of the variables investigated in this study, longer-term hydrologic recovery appears more dependent on burn severity, slope aspect and vegetation type, and less dependent on short-term climatologic events. In addition, initial biomass appears to be the primary factor influencing burn severity, recovery potential, and overall recovery rates. Despite the general recovery of the north aspect and low burn severity areas, vegetation activity and hydrologic behavior are not back to pre-fire conditions after a seven-year period for the two systems studied. Although the difference in pixel numbers (significantly fewer observations in Devil Canyon) and slightly different fire history may influence comparisons between City Creek and Devil Canyon, recovery patterns are generally consistent in both watersheds, and significantly, high burn severity pixels (in any aspect in either watershed) just return within pre-fire ranges (~90%) by the end of the study period. Hydrologic behavior is still altered from pre-fire conditions, and it appears that the high burn pixels, particularly in the upper portion of the watershed, are exerting significant control on post-fire hydrologic recovery. Given the established recovery rates and observed patterns in both watersheds, we estimate that seasonal streamflow patterns will return to pre-fire levels when the high burn areas (across all aspects) have stabilized to pre-fire biomass conditions. Finally, the observed variability in post-fire discharge and precipitation demonstrates the importance of studying seasonal and sub-annual timescales over extended post-fire periods. The simultaneous exploration of vegetation biomass (EVI), slope-aspect, burn severity, and regional climate patterns provides insight on the spatial and temporal controls on hydrologic processes, and, ultimately, will assist in hydrologic predictions and watershed management over extended post-fire periods.

Acknowledgements

This work has been supported by grants from the NSF Hydrologic Sciences Program (EAR #0707162 and EAR #0965236) as well as a NASA Earth System Science Fellowship (#NNX07AO53H). The authors would like to thank Jongyoun Kim and Helen Jung for their technical contributions to this project.

References

Box, G.E.P., Cox, D.R., 1964. An analysis of transformations. Journal of the Royal Statistical Society Series B26 (2), 211–252.

Casady, G.M., Leeuwen, W.J.D., Marsh, S.E., 2009. Evaluating post-wildfire vegetation regeneration as a response to multiple environmental determinants. Environmental Model Assessment. doi:10.1007/s10666-009-9210-x.

Chen, X., Vierling, L., Deering, D., Conley, A., 2005. Monitoring boreal forest leaf area index across a Siberian burn chronosequence: a MODIS validation study. International Journal of Remote Sensing 26 (24), 5433–5451.

Cydzik, K., Hogue, T.S., 2009. Modeling post-fire response and recovery using the Hydrologic Engineering Center Hydrologic Modeling System (HEC-HMS). Journal of the American Water Resources Association 45 (3), 702–714.

Debano, L.F., 2000. The role of fire and soil heating on water repellency in wildland environments: a review. Journal of Hydrology 231–232, 195–206.

Diaz-Delgado, R., Salvado, R., Pons, X., 1998. Monitoring of plant community regeneration after fire by remote sensing. In: Traboud, L. (Ed.), Fire Management and Landscape Ecology. International Association of Wildland Fire, Fairfield, WA, pp. 315–324.

Diaz-Delgado, R., Lloret, F., Pons, X., Terradas, J., 2002. Satellite evidence of decreasing resilience in Mediterranean plant communities after recurrent wildfires. Ecology 83 (8), 2293–2303.

Duguy, B., Vallejo, V.R., 2008. Land-use and fire history effects on post-fire vegetation dynamics in eastern Spain. Journal of Vegetation Science 19, 97–108.

Gao, X., Huete, A.R., Ni, W., Miura, T., 2000. Optical–biophysical relationships of vegetation spectra without background contamination. Remote Sensing of Environment 74, 609–620.

Gitelson, A.A., Kaufman, Y.J., Merzlyak, M.N., 1996. Use of a green channel in remote sensing of global vegetation from EOS-MODIS. Remote Sensing of Environment 58, 289–298.

Gonzalez-Pelayo, O., Andreu, V., Campo, J., Gimeno-Garcia, E., Rubio, J.L., 2006. Hydrological properties of a Mediterranean soil burned with different fire intensities. Catena 68, 186–193.

Hogue, T.S., Sorooshian, S., Gupta, H., 2000. A multistep automatic calibration scheme for river forecasting models. Journal of Hydrolmeteorology 1 (6), 524–542.

Horton, J.S., Kraebel, C.J., 1955. Development of Vegetation after Fire in the Chamise Chaparral of Southern California.

Hromadka, T.V., 1986. San Bernardino County Hydrology Manual. San Bernardino Flood Control District, San Bernardino, California.

Huete, A., Didan, K., Miura, T., Rodriguez, E.P., Gao, X., Ferreira, L.G., 2002. Overview of the radiometric and biophysical performance of the MODIS vegetation indices. Remote Sensing of Environment 83, 195–213.

Ice, G.G., Neary, D.G., Adams, P.W., 2004. Effects of wildfire on soils and watershed processes. Journal of Forestry 16–20.

Jonsson, P., Eklundh, L., 2004. TIMESAT — a program for analyzing time-series of satellite sensor data. Computers and Geosciences 30, 833–845.

Jung, H., Hogue, T.S., Rademacher, L., Meixner, T., 2009. Impact of wildfire on source water contributions in Devil Creek, CA: evidence from end-member mixing analysis. Hydrological Processes 23, 183–200.

Keeley, J.E., Sterling, C.K., 1981. Post-fire regeneration of Southern California chaparral. American Journal of Botany 68 (4), 524–530.

Keeley, J.E., Fotheringham, C.J., Moritz, M.A., 2004. Lessons from the October 2003 Wildfires in Southern California. Journal of Forestry 102 (7), 26–31.

Keeley, J.E., Fotheringham, C.J., Baer-Keeley, M., 2005. Determinants of postfire recovery and succession in Mediterranean-climate shrublands of California. Ecological Applications 15 (5), 1515–1534.

Keeley, J.E., Brennana, T., Pfaff, A.H., 2008. Fire severity and ecosystem responses following crown fires in California shrublands. Ecological Applications 18 (6), 1530–1546.

Key, C.H., Benson, C.N., 2006. Landscape Assessment (LA) Sampling and Analysis Methods. USDA Forest Service Gen. Tech. Rep. RMRS-GTR-164-CD.

Matsushita, B., Yang, W., Chen, J., Onada, Y., Qiu, G., 2007. Sensitivity of the Enhanced Vegetation Index (EVI) and Normalized Difference Vegetation Index (NDVI) to topographic effects: a case study in high-density cypress forest. Sensors 7, 2636–2651.

Mays, L.W., 2001. Water Resources Engineering. John Wiley & Sons, Hoboken, New Jersey.

McMichael, C.E., Hope, A.S., Roberts, D.A., Anaya, M.R., 2004. Post-fire recovery of leaf area index in California chaparral: a remote sensing-chronosequence approach. International Journal of Remote Sensing 25 (21), 4743–4760.

McMichael, C.E., Hope, A.S., Loaiciga, H.A., 2006. Distributed hydrological modeling in California semi-arid shrublands: MIKE SHE model calibration and uncertainty estimation. Journal of Hydrology 317, 307–324.

Meixner, T., Wohlgemuth, P., 2003. Climate variability, fire, vegetation recovery, and watershed hydrology. Proceedings of First Inter-Agency Conference on Research in the Watersheds, Benson, Arizona, pp. 651–656.

Minnich, R.A., 1988. The biogeography of fire in the San Bernardino Mountains of California: a historical study. University of California Publications in Geography 28, 1–121.

Moody, J.A., Martin, D.A., Haire, S.L., Kinner, D.A., 2007. Linking runoff response to burn severity after a wildfire. Hydrological Processes 22, 2063–2074.

Myneni, R.B., Maggion, S., Iaquinta, J., Privette, J.L., Gobron, N., Pinty, B., Kimes, D.S., Verstraete, M.M., Williams, D.L., 1995. Optical remote sensing of vegetation: modeling, caveats, and algorithms. Remote Sensing of Environment 51, 169–188.

NOAA, 2003. National Oceanographic and Atmospheric Administration's Coastal Services Center. Southern California 2000-Era Land Cover/Land Use Metadata. http://www.csc.noaa.gov.

NOAA, 2009a. National Oceanic and Atmospheric Administration, The Second Wettest Rainfall Season in Los Angeles Come to an End. Public Information Statement. National Weather Service, Oxnard, CA.

NOAA, 2009b. National Oceanic and Atmospheric Administration's National Weather Service. The Climate of Los Angeles, California.

NOAA, 2009c. National Oceanic and Atmospheric Administration's National Weather Service. Water Year Rainfall for Downtown Los Angeles (1877–78 thru 2005 Seasons). http://www.weather.gov/climate/.

Pausas, J.G., 2003. The effect of landscape pattern on Mediterranean vegetation dynamics: a modeling approach using functional types. Journal of Vegetation Science 14, 365–374.

Pierson, F.B., Robichaud, P.R., Moffet, C.A., Spaeth, K.E., Hardegree, S.P., Clark, P.E., Eilliams, C.J., 2008. Fire effects on rangeland hydrology and erosion in a steep sagebrush-dominated landscape. Hydrological Processes 22, 2916–2929.

Prater, M.R., DeLucia, E.H., 2006. Non-native grasses alter evapotranspiration and energy balance in Great Basin sagebrush communities. Agricultural and Forest Meteorology 139, 154–163.

Riano, D., Chuvieco, E., Ustin, S., Zomer, R., Dennison, P., Roberts, D., Salas, J., 2002. Assessment of vegetation regeneration after fire through multitemporal analysis of AVIRIS images in the Santa Monica Mountains. Remote Sensing of Environment 79, 60–71.

Roder, A., Hill, J., Duguy, B., Alloza, J.A., Vallejo, R., 2008. Using long time series of Landsat data to monitor fire events and post-fire dynamics and identify driving factors. A case study in the Ayora region (eastern Spain). Remote Sensing of Environment 112 (1), 259–273.

Schenk, H.J., Jackson, R.B., 2002. Rooting depths, lateral spreads, and below-ground/above-ground allometries of plans in water limited ecosystems. Ecology 90, 480–494.

USDA Forest Service, 2007. Slide Fire occurring on the San Bernardino National Forest — 2007 Geospatial_Data_Presentation_Form: raster digital data. http://activefiremaps.fs.fed.us/baer/download.php?year=2007.

Wittenberg, L., Inbar, M., 2009. The role of fire disturbance on runoff and erosion processes — a long-term approach, Mt. Carmel Case Study, Israel. Geographical Research 47 (1), 46–56.

Wittenberg, L., Malkinson, D., Beeri, O., Halutzy, A., Tesler, N., 2007. Spatial and temporal patterns of vegetation recovery following sequences of forest fires in a Mediterranean landscape, Mt. Carmel Israel. Catena 71, 76–83.